University of Alberta

Capillary Electrophoresis with Laser-Induced Fluorescence Detection as a Tool for Glycosyltransferase Characterization

by

Nora Wen Chun Chan

A thesis submitted to the Faculty of Graduate Studies and Research in partial fulfillment of the requirements for the degree of Doctor of Philosophy

Department of Chemistry

Edmonton, Alberta

Spring 1999

National Library of Canada
Acquisitions and Bibliographic Services
395 Wellington Street
Ottawa ON K1A 0N4
Canada

Bibliothèque nationale du Canada
Acquisitions et services bibliographiques
395, rue Wellington
Ottawa ON K1A 0N4
Canada

Your file Votre référence

Our file Notre référence

The author has granted a non-exclusive licence allowing the National Library of Canada to reproduce, loan, distribute or sell copies of this thesis in microform, paper or electronic formats.

L'auteur a accordé une licence non exclusive permettant à la Bibliothèque nationale du Canada de reproduire, prêter, distribuer ou vendre des copies de cette thèse sous la forme de microfiche/film, de reproduction sur papier ou sur format électronique.

The author retains ownership of the copyright in this thesis. Neither the thesis nor substantial extracts from it may be printed or otherwise reproduced without the author's permission.

L'auteur conserve la propriété du droit d'auteur qui protège cette thèse. Ni la thèse ni des extraits substantiels de celle-ci ne doivent être imprimés ou autrement reproduits sans son autorisation.

0-612-39512-X

Canada

University of Alberta

Library Release Form

Name of Author: Nora Wen Chun Chan

Title of Thesis: Capillary Electrophoresis with Laser-Induced Fluorescence Detection as a Tool for Glycosyltransferase Characterization

Degree: Doctor of Philosophy

Year this Degree Granted: 1999

Permission is hereby granted to the University of Alberta Library to reproduce single copies of this thesis and to lend or sell such copies for private, scholarly, or scientific research purposes only.

The author reserves all other publication and other rights in association with the copyright in the thesis, and except as hereinbefore provided, neither the thesis nor any substantial portion thereof may be printed or otherwise reproduced in any material form whatever without the author's prior written permission.

Nora Chan

306-10713 80 Avenue

Edmonton, Alberta T6E 1V7

February 11, 1999

University of Alberta

Faculty of Graduate Studies and Research

The undersigned certify that they have read, and recommend to the Faculty of Graduate Studies and Research for acceptance, a thesis entitled Capillary Electrophoresis with Laser-Induced Fluorescence Detection as a Tool for Glycosyltransferase Characterization submitted by Nora Wen Chun Chan in partial fulfillment of the requirements for the degree of Doctor of Philosophy.

Dr. Monica M. Palcic

Dr. George Kotovych

Dr. Glen R. Loppnow

Dr. Liang Li

Dr. Peter Sporns

Dr. Harry Schachter

(External Examiner)

February 5, 1999

Abstract

Glycosyltransferases are enzymes which catalyze transfer of a monosaccharide from a sugar-nucleotide donor to an acceptor, forming oligosaccharides, glycoproteins, or glycolipids. These products are secreted, and are also expressed on virtually all mammalian cell surfaces. To account for the vast numbers of structures found on glycoproteins and glycolipids, it is estimated that more than one hundred glycosyltransferases exist with each forming a unique glycosidic linkage. Cell surface oligosaccharides are involved in many biological recognition processes, such as binding of viri such as HIV, antibodies, bacteria, toxins, and hormones to their respective binding sites. Unusual oligosaccharides may also be associated with malignant transformations. In some cases these changes are due to altered levels of certain glycosyltransferases. Specific inhibitors that can reduce the formation of these abnormal glycosylations may thus be of therapeutic use.

Difficulties in studying enzymatic activity of glycosyltransferases include limited availability of substrates, low levels of enzymes in tissues leading to problems in isolation procedures, a lack of structural information, and limited ability to detect low levels of oligosaccharide products which themselves have no chromophore. Capillary electrophoresis with laser-induced fluorescence (CE-LIF), with its low detection limit and high separation efficiency, has been used here to overcome several of these problems.

In Chapter 2, CE-LIF was used to detect low levels of activities of an α1,3 fucosyltransferase and a β1,4 galactosyltransferase in *Helicobacter pylori*. The biosynthetic pathway of Lewis^x (a mammalian cell surface structure) was reported in

H. pylori to be identical to that found in humans. A novel glycosidic linkage was detected by CE-LIF and it was confirmed by methylation analysis as an α1→6 linkage between *N*-acetylgalactosamine and galactose.

In Chapter 3, an intracellular inhibition assay was developed for α-glucosidase I in a human colon adenocarcinoma cell line. The potencies and IC_{50} values of two α-glucosidase I inhibitors, 1-deoxynojirimycin and castanospermine, were assessed by monitoring the degradation of a specific synthetic substrate, αGlc(1→2)αGlc(1→3)αGlc in the absence and presence of inhibitors. The method permitted the rapid determination of inhibitor potencies. The efficacy of a novel compound as an inhibitor of α-glucosidase I was tested with this method.

In Chapter 4, the degree of inhibition of a blood group A-transferase by the novel inhibitor, 3-amino-3-deoxy-[αFuc(1→2)]βGal-*O*-octyl, was assessed in the intracellular inhibition assay developed in chapter 3. The intracellular IC_{50} value of this compound in HT29 cells was determined. Effects of 3-amino-3-deoxy-[αFuc(1→2)]βGal-O-octyl on the formation of cell surface structures and glycoprotein formation were also determined in a [^{35}S]-methionine incorporation experiment.

In Chapter 5, CE-LIF was used to determine kinetic constants for enzyme activities of two novel, genetically-engineered glycosyltransferases, *H. pylori* α1,2 fucosyltransferase cloned in *E. coli*, and a Brazilian myxoma viral α2,3 sialyltransferase infected into a European rabbit kidney RK_{13} cell line. The structures of the enzymatic products were identified by co-migration in CE-LIF, which was not possible with radiochemical assays.

Acknowledgments

I am very grateful to Professor Monica Palcic, who not only has been an excellent supervisor but a very knowledgeable figure for every question I have related to academia, and life in general.

Many thanks to past/present members of Monica's research group: Christine Scaman, Gordon Alton, Hong Li, York Liu, Adam Szpacenko, Shawna Mackinnon, Aihua Lu, Kenji Osumi, Kamata Tsuneo. Special thanks to Cathy Compston for all her help and making the lab a wonderful experience, Keiko Sujino for always being a friend and teaching me about carbohydrate synthesis, Lynne Lechelt for keeping me on track at all times, Katja Stangier for showing me how to be an organized researcher. Most of all, Andy Holt for sharing his thoughts, knowledge, and experiences, and spending many hours proof-reading my publications, including this thesis.

I would like to thank Professor Ole Hindsgaul for career advice and trusting me to safeguard his home and his dogs. I also thank members of his group, especially Vivek Kamath and Minghui Du for showing me the steps for fluorescent labeling.

I thank Professor Norm Dovichi for cheerful hallway and serious meeting conversations, and for the CE-LIF instrument that was built in his research group. I thank members of his group, especially Edgar Arriaga and Darren Lewis, for helping me fixing the instrument at many desperate times.

I thank my parents for their faith in me and send me to Canada to pursue my goals. Finally, to my husband, Thompson, for hanging in there at times I don't want to mention, and giving me all the support when I needed it the most.

Table of Contents

1. Introduction 1

1.1 Introduction to Glycobiology 2

1.1.1 Mammalian Monosaccharides 2

1.1.2 Glycosyltransferases 2

1.1.3 Types of Glycoconjugates 6

1.1.3.1 Glycoproteins 6

1.1.3.1.1 *N*-Glycans 7

1.1.3.1.2 *O*-Glycans 10

1.1.3.2 Glycolipids 10

1.1.4 Blood Group Antigenic Determinants 12

1.1.5 Role of Oligosaccharides in Mammalian Cells, and Their Association with Oncogenesis 17

1.1.6 Inhibition of Glycosylation 18

1.2 Capillary Electrophoresis 22

1.2.1 Principles of Capillary Zone Electrophoresis 23

1.2.1.1 Electroosmotic Flow and Zeta Potential 25

1.2.1.2 Electrophoretic Mobility 27

1.2.2 Principles of MEKC 29

1.2.2.1 Parameters Governing MEKC 29

1.2.2.1.1 Micelle Formation 29

1.2.2.1.2 Capacity Factor 30

1.2.2.1.3 Borate Buffer Complexation with Oligosaccharides 33
1.2.3 Sample Injection 34
1.2.4 Sample Detection 35
1.2.4.1 Post-Column Laser-Induced Fluorescence Detection 35
1.2.5 Pre-Column Derivatization 35
1.2.6 Advantages of CE-LIF over Conventional Separation Methods 36
1.3 References 38
2. The Biosynthesis of Lewis^x in *Helicobacter pylori* 47
2.1 Introduction 48
2.2 Experimental Section 50
2.2.1 Materials 50
2.2.2 Cell Growth and Immuno-electron Microscopy 51
2.2.3 Enzyme Extract Preparation 52
2.2.4 Activity Screening 52
2.2.5 Kinetic Characterizations 53
2.2.6 Capillary Electrophoresis 54
2.2.7 Preparative Syntheses 55
2.2.8 Methylation Analysis 55
2.3 Results and Discussion 57
2.3.1 Detection of Lewis^x on *H. pylori* Cell Surface 57
2.3.2 Fucosyltransferase and Galactosyltransferase Activities 57
2.3.3 Detection of Lewis^x and a New Product by CE-LIF 59
2.3.4 Identification of the New Product by ^{1}H-NMR and Methylation Analysis 61

2.3.5 Identification of Lewis^x by ^{1}H NMR 64

2.3.6 Biosynthetic Pathway of Lewis^x in *H. pylori* 66

2.3.7 Kinetic Variation in Different Strains of *H. pylori* 66

2.4 Conclusions 70

2.5 References 71

3. Intracellular Glucosidase I Inhibition in Cultured Cells Measured by Capillary Electrophoresis with Laser-Induced Fluorescence Detection 73

3.1 Introduction 74

3.2 Experimental Section 78

3.2.1 Materials 78

3.2.2 Preparation of Ethylenediamine monoamides 79

3.2.3 Preparation of TG-TMR 80

3.2.4 Culture of HT29 cells 80

3.2.5 Confocal Laser Scanning Microscopic Image of HT29 Cells Incubated with TG-TMR 81

3.2.6 Inhibition Assays with 1-Deoxynojirimycin and Castanospermine 82

3.2.7 Sample Preparation for Analysis by Capillary Electrophoresis with Laser-Induced Fluorescence Detection 82

3.2.8 Data Analysis 83

3.3 Results and Discussion 85

3.3.1 ^{1}H NMR and ESI-MS characterization of TG-TMR 85

3.3.2 Intracellular Localization of Fluorescent Substrate using Confocal Scanning Laser Microscopy 85

3.3.3 Detection Of α-Glucosidase Products by CE-LIF 86

3.3.4 Intracellular Inhibition of α-Glucosidase 92

3.4 Conclusions 100

3.5 References 101

4. First Demonstration of Intracellular Inhibition of a Glycosyltransferase 104

4.1 Introduction 105

4.2 Experimental Section 108

4.2.1 Materials 108

4.2.2 Capillary Electrophoresis Assays for *In Vitro* Studies with Isolated Cloned Blood Group A-Transferase 109

4.2.3 Detection of Intracellular A-Transferase Activity in HT29 Cells 110

4.2.4 Intracellular Inhibition Assays with 3-Amino-3-Deoxy-[αFuc(1→2)]βGal-*O*-Octyl by CE-LIF 111

4.2.5 Data Analysis 111

4.2.6 Intracellular Inhibition Assay with 3-Amino-3-Deoxy-[αFuc(1→2)]βGal-*O*-Octyl by ^{35}S-Methionine Radiolabeling 112

4.2.6.1 Preparation of Monoclonal Antibodies 112

4.2.6.2 Preparation of BSA-Glycan Conjugates 113

4.2.6.3 Metabolic Labeling of Cells 113

4.2.6.4 Immunoprecipitation and SDS-PAGE Detection 114

4.3 Results And Discussion 115

4.3.1 *In Vitro* Inhibition of Isolated Cloned A-Transferase by 3-Amino-3-Deoxy-[αFuc(1→2)]βGal-*O*-Octyl 115

4.3.2 Detection of A-Transferase Uptake Product by CE-LIF 115

4.3.3 Intracellular Inhibition of A-transferase in HT29 Cells 120

4.3.4 Determination of The Intracellular IC_{50} Value for 3-Amino-3-Deoxy-[αFuc(1→2)]βGal-*O*-Octyl 122

4.3.5 Inhibitory Effects of 3-Amino-3-Deoxy-[αFuc(1→2)]βGal-*O*-octyl on Glycoprotein Formation in HT29 cells 124

4.4 Conclusions 130

4.5 References 132

5. Detection and Characterization of Novel Glycosyltransferases with CE-LIF 135

5.1 Introduction 136

5.2 Experimental Section 143

5.2.1 Materials 143

5.2.2 Characterization of *H. pylori* α1,2 Fucosyltransferase 144

5.2.2.1 Preparation of Extract Containing the Cloned α1,2 Fucosyltransferase 144

5.2.2.2 Radiochemical Synthesis of α1,2 Fucosylated Products 145

5.2.2.3 α1,2 Fucosylated Product Analyses by CE-LIF 146

5.2.3 Characterization of Brazilian Myxoma Viral α2,3 Sialyltransferase 147

5.2.3.1 Cell Extract Preparation Containing the myxoma viral α2,3 Sialyltransferase 147

5.2.3.2 Radiochemical Synthesis of Sialylated Lewis^x and Lewis^a 147

5.2.3.3 Confirmation of a 2,3 Linkage between Sialic Acid and Lewis^x or Lewis^a 148

5.2.3.4 Peak Identification Using a Neuraminidase 149

5.2.3.5 One-Pot Syntheses of Sialylated Lewis^x-TMR from GlcNAc-TMR & Sialylated Lewis^a-TMR from Lewis^c-TMR 149

5.3 Results And Discussion 151

5.3.1 *Helicobacter pylori* α1,2 Fucosyltransferase Results 151

5.3.1.1 Radiochemical Synthesis of α1,2 Fucosylated Products 151

5.3.1.2 Analysis of the α1,2 Fucosylation Products by Capillary Electrophoresis with Laser-Induced Fluorescence Detection 151

5.3.2 Brazilian Myxoma Viral α2,3 Sialyltansferase Results 160

5.3.2.1 Transfer of Sialic Acid to Lewis^a-gr and Lewis^x-gr 160

5.3.2.2 Confirmation of the α2,3 Sialylated Le^x- and Le^a-TMR Products by CE-LIF 160

5.3.2.3 Analysis of the One-Pot Syntheses 163

5.4 Conclusions 173

5.5 References 175

6. Conclusions 178

6.1 General Discussion and Conclusions 179

6.2 References 186

List of Nomenclature of Sugars, Abbreviations, and Symbols

HO-TMR	$HO(CH_2)_8CONH(CH_2)_2NHCO$-TMR, Linker arm, **1**
GlcNAc-TMR	βGlcNAc-OTMR, *N*-acetylglucosamine, **2**
LacNAc-TMR	βGal(1→4)βGlcNAc-OTMR, *N*-acetyllactosamine, **3**
H type II-TMR	αFuc(1→2)βGal(1→4)βGlcNAc-OTMR, **4**
Lewis^x-TMR (Le^x)	βGal(1→4)[αFuc(1→3)]βGlcNAc-OTMR, **5**
Lewis^y-TMR (Le^y)	αFuc(1→2)βGal(1→4)[αFuc(1→3)]βGlcNAc-OTMR, **6**
Lewis^c-TMR (Le^c)	βGal(1→3)βGlcNAc-OTMR, **7**
H type I-TMR	αFuc(1→2)βGal(1→3)βGlcNAc-OTMR, **8**
Lewis^a-TMR (Le^a)	βGal(1→3)[αFuc(1→4)]βGlcNAc-OTMR, **9**
Lewis^b-TMR (Le^b)	αFuc(1→2)βGal(1→3)[αFuc(1→4)]βGlcNAc-OTMR, **10**
2,3 sialyl LacNAc-TMR	αNeu5Ac(2→3)βGal(1→4)βGlcNAc-OTMR, **11**
2,6 sialyl LacNAc-TMR	αNeu5Ac(2→6)βGal(1→4)βGlcNAc-OTMR, **12**
sialyl Lewis^x-TMR	αNeu5Ac(2→3)βGal(1→4)[αFuc(1→3)]βGlcNAc-OTMR, **13**
2,3 sialyl Lewis^c-TMR	αNeu5Ac(2→3)βGal(1→3)βGlcNAc-OTMR, **14**
TG-TMR	αGlc(1→2)αGlc(1→3)αGlc-OTMR, Triglucose-*O*TMR
DG-TMR	αGlc(1→3)αGlc-OTMR, Diglucose-*O*TMR
MG-TMR	αGlc-OTMR, Monoglucose-*O*TMR
FucGal-TMR	αFuc(1→2)βGal-*O*TMR
A-trisaccharide-TMR	αGalNAc(1→3)[αFuc(1→2)]βGal-*O*TMR
H*O*-gr	$HO(CH_2)_8COOCH_3$
GlcNAc-*O*gr	βGlcNAc-$O(CH_2)_8COOCH_3$

LacNAc-*O*gr	βGal(1→4)βGlcNAc-O$(CH_2)_8COOCH_3$
H type II-*O*gr	αFuc(1→2)βGal(1→4)βGlcNAc-O$(CH_2)_8COOCH_3$
Lewis^x-*O*gr	βGal(1→4)[αFuc(1→3)]βGlcNAc-O$(CH_2)_8COOCH_3$
Lewis^y-*O*gr	αFuc(1→2)βGal(1→4)[αFuc(1→3)]βGlcNAc-O$(CH_2)_8COOCH_3$
Lewis^c-*O*gr	βGal(1→3)βGlcNAc-O$(CH_2)_8COOCH_3$
H type I-*O*gr	αFuc(1→2)βGal(1→3)βGlcNAc-O$(CH_2)_8COOCH_3$
Lewis^a-*O*gr	βGal(1→3)[αFuc(1→4)]βGlcNAc-O$(CH_2)_8COOCH_3$
Lewis^b-*O*gr	αFuc(1→2)βGal(1→3)[αFuc(1→4)]βGlcNAc-O$(CH_2)_8COOCH_3$
3NH_2FucGal-*O*-octyl	3-amino-3-deoxy-[αFuc(1→2)]βGal-O$(CH_2)_7CH_3$
D-Glc	D-glucose
D-Gal	D-galactose
D-GlcNAc	D-*N*-acetylglucosamine
D-GalNAc	D-*N*-acetylgalactosamine
D-Man	D-mannose
D-GlcA	D-glucuronic acid
D-Xyl	D-xylose
Neu5Ac	*N*-acetylneuraminic acid (sialic acid)
L-Fuc	L-fucose
UDP	uridine-5'-diphosphate
GDP	guanosine-5'-diphosphate
CMP	cytidine-5'-monophosphate

AIDS	acquired immune-deficiency syndrome
Asn	asparagine
BSA	bovine serum albumin
CAST	castanospermine
CE	capillary electrophoresis
Cer	ceramide
CGE	capillary gel electrophoresis
CIEF	capillary isoelectric focusing
CITP	capillary isotachophoresis
CMC	critical micelle concentration
CZE	capillary zone electrophoresis
D-MEM	Dulbecco's modified Eagle's medium
1-dNJ	1-deoxynojirimycin
DMF	dimethylformamide
E	electric field
E. coli	*Escherichia coli*
EDTA	ethylenediaminetetraacetic acid
ELISA	enzyme-linked immunosorbent assay
EOF	electroosmotic flow
ESI-MS	electrospray mass spectrometry
FucT	fucosyltransferase
GalT	galactosyltransferase
GC-MS	gas-liquid chromatography-mass spectrometry

GnT-V	*N*-acetyl glucosaminyltransferase V
α-Glc I	α-glucosidase I
H. pylori	*Helicobacter pylori*
HEPES	*N*-(2-hydroxyethyl)piperazine-*N'*-ethanesulphonic acid
HIV	human immune-deficiency virus
i.d.	inner diameter
Ig	immunoglobulin
IP	immunoprecipitation
k'	capacity factor
L_c	capillary length
L_d	length of capillary from injection end to detection end
LIF	laser-induced fluorescence
MAB	monoclonal antibody
MEKC	micellar electrokinetic capillary chromatography
MES	2-[*N*-morpholino]ethanesulfonic acid
^{1}H NMR	proton nuclear magnetic resonance
NMS	normal mouse serum
obs.	observed
PBS	phosphate-buffered saline (2.5 mM NaH_2PO_4, 7.3 mM Na_2HPO_4, 144 mM NaCl, pH 7.2)
PMSF	phenylmethylsulfonylfluoride
q	ion charge
r	ion radius

SDS	sodium dodecyl sulphate
SDS-PAGE	sodium dodecylsulphate-polyacrylamide gel electrophoresis
Ser	serine
SSEA	stage-specific embryonic antigen
t_0	migration time of analyte with *k'* equals zero
TFA	trifluoroacetic acid
Thr	threonine
t_M	migration time of analyte with *k'* equals values between zero and infinity
t_{mc}	migration time of micelles
TMR	tetramethylrhodamine
Triton X-100	t-octylphenoxypolyethoxyethanol
V_c	capillary volume
V_{inj}	injection voltage
V_{inj}	injection volume
V_{sep}	separation voltage
ζ	zeta potential
ε	dielectric constant
η	viscosity
ν_{eo}	electroosmotic velocity
ν_{ep}	electrophoretic velocity
μ_{eo}	electroosmotic mobility
μ_{ep}	electrophoretic mobility

List of Figures

Figure 1.1 Nine monosaccharide units commonly found in mammalian cells. 3

Figure 1.2 Generalized glycosyltranferase catalyzed reaction..... 4

Figure 1.3 Nine sugar-nucleotides commonly found in mammalian cells. 5

Figure 1.4 *N*-glycan core structures (core structures are boxed)..... 8

Figure 1.5 Examples of *O*-glycans with cores 1 to 7..... 9

Figure 1.6 Classification of glycolipids..... 11

Figure 1.7 Blood group antigens found on glycoproteins and glycolipids of mammalian cell surface. 13

Figure 1.8 Structures of some Lewis antigenic determinants with the type I backbone. 15

Figure 1.9 Structures of some Lewis antigenic determinants with the type II backbone. 16

Figure 1.10 Basic configuration of a capillary electrophoresis system. 24

Figure 1.11 Diagram of a capillary section and the ionic layer. 26

Figure 1.12 The elution window in MEKC 31

Figure 1.13 Separation process in MEKC 32

Figure 1.14 Steps in synthesizing TMR-labeled oligosaccharides..... 37

Figure 2.1 Transmission electron micrograph of unstained, unfixed *H pylori* strain UA 1182 incubated with anti-human CD15 IgM MAB and goat anti-mouse IgM-colloidal gold 10 nm particles. 58

Figure 2.2 Analysis of reaction mixtures from *H. pylori* UA 861 and UA 802 incubations by CE-LIF 62-63

Figure 2.3 Partial 500 MHz ^{1}H NMR spectra of reaction products. 65

Figure 3.1 Structures of inhibitors used in chapter 3..... 84

Figure 3.2 Partial 300 MHz ^{1}H NMR spectrum of TG-TMR in CD_3OD. 87

Figure 3.3 Confocal laser scanning microscopic image of HT29 cells incubated with TG-TMR. 88

Figure 3.4 Diglucose-TMR incubation data. 89

Figure 3.5 Electropherogram of TMR-labeled compounds obtained from CE separation of the contents of HT29 cells incubated with TG-TMR. 90

Figure 3.6 Electropherograms of TMR-labeled species obtained from CE separation of the contents of lysed HT29 cells. 91

Figure 3.7 Electropherograms of HT29 cell contents after incubation with inhibitors followed by TG-TMR..... 93

Figure 3.8 Inhibition of α-glucosidase I by a range of concentrations of 1-dNJ and CAST. 94

Figure 3.9 Electropherogram of HT29 cell contents after pretreatment with a mannosidase inhibitor, swainsonine, as negative control followed by TG-TMR incubation..... 95

Figure 3.10 Electropherogram of HT29 cell contents after incubation with a novel carbohydrate-based inhibitor, 1,5-trans-*C*-glucoside (5 mM) followed by TG-TMR.96

Figure 4.1 Structure of 3-amino-3-deoxy-[αFuc(1→2)]βGal-*O*-octyl. 109

Figure 4.2 Electropherograms of isolated cloned A-transferase after incubation with αFuc(1→2)βGal-OTMR and the inhibtory effects of 3-amino-3-deoxy-[αFuc(1→2)]βGal-*O*-octyl..... 116

Figure 4.3 Capillary electropherograms of the *in vitro* incubation experiment vs the intracellular uptake experiment (18 hr). 117

Figure 4.4 Electropherogram of FucGal-OTMR and its metabolites following incubation of HT29 cells for 2 days with 100 μM substrate. 119

Figure 4.5 Electropherograms of HT29 cell contents after incubation with 3-amino-3-deoxy-[αFuc(1→2)]βGal-*O*-octyl followed by αFuc(1→2)βGal-OTMR. 121

Figure 4.6 Inhibition of blood group A-transferase by a range of concentrations of 3-amino-3-deoxy-[αFuc(1→2)]βGal-*O*-octyl.. 123

Figure 4.7 Effects of 3-amino-3-deoxy-[αFuc(1→2)]βGal-*O*-octyl on glycosylation of the cell-associated glycoprotein gp140/α3β1 integrin with blood group A determinants 127

Figure 4.8 Solid-phase immunosorbent assay of BSA-glycan conjugates with MAB 8D5.. 129

Figure 5.1 Analysis by CE-LIF of reaction mixtures from the *E. coli* whole cell extract incubations..... 153

Figure 5.2 Analysis of reaction mixtures containing *H. pylori* α1,2 fucosyltransferase with 1.8 mM LacNAc and 0.1 M (**A**), 0.5 M (**B**), 1.0 M (**C**) lactose. 155

Figure 5.3 Analysis of reaction mixtures from the *E. coli* whole cell extract with 1.8 mM Lewis^x-TMR incubations by CE-LIF..... 156

Figure 5.4 Analysis of Le^a-TMR reaction mixtures from the *E. coli* whole cell extract incubations by CE-LIF 158

Figure 5.5 Analysis of Le^c-TMR reaction mixtures from the *E. coli* whole cell extract incubations by CE-LIF 159

Figure 5.6 Analysis of reaction mixtures from the myxoma virus enzyme extract with Le^x-TMR and Le^a-TMR incubations by CE-LIF 162

Figure 5.7 Analysis by CE-LIF of the Le^x-TMR reaction mixture from the neuraminidase incubations 164

Figure 5.8 Analysis by CE-LIF of the Le^a-TMR reaction mixture from the neuraminidase incubations 165

Figure 5.9 Electropherograms of the α2,3 sialylated Le^x-TMR one-pot synthesis after different times. 166

Figure 5.10 Electropherograms of the α2,3 sialylated Le^a-TMR one-pot synthesis after different times. 167

List of Tables

Table 1.1 Examples of recently developed carbohydrate drugs..... 21

Table 2.1 Cellular distribution of galactosyltransferase and fucosyltransferase activities in *H. pylori* extracts.. 60

Table 2.2 K_m values for the substrates of the membrane bound glycosyltransferases from *H. pylori* strains..... 69

Table 4.1 Structure of oligosaccharide moiety of BSA-glycan conjugates. 128

Table 5.1 Relative *H. pylori* α1,2 fucosyltransferase activity with each acceptors. 152

Table 5.2 Relative myxoma viral α2,3 sialyltransferase activity with Le^a- and Le^x-gr acceptors. 161

Table 5.3 Percent area of each peak in the electropherograms of the αNeu5Ac(2→3)Le^x-TMR one-pot synthesis. 169

Table 5.4 Percent area of each peak in the electropherograms of the αNeu5Ac(2→3)Le^a-TMR one-pot synthesis.. 170

List of Schemes

Scheme 2.1 Biosynthesis of Lewis^x in *H. pylori*. 68

Scheme 3.1 Metabolism of TG-TMR by glucosidases to DG-, MG-, and HO-TMR. 77

Scheme 4.1 Synthesis of A-trisaccharide from αFuc(1→2)βGal-*O*-octyl and UDP-GalNAc... 107

Scheme 5.1 Biosynthetic pathway of Lewis^y-OR involving α1,2 fucosyltransferase: comparison between the normal mammalian and the novel cloned *H. pylori* enzymes. 139

Scheme 5.2 Biosynthetic pathway of Lewis^b-OR involving α1,2 fucosyltransferase: comparison between the normal mammalian and the novel cloned *H. pylori* enzymes 140

Scheme 5.3 Biosynthetic pathway of sialylated Lewis^x-OR involving α2,3 sialyltransferase: comparison between the normal mammalian and the novel myxoma viral enzymes... 141

Scheme 5.4 Biosynthetic pathway of sialylated Lewis^b-OR involving α2,3 sialyltransferase: comparison between the normal mammalian and the novel myxoma viral enzymes..... 142

Chapter One

Introduction

1.1 Introduction to Glycobiology

1.1.1 Mammalian Monosaccharides

Carbohydrates of biological relevance usually consist of several covalently-linked monosaccharides and are referred to as oligosaccharides or glycans. There are nine commonly found monosaccharides in mammalian systems (**Fig. 1.1**), all of which have the D-configuration, except fucose, which has the L-configuration. Monosaccharides are normally linked together by a condensation reaction, in which the hydroxyl (-OH) group of C-1' of one monosaccharide is reacted with any available -OH, other than that at C-1, of a second monosaccharide. Since the configuration at C-1' can vary, then either an α- or β-glycosidic linkage can be formed. In an α-linkage, the hydroxyl group at C-1 of a D-sugar (in its $^4C_1$ chair conformation) is in the axial position, and in a β-linkage, it is in the equatorial position (as shown below).

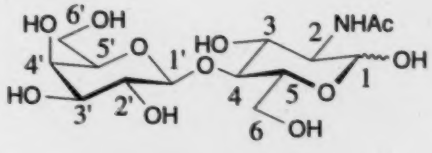

β-D-Gal(1→4)-D-GlcNAc

1.1.2 Glycosyltransferases

The enzymes directly involved in the biosynthesis of oligosaccharides are known collectively as glycosyltransferases. The basic reaction catalyzed is transfer of a sugar from an activated, high energy derivative (usually a sugar-nucleotide donor) to a suitable acceptor (**Fig. 1.2**; reviewed in 1, 2). The acceptor may be an asparagine

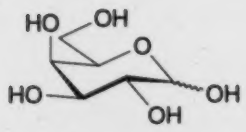

D-Galactose (D-Gal)

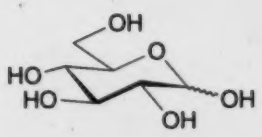

D-Glucose (D-Glc)

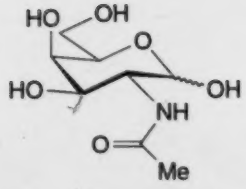

D-*N*-Acetyl galactosamine (D-GalNAc)

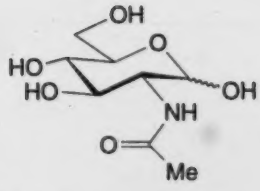

D-*N*-Acetyl glucosamine (D-GlcNAc)

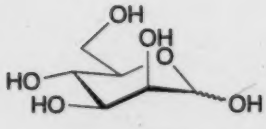

D-Mannose (D-Man)

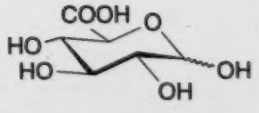

D-Glucuronic acid (D-GlcA)

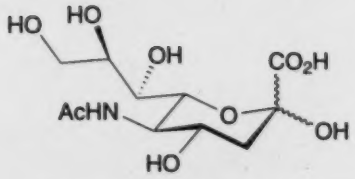

Sialic acid (Neu5Ac)

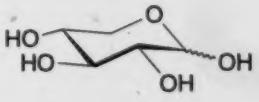

D-Xylose (D-Xyl)

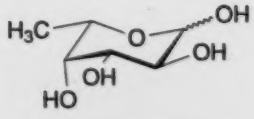

L-Fucose (L-Fuc)

Figure 1.1 Nine monosaccharide units commonly found in mammalian cells.

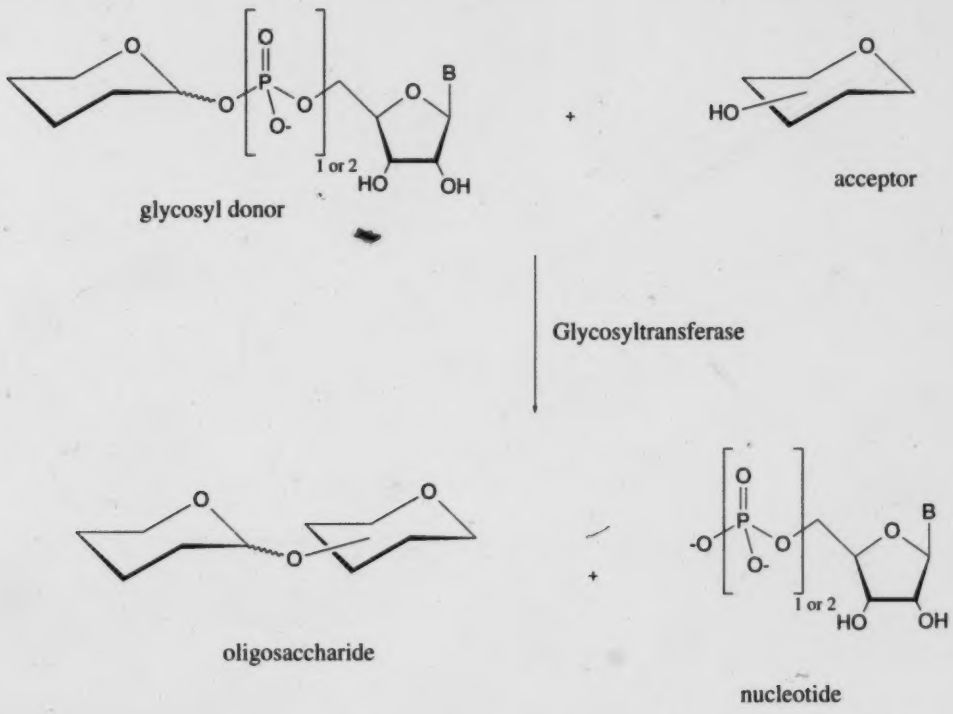

Figure 1.2 Generalized glycosyltranferase catalyzed reaction.

(in *N*-glycans), serine or threonine (in *O*-glycans), the primary -OH group of ceramide (in glycolipids), or an hydroxyl group of an incomplete carbohydrate sequence (in oligosaccharides; reviewed in 2-4). The nine most common sugar-nucleotide donors found in mammalian cells are shown in **Fig. 1.3**.

In general, glycosyltransferases exhibit strict specificities toward the nature of donors and acceptors. The product of the catalysis is highly regio- and stereo-specific. For example, the most extensively studied β1,4 galactosyltransferase (EC 2.4.1.38) from bovine milk (5) transfers a galactose to the 4-OH position of *N*-acetylglucosamine through a β-glycosidic linkage.

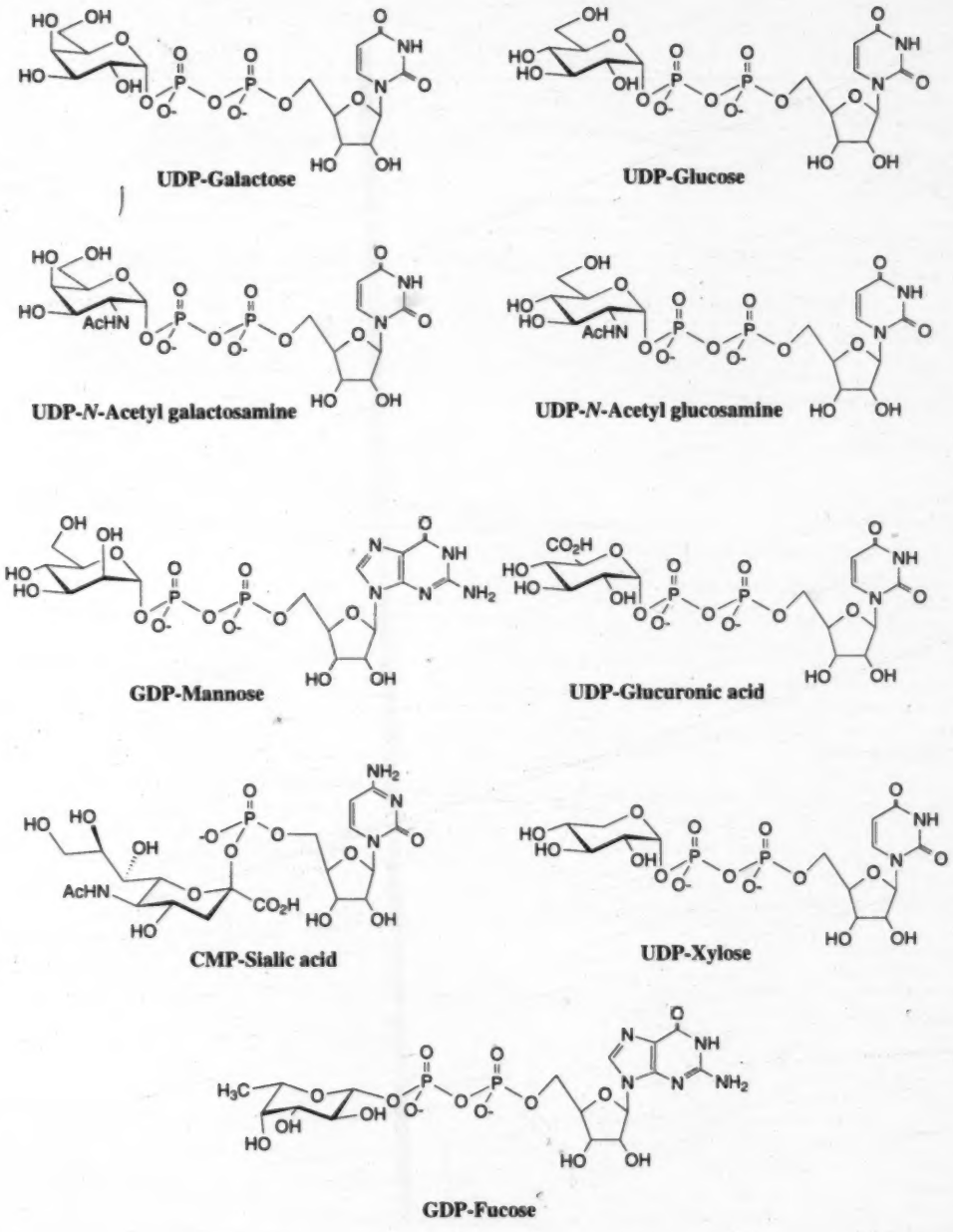

Figure 1.3 Nine sugar-nucleotides commonly found in mammalian cells.

It is estimated that one hundred or more glycosyltransferases are required for the synthesis of known carbohydrate structures on glycoproteins and glycolipids (1, 6). As indicated in reviews by Paulson and Colley (6) and more recently by Sears and Wong (7), all glycosyltransferases share a common domain structure in that they are Type II membrane proteins. They all have a short NH_2-terminal cytoplasmic tail, a signal-anchor domain (16-20 amino acids), and an extended, proteolytically-sensitive stem region followed by the large COOH-terminal catalytic domain (2, 6-8). The signal-anchor region acts as both uncleavable signal peptides and membrane-spanning regions (trans-membrane domain), and it is also responsible for orienting the catalytic domains of these membrane-bound glycosyltransferases within the lumen of the Golgi compartments, compared to that of the Type I membrane-proteins (2). The soluble forms of glycosyltransferases are thought to result from proteolytic cleavage of the catalytic domain from the trans-membrane domain (9, 10).

1.1.3 Types of Glycoconjugates

1.1.3.1 Glycoproteins

About 80% of all proteins, with exceptions such as bovine serum albumin (BSA) and all cytoplasmic proteins, are glycosylated. The interest in the effects of glycosylation, and thus in structural analysis of carbohydrates attached to proteins, has increased greatly during the past decade (3, 7). This has resulted in an accumulation of a wealth of information concerning the chemical structures of carbohydrates. Glycoproteins can be classified into two main categories, *N*-glycans and *O*-glycans. Proteoglycans are proteins that contain one or more polysaccharide

chains carrying high negative charge and molecular weight, and are not discussed in this thesis (reviewed in 3, 11).

1.1.3.1.1 *N*-Glycans

N-linked glycans in eukaryotes fall into three categories (3, 7, 12) shown in **Fig. 1.4**, with the core structures in boxes. The core structure in each category represents the combination of oligosaccharides that is the core for further elaboration. All three classes contain the chitobiose core, βGlcNAc(1→4)βGlcNAc, which is covalently linked to an asparagine residue on a protein structure with the sequence Asn-X-Thr/Ser (7), where X is any amino acid.

The high mannose type consists almost entirely of mannose residues, with a variety of linkages, and the core structure is a heptasaccharide (**Fig. 1.4**). Variations are formed by the locations and the numbers of up to four αMan(1→2) residues linked to the nonreducing end of the heptasaccharide core.

The complex type *N*-glycans consist of a core pentasaccharide (the trimannosyl core) with variations resulting from proximal GlcNAc substitution with a fucose, and β-Man substitution with a bisecting GlcNAc. The outer chain moieties are extended typically with Gal and GlcNAc (12, 13), and are capped with Gal, GlcNAc, Fuc, and/or sialic acid. The additions of these sugar units show very high variations, which will be discussed in **section 1.1.4**.

The hybrid type *N*-glycans exhibit structural features common to both the high mannose and complex types. They show the characteristics of high mannose glycans

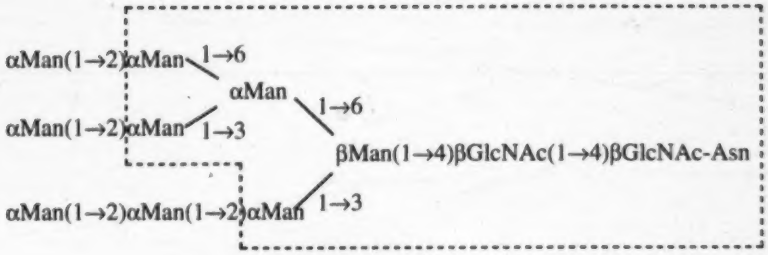

High Mannose

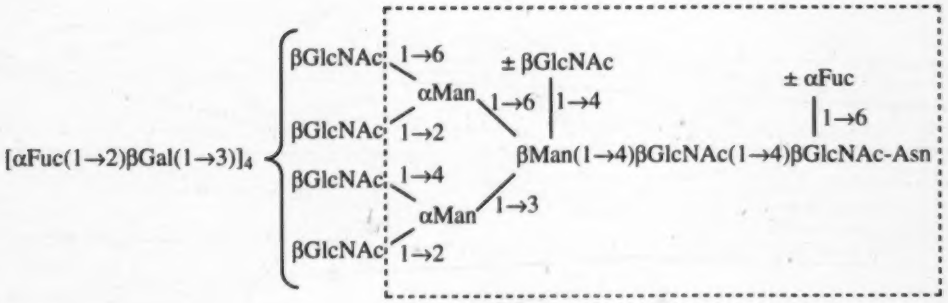

Complex

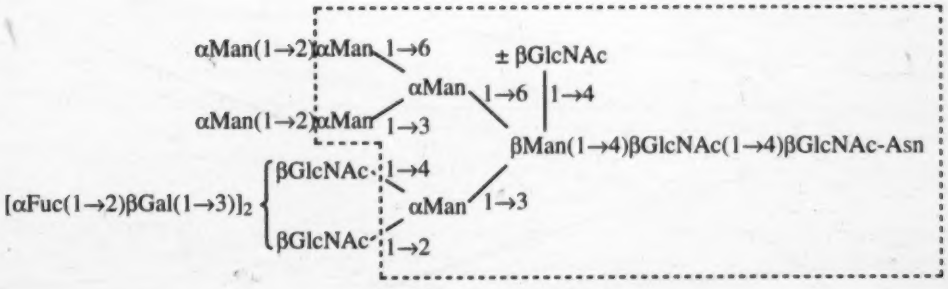

Hybrid

Figure 1.4 *N*-glycan core structures (core structures are boxed). Adapted from Kobata and Takasaki (3).

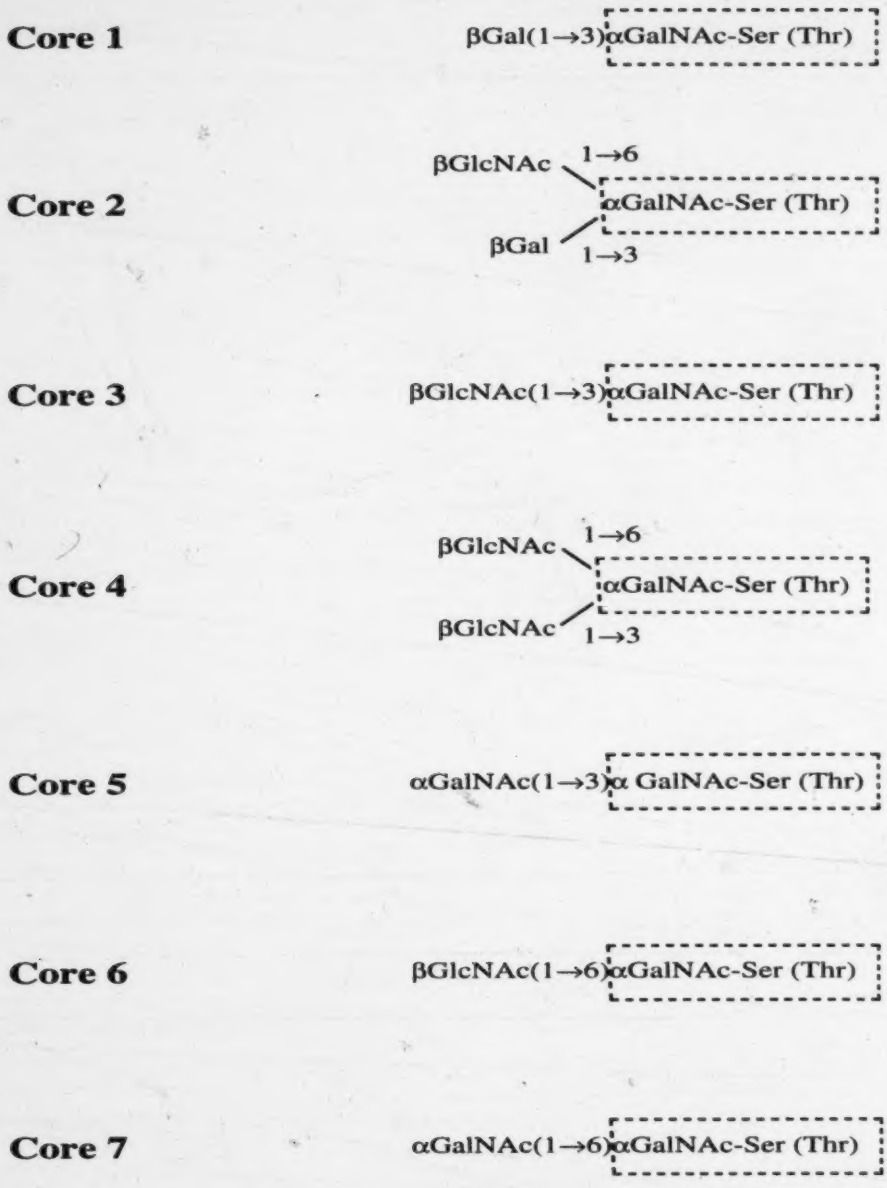

Figure 1.5 Examples of *O*-glycans with cores 1 to 7. Adapted from Sears and Wong (7). Core structures [αGalNAc-Ser (Thr)] are boxed.

on the mannose α1,6 branch, and characteristics of the outer chain moieties of the complex type *N*-glycans expressed on the mannose α1,3 branch.

The three types of *N*-glycans are closely related in their biosynthetic route: high mannose type glycans are processed to hybrid types and then to complex type glycans (2). Therefore, structural variations are mainly formed in the outer chain moieties of complex type glycans.

1.1.3.1.2 *O*-Glycans

O-Glycans, also known as mucin-type glycans, are linked via an αGalNac at the reducing end, to serine or threonine residues of mucinous glycoproteins, secreted serum glycoproteins, and cell surface membrane-bound glycoproteins (core structures in boxes in **Fig. 1.5**). They are less easy to categorize due to the high degree of variation in structure as extensive studies have revealed that a number of different structures are present in these glycans (2, 7). These glycans are grouped into seven classes according to their core structures (**Fig. 1.5**).

1.1.3.2 Glycolipids

Glycolipids found in mammalian cells mostly occur as glycosphingolipids, which are composed of a sphingosine moiety, a fatty acid, and a sugar (see **Fig. 1.6**). The hydrophobic moiety, shown on the top of **Fig. 1.6**, is called a ceramide. The

R = ceramide =

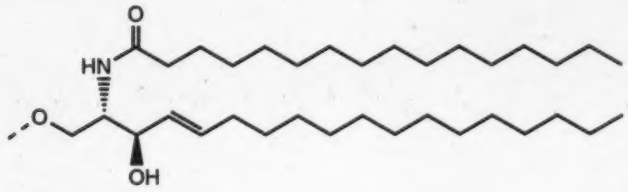

Lacto-series glycolipids type I βGal(1→3)βGlcNAc(1→3)βGal(1→4)βGlc-R

Lacto-series glycolipids type II βGal(1→4)βGlcNAc(1→3)βGal(1→4)βGlc-R

Globo-series glycolipids βGalNAc(1→3)αGal(1→4)βGal(1→4)βGlc-R

Ganglio-series glycolipids βGal(1→3)βGalNAc(1→4)βGal(1→4)βGlc-R

Figure 1.6 Classification of glycolipids. The skeletal structure of each series is boxed. The examples shown for each series are: lacto-series type I, lactotetraosylceramide; lacto-series type II, neolactotetraosylceramide; globo-series, globotetraosylceramide; ganglio-series, gangliotetraosylceramide. Adapted from Hakomori (14).

oligosaccharide chain is synthesized by the stepwise addition of sugars to a ceramide. Glycolipids can be categorized into 4 major classes: the lacto-series type I and type II, the globo-series, and the ganglio-series. They are synthesized by addition of a glucose at the reducing end, with further addition of a galactose through a β1,4 linkage. The lacto-series (type I and type II) of glycolipids contains structural moieties similar to the outer chain moieties of both complex type *N*-glycans and *O*-glycans. These are the blood group antigenic determinants found on glycoproteins and glycolipids.

1.1.4 Blood Group Antigenic Determinants

Extensions of the mammalian core structures of *N*-, and *O*-glycans and glycolipids most commonly ends in type I (βGal(1→3)βGlcNAc) or type II (βGal(1→4)βGlcNAc) saccharides that can be capped with Fuc, GalNAc, Gal, or Neu5Ac with a variety of linkages. **Fig. 1.7** depicts the blood group O(H), A, and B antigenic determinants, found on both the type I and type II backbones. For example, blood group O(H) determinant can be in the type I form, αFuc(1→2)βGal(1→3)βGlcNAc, or the type II form, αFuc(1→2)βGal(1→4) βGlcNAc. The blood group A antigen is formed by the transfer of a GalNAc by α1,3 *N*-acetylgalactosaminyltransferase, also known as blood group A-transferase (EC 2.4.1.40), to the O(H) antigen. Similarly, the B antigen is formed by the transfer of a galactose by α1,3 galactosyltransferase (blood group B-transferase, EC 2.4.1.37) to the O(H) antigen.

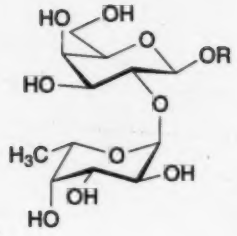

O (H) antigen

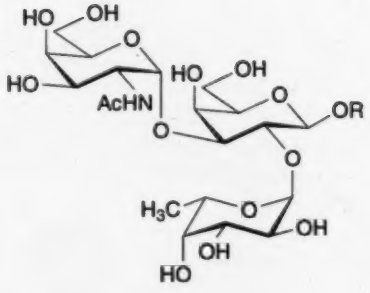

Blood group A antigen

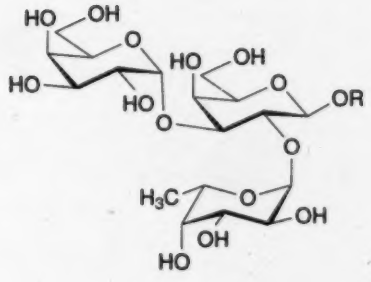

Blood group B antigen

Figure 1.7 Blood group antigens found on glycoproteins and glycolipids of mammalian cell surface. R represents GlcNAc residue of glycoproteins or glycolipids.

The histo-blood group ABO(H) antigens are present on the surface of red blood cells and are largely responsible for failure of mismatched blood transfusions. Blood group A individuals express the A-transferase to form the A determinant, whereas blood group B individuals express the B-transferase to form the B determinant. Blood group O individuals do not express either enzyme, and AB individuals express both (15). These ABO carbohydrate antigens occur on other cell types and in soluble form in the cytoplasm (16). They are also important in cell development, cell differentiation, and oncogenesis (17-19).

The elaboration of the type I backbone (βGal(1→3)βGlcNAc, or Lewis^c) with the addition of fucose and sialic acid by a variety of fucosyltransferases and sialyltransferases in a concerted manner, results in the type I series Lewis antigenic determinants (**Fig. 1.8**). H type I is the result of the transfer of a Fuc to the 2-OH of Gal in Lewis^c by an α1,2 fucosyltransferase. Addition of α-Fuc to the 4-OH of the GlcNAc residue by an α1,4 fucosyltransferase forms Lewis^a, while Lewis^b is the difucosylated product of the sequential addition by α1,2 fucosyltransferase followed by α1,4 fucosyltransferase. α2,3 Sialyltransferase adds sialic acid to the 3-OH of Gal to form sialyl Lewis^c. By a combination of fucosylation and sialylation, sialyl Lewis^a is formed.

The type II backbone chain (βGal(1→4)βGlcNAc, or LacNAc) is elaborated upon in a manner similar to that described above for the type I backbone (**Fig. 1.9**). Addition of α-Fuc residues to the Gal and/or the GlcNAc residue of LacNAc by different linkages in a sequential manner, produces the following blood group antigenic structures: H type II (αFuc(1→2)βGal(1→4)βGlcNAc), Lewis^x

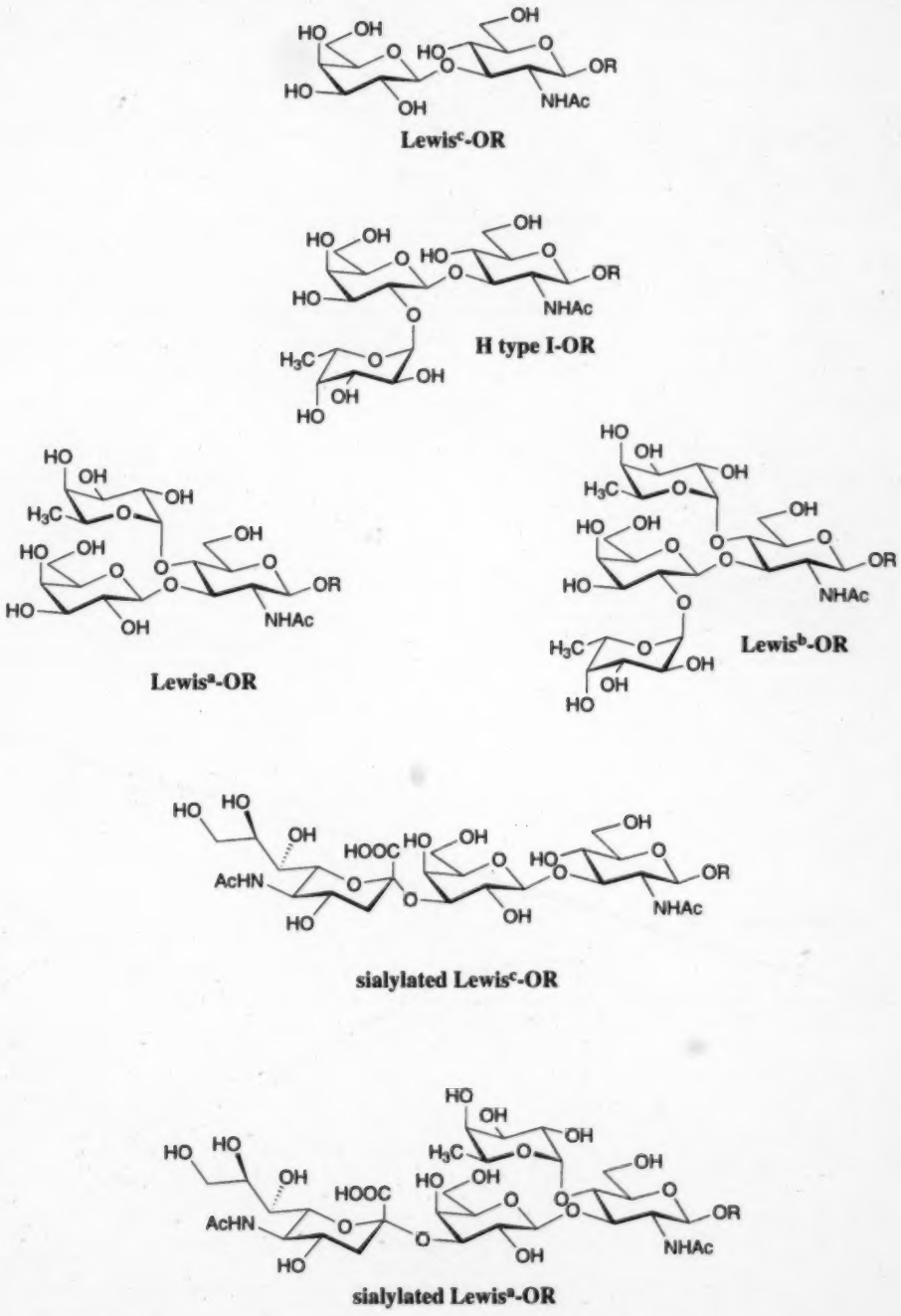

Figure 1.8 Structures of some Lewis antigenic determinants with the type I backbone.

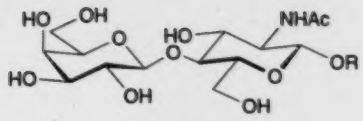

LacNAc-OR

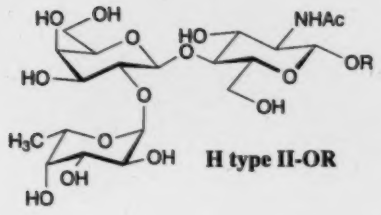

H type II-OR

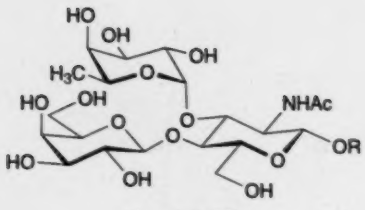

Lewis^x-OR

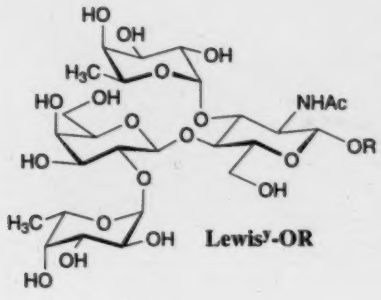

Lewis^y-OR

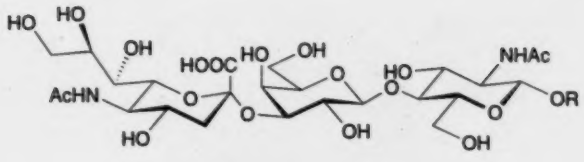

sialylated LacNAc-OR

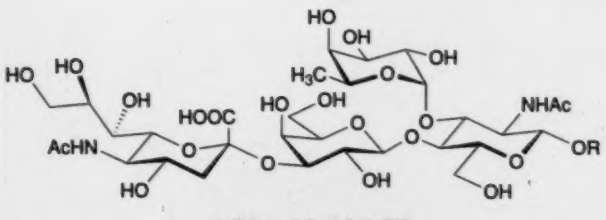

sialylated Lewis^x-OR

Figure 1.9 Structures of some Lewis antigenic determinants with the type II backbone.

(βGal(1→4)[αFuc(1→3)]βGlcNAc), and Lewis^y (α Fuc(1→2)βGal(1→4) [αFuc(1→3)]βGlcNAc). Sialylation of LacNAc forms sialyl LacNAc, and when this is followed by the transfer of Fuc by α1,3 fucosyltransferase, forms sialyl Lewis^x.

1.1.5 Role of Oligosaccharides in Mammalian Cells, and Their Association with Oncogenesis

Cell surface oligosaccharides have been implicated in many physiological and pathological phenomena (20). They can function in biological recognition processes by serving as receptor binding sites for lectins (reviewed in 21-23), bacteria (24, reviewed in 25), viri (26, 27) such as HIV (reviewed in 28), parasites (29), antibodies (30), toxins (31), hormones (32), and enzymes (33). They also play a role in cell-cell interactions and intracellular signaling as reviewed by Hakomori and Igarashi (34), and in adhesion of leukocytes to vascular endothelium during early stages of inflammation (35).

These antigenic structures are also cell- and tissue-specific. Some are related to processes of differentiation, such as in the case where HL60 (undifferentiated promyelocytes; 36) cells are induced to differentiate to granulocytes, with a resulting decrease in G_{M3} (Neu5Ac(2→3)βGal(1→4)βGlc-Cer), but which increases again upon differentiation to macrophages (37). Some are related to development (ontogenesis). For example, Lewis^x is a stage-specific embryonic antigen (SSEA-1) which is found in the eight-cell stage of a mouse embryo (38-40). Increased Lewis and sialylated Lewis structure expressions are involved in malignant transformation (oncogenesis;

41-45, reviewed in 46, 47) and β1,6-linked branching of the complex type *N*-glycans (that is βGlcNAc(1→6)αMan(1→6)βMan-) are associated with metastasis (48, 49).

These changes in glycosylation pattern have been associated with altered levels of the relevant glycosyltransferases (50). Concentrations of *N*-acetyl glucosaminyltransferase-V (GnT-V) have been shown to be elevated in tumour cells, explaining the increase in β1,6-linked branching of the complex type *N*-glycans (48, 51). In addition to increased levels of GnT-Vs, the increased levels of α2,3 sialyltransferases and α1,3 fucosyltransferase found in malignant tumour cells have been described as one of the most reproducible correlates to oncogenesis in cells (51, 52).

Some strains of *Helicobacter pylori*, a human pathogen associated with gastritis, gastric and duodenal ulcers and gastric adenocarcinoma (53), were first reported by our laboratory to express β1,4 galactosyltransferase and α1,3 fucosyltransferase activities (54), and to express Lewis^x on the cell surface and flagella sheaths (55). This is thought to protect the pathogens from recognition by the immune system of the mammalian host cells.

1.1.6 Inhibition of Glycosylation

In many of the diseases described above, specific inhibition of key glycosyltransferases may be of therapeutic benefit. For example, since the increased branching in *N*-glycans of tumour cells correlates with metastatic potential, selective inhibition of GnT-V might help prevent metastasis. Similarly, inhibition of α1,3 fucosyltransferase might be of benefit in the treatment of some cancers by reducing

production of the Lewis and sialylated Lewis blood group structures observed in tumours. The potential of this approach has been demonstrated by two main classes of glycosylation inhibitors; tunicamycin, which inhibits UDP-GlcNAc: dolichylphosphate GlcNAc-1-phosphotransferase (56) and glycosidase inhibitors (reviewed in 57, 58), such as swainsonine (α-mannosidase inhibitor), nojirimycin and castanospermine (α-glucosidase I inhibitors). Unfortunately, these inhibitions are non-specific and are cytotoxic since they inhibit biosynthesis of all *N*-glycans.

One of the main objectives in our laboratory is to use basic mechanistic enzymology to design and study specific inhibitors of glycosylation that target a unique perturbation in the latter stages of biosynthesis of cell surface glycolipids and glycoproteins. Examples of enzymes on which such studies have been performed in our laboratory include α1,3 *N*-acetylgalactosaminyltransferase (59, 60), α1,2 fucosyltransferase (61) and GnT-V (62, 63). As reviewed by McAuliffe and Hindsgaul (64), a number of novel carbohydrate drugs have been recently released on the market, and many more are in the latter stage of evaluation (**Table 1.1**). It is interesting that the list does not include any glycosyltransferase inhibitors; while many such compounds are effective inhibitors *in vitro*, they are far less efficacious *in vivo*, due both to poor stability and to extremely low bioavailability.

Until recently, little mechanistic work was possible on glycosyltransferases due to the limited availability of substrates, problems associated with isolation of low amounts of glycosyltransferases from natural sources, very little crystal structure information (65, 66), and lack of sensitivity with respect to the detection of products with conventional assay methods (67-69). In addition, carbohydrates are not

naturally chromophoric, a property which would facilitate detection. An ultra-sensitive assay for glycosyltransferases is thus required which will allow separation and detection of oligosaccharides, labeled with a chromophore or fluorophore. Through a collaboration between M. M. Palcic, O. Hindsgaul, and N. J. Dovichi, an assay for fucosyltransferases was developed which used fluorescently labeled oligosaccharide substrates. This method uses capillary electrophoresis (CE) to separate the substrate from the product(s), prior to detection of product with laser-induced fluorescence (LIF) which can achieve a detection limit of 100 molecules of products (70).

In this thesis, CE-LIF was used to detect low levels of glycosyltransferase activities from the bacterium, *Helicobacter pylori*, this being the first report of mammalian-like glycosyltransferases in *H. pylori*. The method was also used to detect and identify low levels of products synthesized from genetically engineered enzymes (*H. pylori* α1,2 fucosyltransfase and myxoma viral α2,3 sialyltransferase), and to develop an intracellular inhibition assay for specific α-glucosidase I inhibitors, which was then used to examine a potential blood group A-transferase inhibitor.

Table 1.1 Examples of recently developed carbohydrate drugs.

Substance	Target	Structure	Company	Status	Refs
Acarbose	Diabetes	Maltotetrose analogue	Bayer AG	Released	71
Acemannan	Infection	Acelylated β1,4-D-manan	Carrington Labs	Released	72,73
Cylexin®	Reperfusion injury	Sialylated Lewis^x	Cytel	Phase II	74,75
Cordox®	Asthma/ Reperfusion	Fructose-1,6-diphosphate	Cypros	Phase II	76
GBC-590	Cancer	Pectin-based oligosaccharide	SafeScience	Phase II	77
MDL-24,574A	HIV/AIDS	Castanospermine analogue	Hoeschst Roussel	Phase II	78
NE-0080	*H. pylori* infection	Oligosaccharide	Neose Tech.	Phase II	79,80
Relenza™	Influenza	Sialic acid analogue	Biota/Glaxo Wellcome	FDA pending	81
SYNSORB PK™	*E. coli* O157:H7	Oligosaccharide conjugate	SYNSORB Biotech	Phase II	82-84
Theratope®	Metastatic cancer	Sialyl Tn antigen conjugate	Biomira/ Chiron	Phase III	85

1.2 Capillary Electrophoresis

The term, capillary electrophoresis (CE), encompasses a family of related techniques that employ capillaries of 10-200 μm inner diameter (i.d.) to perform high efficiency separations of molecules based on differences in their electrophoretic mobilities. These separations are facilitated by an externally applied electric gradient (as high as 500 V/cm), which may generate electroosmotic flow of buffer solutions within the capillary. Use of narrow-bore capillaries facilitates the dissipation of heat generated from the high voltage applied across the two electrodes. Capillaries of 10-75 μm i.d. have a large surface area to volume ratio, thus providing more efficient heat dissipation to prevent joule heating (heating of a conducting medium as current flows through it). This leads to improved resolution as a result of decreased band broadening caused by fluid convection inside the capillary. Other advantages of using small diameter capillaries include a requirement for minute amounts of sample, and reduced consumption of reagents.

The main modes of CE include capillary zone electrophoresis (CZE), capillary gel electrophoresis (CGE), capillary isoelectric focusing (CIEF), capillary isotachophoresis (CITP), and micellar electrokinetic capillary chromatography (MEKC). The basic principle of CZE will be covered and details of MEKC will be discussed in this section as this is the mode of CE used in experiments described in this thesis.

1.2.1 Principles of Capillary Zone Electrophoresis

Capillary zone electrophoresis (CZE), often referred to as free solution capillary electrophoresis, is the simplest and most commonly used form of CE. The addition of specialized reagents to the separation buffer readily allows the same instrument to be used with other modes: MEKC (surfactants), CIEF (ampholytes), or CGE (unpolymerized or polymerized sieving matrix). Therefore, a discussion of CZE is required to understand the basic principle governing the separations in all these modes.

The basic instrumental configuration for CE is relatively simple. The components include a controllable high voltage power supply, a fused silica capillary, two buffer reservoirs that can accommodate both the capillary and the two electrodes connected to the power supply, and a detector (**Fig. 1.10**). The capillary is filled with the appropriate separation buffer at the desired pH and a sample plug is introduced hydrodynamically (pressure-driven) or electrokinetically (voltage-driven) at the inlet. When voltage is applied to the capillary, the ionic species in the sample plug migrate with an electophoretic mobility determined by their charge and mass. The analytes are separated and will eventually pass the detector where information is collected and stored in a data acquisition system.

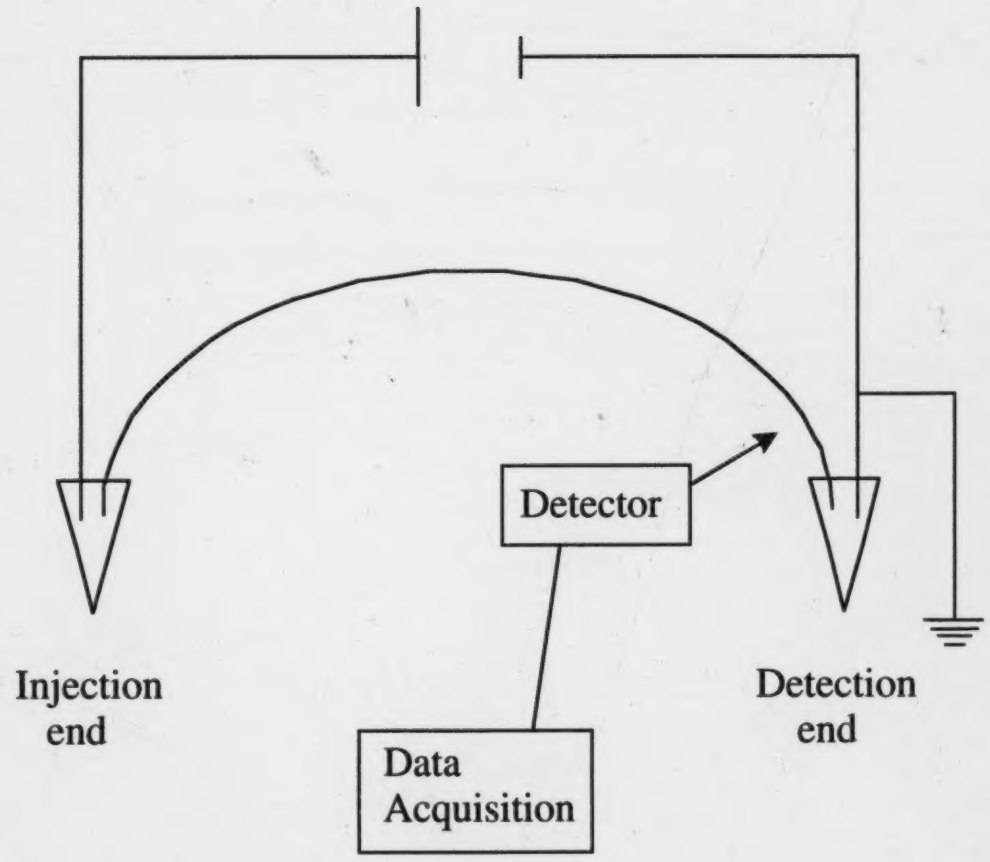

Figure 1.10 Basic configuration of a capillary electrophoresis system.

1.2.1.1 Electroosmotic Flow and Zeta Potential

If an electric field is applied tangentially along a buffer-filled capillary, there are two important electrokinetic phenomena which occur (86-90): electrophoresis and electroosmosis. Electrophoresis is the movement of a *charged surface* plus attached material (dissolved or suspended material) relative to stationary liquid by an electric field. Electroosmosis is the movement of *liquid* relative to a stationary charged surface (fused silica capillary wall) by an applied electric field. The pressure necessary to counterbalance electroosmotic flow (EOF) is termed the electroosmotic pressure. EOF (91) is pH dependent because it governs the degree of ionization of the silanol groups on the capillary wall. The equilibrium between SiOH and SiO^- lies towards SiO^- at higher pH values, resulting in increased EOF. If EOF is greater in magnitude and opposite in direction to the electrophoretic mobilities of all anions in the buffer, than all ions will migrate in the same direction and reach the detector in the following order: cations, neutrals, anions.

As shown in the expanded region of the inner wall of a capillary (**Fig. 1.11A**), the ionized silanol groups will attract cationic species from the buffer. The double layer that is formed has a positive potential that decreases exponentially as the distance increases from the surface of the wall into the diffusive layer (**Fig. 1.11B**). Counterions to those ionized silanol groups are essentially stagnant and form a plane of sheer adjacent to the capillary wall. The potential at the plane of sheer is termed the zeta potential (ζ), and is given by:

$$\zeta = \frac{4\pi\eta\mu_{eo}}{\varepsilon} \qquad (1.1)$$

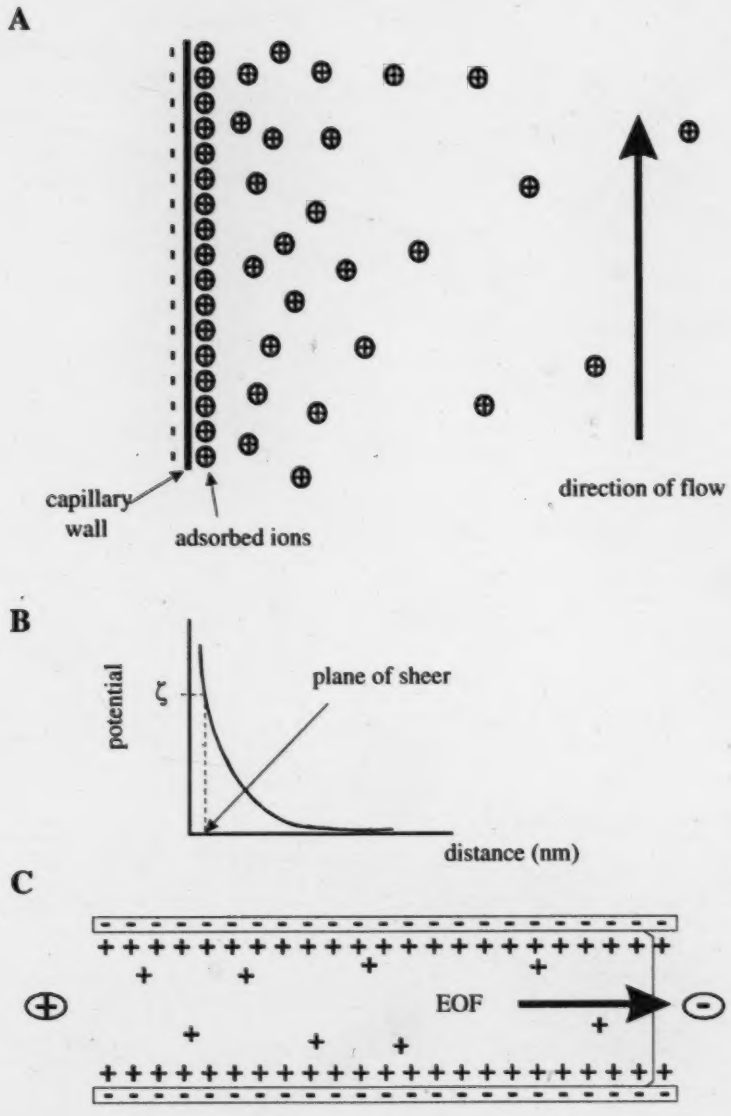

Figure 1.11 Diagram of a capillary section and the ionic layer. **(A)** shows the region near the capillary wall and the double layer formed critical in generating electoosmotic flow. **(B)** shows the ζ potential at the plane of sheer. **(C)** illustrates the generation of EOF in a capillary upon voltage application and the flat elution profile.

where η is the viscosity, ε is the dielectric constant of the solution, and μ_{eo} is the electoosmotic mobility.

When a voltage is applied across the capillary, cations in the diffusive layer adjacent to the plane of sheer migrate in the direction of the cathode, carrying water with them. The result is a net flow of buffer solution in the direction of the negative electrode. The electoosmotic velocity (ν_{eo}) is calculated by:

$$\nu_{eo} = \mu_{eo}E \tag{1.2}$$

where E is the electric field.

Electroosmotic velocity (ν_{eo}) is highest at the diffusive portion of the plane of sheer where μ_{eo} is largest (ζ is maximum). Since the flow originates from near the wall of the capillary, the flow profile is flat at the detection end (**Fig. 1.11C**).

1.2.1.2 Electrophoretic Mobility

A charged particle in a solution will become mobile when placed in an electric field. The velocity, ν_{ep}, acquired by the solute is the product of μ_{ep}, the electophoretic mobility, and the applied field, E.

$$\nu_{ep} = \mu_{ep}E = \mu_{ep}(V/L_c) \tag{1.3}$$

where V is the applied voltage and L_c is the length of the capillary.

The electrophoretic mobility, μ_{ep} is given by:

$$\mu_{ep} = \frac{\nu_{ep}}{E} = \frac{q}{6\pi\eta r} \qquad (1.4)$$

where r is the radius and q (+/- value) is the charge of the ion.

From Eq.1.4, it is evident that the ion mobility is a property of both the charge and size: a small, highly charged particle will have a high mobility, while a large, minimally-charged particle will have a low mobility. The observed velocity, ν_{ep}(obs.) of a particle (charged or neutral) is given by:

$$\nu_{ep}(\text{obs.}) = (\mu_{ep} + \mu_{eo})\,(V/L_c) \qquad (1.5)$$

and the time (t_M) needed for the particle to migrate from the injection end to the detection end is:

$$t_M = \frac{L_c^2}{(\mu_{ep} + \mu_{eo})V} \qquad (1.6)$$

The migration time (t_M) is proportional to the square of the length of the capillary (for post-column detection) and inversely proportional to the sum of the electrophoretic and electroosmotic mobilities. It can be noted from Eq. 1.5 & Eq. 1.6 that if μ_{eo} is greater in magnitude than μ_{ep} of all particles, charged or neutral, all analytes will migrate to the cathode. The neutral species are being carried by electroosmosis and are not separated by capillary zone electrophoresis alone.

1.2.2 Principles of MEKC

To perform separations of neutral analytes by CE, Terabe and coworkers (92, 93) introduced electrokinetic chromatography (EKC). MEKC (94) is one mode of EKC where surfactants (such as SDS) are added to the buffer at or above the critical micelle concentration (CMC). The micelles in the buffer act as pseudo-stationary phase in a manner similar to reverse-phase liquid chromatography, in which partition occurs between the stationary phase and the mobile phase. The analyte (small charged or neutral molecules) such as oligosaccharides can be separated based on their partition between the micelles and the buffer.

A few recent reviews have been able to show the broad applications of MEKC in the separation of proteins and peptides (95), drug analyses (96-98), carbohydrates (99), and coupling to mass spectometry (100).

1.2.2.1 Parameters Governing MEKC

1.2.2.1.1 Micelle Formation

In MEKC, sodium dodecyl sulphate (SDS) is the most commonly used surfactant. SDS forms micelles at or above the CMC (7-10 mM) with an aggregation number of 62 at 20-25°C (101). The micelles are negatively charged on the surface facing the bulk solution. Generally the electrophoretic mobility (μ_{ep}) of the SDS micelles is less than the electroosmotic mobility (μ_{eo}), and they move slowly toward the cathode. For neutral molecules, an effective micellar separation occurs in the region between the electroosmotic flow time, t_0, and the micelle migration time, t_{mc}. This region is often referred to as the migration time window (**Fig. 1.12**) in MEKC.

The migration velocity of the analyte thus depends on the distribution coefficient between the micellar and the aqueous phases. The greater the percentage of analyte that is distributed into the micelle, the slower it migrates.

1.2.2.1.2 Capacity Factor

This percentage of analyte partitioning into the micelles is termed similar to that of chromatography as the capacity factor (k'):

$$k' = \frac{n_{mc}}{n_{aq}} \tag{1.7}$$

where n_{mc} and n_{aq} are the amount of the analyte incorporated into the micelle and that in the aqueous phases, repectively. We can obtain the relationship between the capacity factor and the migration times (t_M) as:

$$t_M = \frac{1 + k'}{1 + (t_0/t_{mc})\, k'} t_0 \tag{1.8}$$

From Eq. 1.8, the migration time of the analyte equals t_0 when k' equals zero, or when the analyte does not partition into the micelle at all. The migration time becomes t_{mc} when k' is infinity or when all the analyte is incorporated into the micelle and no analyte is present in the aqueous phase. Neutral analytes which partition between the two phases will migrate at an intermediate time, t_M, within the migration time window (**Fig. 1.12**). This separation process is illustrated in **Fig. 1.13**.

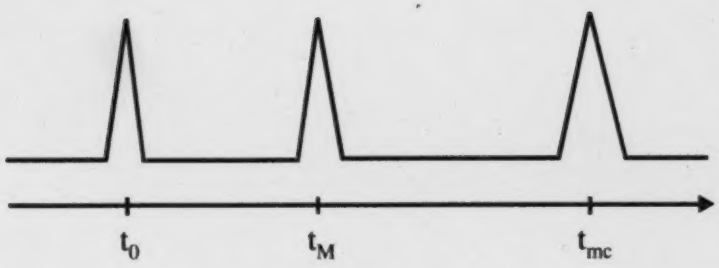

t_0	k' = zero
t_M	zero < k' < infinity
t_{mc}	k' = infinity

Figure 1.12 The elution window in MEKC.

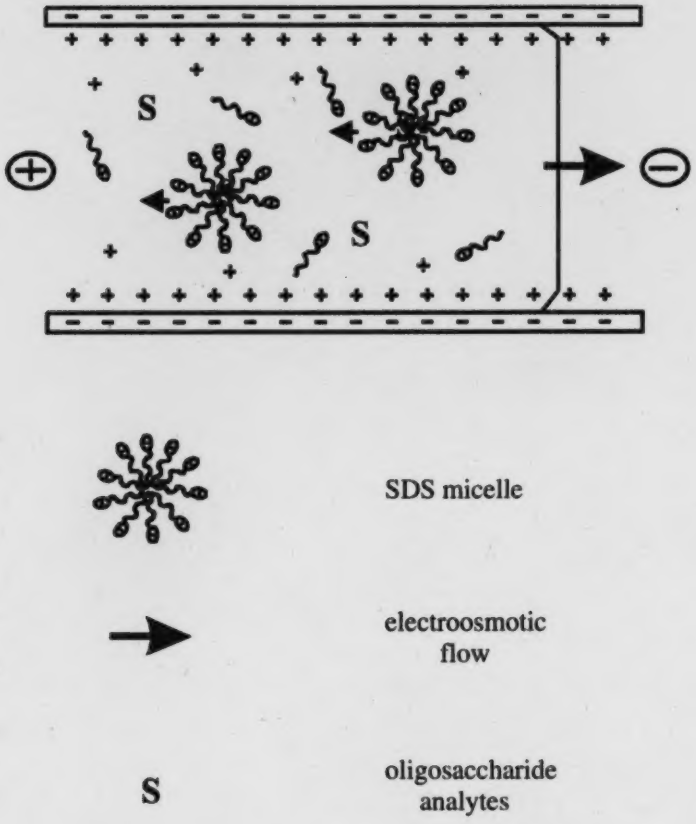

Figure 1.13 Separation process in MEKC. Analytes separate according to their partition between the buffer (mobile phase) and the SDS micelles (peudo-stationary phase).

1.2.2.1.3 Borate Buffer Complexation with Oligosaccharides

The most commonly used background electrolytes for the electrophoretic separations of carbohydrates are borate buffers. Use of boric acid to determine the configuration of carbohydrates was described by Böeseken in 1949 (102). Borate complexes with polyhydroxy compounds (such as saccharides) in general, both cyclic and non-cyclic. The complexations can be formulated as follows:

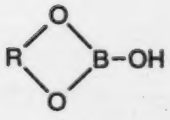

[1]

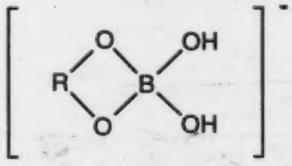

[2]

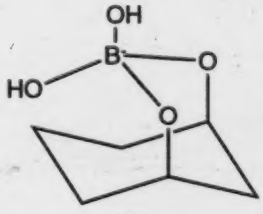

[5]

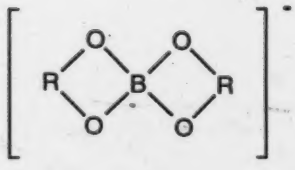

[3]

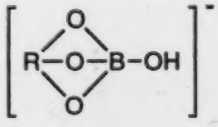

[4]

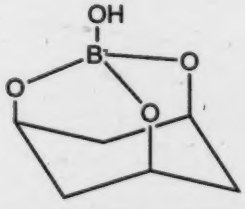

[6]

where ionic species, non-cyclic complexes [2], [3], [4] and cyclic complexes [5], [6], migrate during electrophoresis (103, 104). These borate complexes effectively changed the capacity factor (k') of each oligosaccharide and, therefore, improve resolution in MEKC.

1.2.3 Sample Injection

There are 2 principal methods for introducing sample into the capillary column: hydrodynamic injection and electrokinetic injection. Hydrodynamic injection is driven by the bulk movement of the buffer to introduce sample into the capillary. This bulk movement is based on the pressure difference between the sample reservoir and the waste reservoir and is dependent on the buffer density, capillary radius, and most of all the height difference between reservoirs. Hydrodynamic injection can be used provided that the inner diameter of the capillary is not so small that it distorts the injection front seriously (105).

In experiments described in this thesis, electrokinetic injection, sometimes known as electromigration, was used. Samples are injected into the capillary by applying voltage to the sample vial for a very short period of time (1-5 sec). The amount of each analyte injected depends on the electrophoretic mobility of each analyte. This effect causes a distortion in the ratio of peak areas for species having different mobilities (105). The injection volume (V_{inj}) of an individual analyte can be calculated from Eq. 1.9:

$$V_{inj} = V_c \left(\frac{V_{inj}}{V_{sep}}\right)\left(\frac{t_{inj}}{t_M}\right) \qquad (1.9)$$

where V_c is the total volume of the capillary, V_{inj} and V_{sep} are the injection and separation voltages, respectively, and t_{inj} and t_M are the injection time and migration time of the analyte.

1.2.4 Sample Detection

Sample detection can be done on-column or post-column. Most commercially-available CE machines are equipped with on-column detection where a detection window is burned in the capillary. The detection distance from the injection end to the detection end is termed L_d, this value being less than L_c. The detection methods used include UV absorption (106), fluorescence (107), electrochemical detection (108), and photo-thermal effect (109).

1.2.4.1 Post-Column Laser-Induced Fluorescence Detection

The CE instrument used throughout this thesis uses post-column laser-induced fluorescence detection to monitor the separation of oligosaccharides in the capillary. With on-column detection, fluorescence reflection and refraction at the glass capillary wall cause high background signals, and thus lower the signal-to-noise ratio. Dovichi and Cheng (110, 111) reported the use of a post-column quartz sheath-flow cuvette to improve detection by decreasing band-broadening and reflection. Moreover, the laser monochromicity reduces stray light and increases detection sensitivity. Therefore, this method of post-column laser-induced fluorescence detection is one of the most sensitive detection methods available for CE, it can detect as low as one enzyme molecule (112).

1.2.5 Pre-Column Derivatization

Oligosaccharides do not absorb in the UV-VIS region and are not inherently fluorescent. The oligosaccharide acceptors used in this thesis are labeled with a

fluorescent compound, tetramethylrhodamine (TMR). The maximum absorption wavelength of TMR is 552 nm, and the excited molecule emits at 570 nm. The laser used to excite TMR is a green He-Ne laser with a 543.5 nm wavelength. TMR is attached to the oligosaccharide acceptors through an ethylenediamine linker that is covalently bound to an 8-methoxycarbonyloctyl glycoside (**Fig. 1.14**) (113).

1.2.6 Advantages of CE-LIF over Conventional Separation Methods

CE-LIF provides fast (separation within 15 min), high sensitivity with low detection limit (200 rhodamine 6G molecules), and high separation efficiency (typically number of theoretical plates are in the order of 10^6) for the detection of minute glycosyltransferase activities. Compare to conventional assay methods such as Sep-Pak C18 assay (67), HPLC (68, 69), TLC (114), and size-exclusion chromatography (115), where these assay methods required use of radioisotopes, longer separation time, and insufficient separation which sometimes required re-chromatograph pooled fractions. ELISA-based assay (116) allows fast analysis with the possibility of up to 96 samples but it can only test one enzyme, compare to CE-LIF monitoring several enzymes, including hydrolytic enzymes, simultaneously.

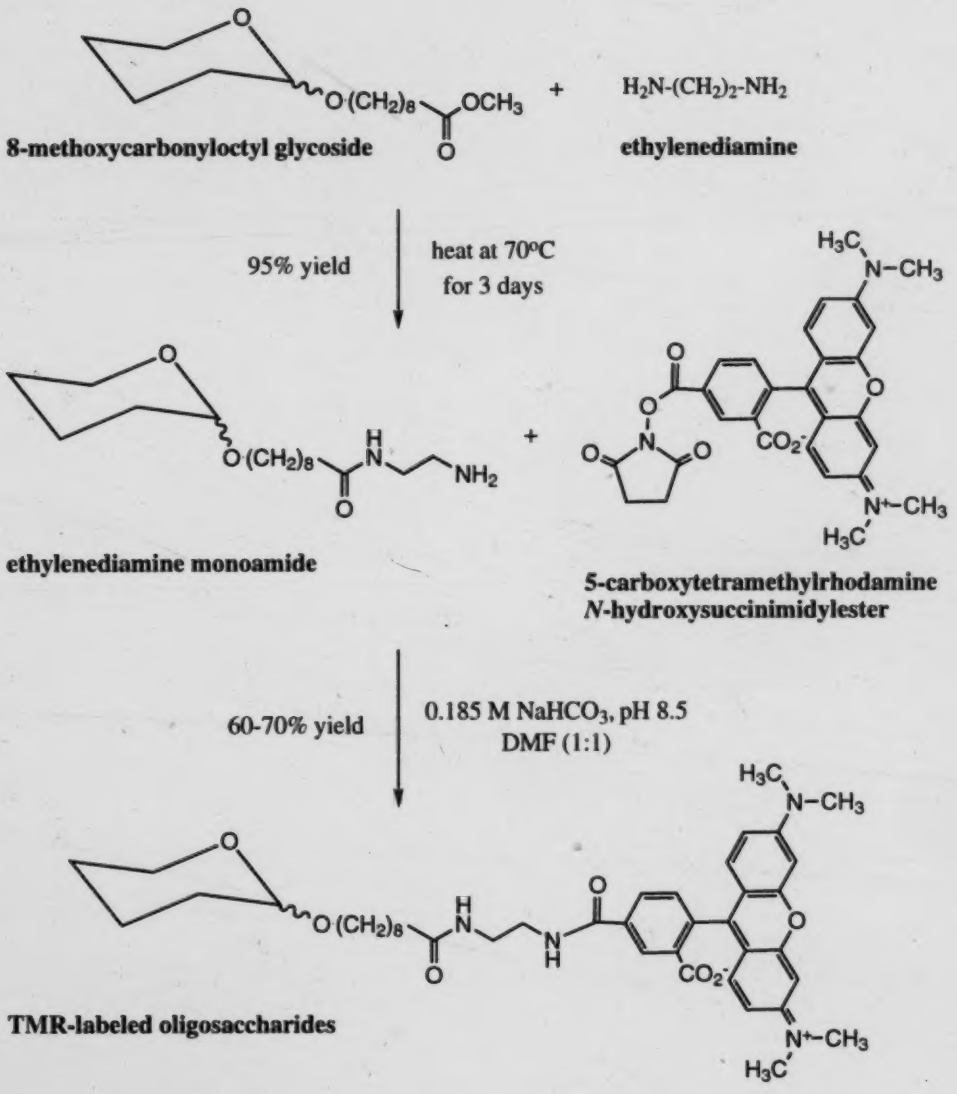

Figure 1.14 Steps in synthesizing TMR-labeled oligosaccharides.

1.3 References

1. Kleene, R., and Berger, E. G. (1993) *Biochim. Biophys. Acta* **1154**, 283-325.
2. Schachter, H. (1994) in *Molecular Glycobiology* (Fukuda, M., and Hindsgaul, O. eds.) pp.88-162, Oxford University Press, Oxford, UK.
3. Kobata, A., and Takasaki, S. (1992) in *Cell Surface Carbohydrates and Cell Development* (Fukuda, M. ed.) pp. 1-24, CRC Press, Boca Raton.
4. Hughes, R. C. (1983) in *Outline Studies in Biology, Glycoproteins* (Brammar, W. J., and Edidin, M. eds.) pp.36-37, Chapman and Hall Ltd., London, UK.
5. Barker, R., Olsen, K. W., Shaper, J. H., and Hill, R. L. (1972) *J. Biol. Chem.* **247**, 7135-7147.
6. Paulson, J. C., and Colley, K. J. (1989) *J. Biol. Chem.* **264**, 17615-17618.
7. Sears, P, and Wong, C.-H. (1998) *Cell. Mol. Life Sci.* **54**, 223-252.
8. Seto, N. O., Palcic, M. M., Compston, C. A., Li, H., Bundle, D. R., and Narang, S. A. (1997) *J. Biol. Chem.* **272**, 14133-14138.
9. Paulson, J. C., Weinstein, J., Ujita, E. L., Riggs, K. J., and Lai, P.-H. (1987) *Biochem. Soc. Trans.* **15**, 618-620.
10. Lammers, G., and Jamieson, J. C. (1989) *Biochem. J.* **261**, 389-393.
11. Carson, D. D. (1992) in *Cell Surface Carbohydrates and Cell Development* (Fukuda, M. ed.) pp. 258-283, CRC Press, Boca Raton.
12. Schachter, H. (1984) *Biol. Cell* **51**, 133-146.
13. Brockhausen, I., Narashimhan, S., and Schachter, H. (1988) *Biochimie* **70**, 1521-1533.
14. Hakomori, S.-I. (1985) *Cancer Res.* **45**, 2405-2414.

15. Yamamoto, F.-I., Clausen, H., White, T., Marken, J., and Hakomori, S.-I. (1990) *Nature* **345**, 229-233.

16. Watkins, W. M. (1991) *Pure Appl. Chem.* **63**, 561-568.

17. Davidsohn, I., and Stejskal, R. (1972) *Haematologia* **6**, 177-184.

18. Feizi, T. (1985) *Nature* **314**, 53-57.

19. Singhal, A, and Hakomori, S.-I. (1990) *Bioessays* **12**, 223-230.

20. Varki, A. (193) *Glycobiology* **3**, 97-130.

21. Feizi, T. (1993) *Curr. Opin. Struct. Biol.* **3**, 701-710.

22. Crocker, P. R., and Feizi, T. (1996) *Curr. Opin. Struct. Biol.* **6**, 679-691.

23. Liener, I. E., Sharon, N., and Goldstein, I. J. eds. (1986) *The Lectins: Properties, Functions and Applications in Biology and Medicine*, Academic Press, New York.

24. Miller-Podraza, H., Milh, M. A., Bergström, J., and Karlsson, K.-A. (1996) *Glycoconjugate J.* **13**, 453-460.

25. Karlsson, K.-A. (1995) *Curr. Opin. Struct. Biol.* **5**, 622-635.

26. Pritchett, T. J., Brossmer, R., Rose, U., and Paulson, J. C. (1988) *Virology* **160**, 502-506.

27. Gruters, R. A., Neefjes, J. J., Termette, M., de Goede, R. E. Y., Tulp, A., Husiman, G., Miedema, F., and Ploegh, L. (1987) *Nature* **330**, 74-77.

28. Feizi, T., and Larkin, M. (1990) *Glycobiology* **1**, 17-23.

29. Cummings R. D., and Nyame, A. K. (1996) *FASEB J.* **10**, 838-848.

30. Hakomori, S.-I., and Kannagi, R. (1983) *J. Natl. Cancer Inst.* **71**, 231-251.

31. Wiegandt, H. (1985) *New Comprehesive Biochem.* **10**, 199-260.

32. Calveo, F. O., and Ryan, R. J. (1985) *Biochemistry* **24**, 1953-1959.

33. Koro, L. A., and Marchase, R. B. (1982) *Cell* **31**, 739-748.

34. Hakomori, S.-I., and Igarashi, Y. (1995) *J. Biochem.* **118**, 1091-1103.

35. Brandley, B. K., Swiedler, S. J., and Robbins, P. W. (1990) *Cell* **63**, 861-863.

36. Collins, S. J., Gallo, R. C., and Gallagher, R. E. (1977) *Nature* **270**, 347-349.

37. Momoi, T., and Yokota, J. (1983) *J. Natl. Cancer. Inst.* **70**, 229-236.

38. Solter, D., and Knowles, B. B. (1978) *Proc. Natl. Acad. Sci. USA* **75**, 5565-5569.

39. Fox, N., Damjanov, I., Martinez-Hernandez, A., Knowles, B. B., and Solter, D. (1981) *Dev. Biol.* **83**, 2248-2252.

40. Kleene, R., and Berger, E. G. (1993) *Biochim. Biophys. Acta* **1154**, 283-325.

41. Chia, D., Terasaki, P. I., Suyama, N., Galton, J., Hirots, M., and Katz, D. (1985) *Cancer Res.* **45**, 435-437.

42. Fukushima, K., Hirota, M., Terasaki, P. I., Wakisaka, A., Togashi, H., Chia, D., Suyama, N., Fukushi, Y., Nudelman, E., and Hakomori, S.-I. (1984) *Cancer Res.* **44**, 5279-5285.

43. Koprowski, H., Steplewski, Z., Mitchell, K., Herlyn, M., Herlyn, D., and Fuhrer, P. (1979) *Somat. Cell Genet.* **5**, 957-972.

44. Magnani, J. L., Nilsson, B., Brockhaus, M., Zopf, D., Steplewski, Z., Koprowski, H., and Ginsburg, V. (1982) *J. Biol. Chem.* **257**, 14365-14369.

45. Takada, A., Ohmori, K., Takahashi, N., Tsuyuoka, K., Yago, A., Zenita, K. Hasegawa, A., and Kannagi, R. (1991) *Biochem. Biophys. Res. Commun.* **179**, 713-719.

46. Hakomori, S.-I. (1989) *Adv. Cancer Res.* **52**, 257-331.

47. Hakomori, S.-I. (1996) in *Glycoproteins and Disease* (Montreuil, J., Viegenthart, J. F. G., and Schachter, H. eds.) **vol. 30**, pp.243-276, Elsevier, Amsterdam.

48. Dennis, J. W., Laferté, S., Waghorne, C., Breitman, M. L., and Kerbel, R. S. (1987) *Science* **236**, 582-585.

49. Pierce, M., and Arango, J. (1986) *J. Biol. Chem.* **261**, 10772-10777.

50. Schachter, H. (1998) *Adv. Exp. Med. Biol.* **435**, 9-27.

51. Yamashita, K., Tachibana, Y., Okhura, T., and Kobata, A. (1985) *J. Biol. Chem.* **260**, 3963-3939.

52. Dennis, J. W. (1992) in *Cell Surface Carbohydrates and Cell Development* (Fukuda, M. ed.) pp. 161-194, CRC Press, Boca Raton.

53. Moran, A. P., Helander, I. M., and Kosunen, T. U. (1992) *J. Bacteriol.* **174**, 1370-1377.

54. Chan, N. W. C., Stangier, K., Sherburne, R., Taylor, D. E., Zhang, Y., Dovichi, N. J., and Palcic, M. M. (1995) *Glycobiology* **5**, 683-688.

55. Aspinall, G. O., Monteiro, M. A., Pang, H., Walsh, E. J., and Moran A. P. (1994) *Carbohydr. Lett.* **1**, 151-156.

56. Irimura, T., Gonzalez, R., and Nicolson, G. L. (1981) *Cancer Res.* **46**, 3411-3418.

57. Jacob G. S. (1995) *Curr. Opin. Struct. Biol.* **5**, 605-611.

58. Winchester B., and Fleet, G. W. J. (1992) *Glycobiology* **2**, 199-210.

59. Lowary, T. L., and Hindsgaul, O. (1993) *Carbohydr. Res.* **249**, 163-195.

60. Lowary, T. L., and Hindsgaul, O. (1994) *Carbohydr. Res.* **251**, 33-67.

61. Palcic, M. M., Heerze, L. D., Srivastava, O. P., and Hindsgaul, O. (1989) *J. Biol. Chem.* **264**, 17174-17181.

62. Lu, P. P., Hindsgaul, O., Li, H., and Palcic, M. M. (1997) *Carbohydr. Res.* **303**, 283-291.

63. Lu, P. P., Hindsgaul, O., Compston, C. A., and Palcic, M. M (1996) *Bioorg. Med. Chem.* **4**, 2011-2022.

64. McAuliffe, J. C., and Hindsgaul, O. (1997) *Chem. Ind.* **5**, 170-174.

65. Gastinel, L. N.,Cambillau, C., and Bourne, Y. (1998) in *Glycobiology '98: 3rd Annual Conference of the Society of Glycobiology*, 11-14 November, 1998, special presentation, Baltimore, MD.

66. Virelink A., Ruger, W., Driessen H. P. C., and Freemont P. S. (1994) *EMBO J.* **13**, 3413-3422.

67. Palcic, M. M., Heerze, L. D., Pierce, M., and Hindsgaul, O. (1988) *Glycoconj. J.* **5**, 49-63.

68. Schachter, H., Brockhausen, I., and Hull, E. (1989) *Methods Enzymol.* **179**, 351-397.

69. Brockhausen, I., Carver, J. P., and Schachter, H. (1988) *Biochem. Cell Biol.* **66**, 1134-1151.

70. Zhao, J. Y., Dovichi, N. D., Hindsgaul, O., Gosselin, S., and Palcic, M. M. (1994) *Glycobiology* **4**, 239-242.

71. Balfour, J. A., and McTavish, D. (1993) *Drugs* **46**, 1025-1054.

72. Keikawus, A., *et al.* (1996) in *XIth International Conference on AIDS*, 7-12 July 1996, abstract Mo.B., Vancouver, B.C.

73. Egger, S. F., Brown, G. S., Kelsey, L. S., Yates, K. M., Rosenberg, L. J., and Talmadge, J. E. (1996) *Int. J. Immnuopharmac.* **18**, 113-126.

74. Cytel Corporation (Nasdaq: CYTLD) San Diego, CA, press release, 18 December, 1997.

75. Cytel Corporation (Nasdaq: CYTLD) San Diego, CA, press release, 30 September, 1998.

76. Cypros Pharm. Corp. (Nasdaq: CYP) Carlsbad, CA, press release, 27 May, 1998.

77. SafeScience Inc. (Nasdaq: SAFS) Boston, MA, press release, 5 November, 1998.

78. Fischl, M. A., Resnick, L., Coombs, R., Kremer, A. B., Pottage, J. C. Jr., Fass, R. J., Fife, K. H., Powderly, W. G., Collier, A. C., Aspinall, R. L., Smith, S. I., Kowalski, K. G., and Wallemark, C. B. (1994) *J. Acquir. Immun. Defic. Syn.* **7**, 139-147.

79. Zopf, D. and Roth, S. (1996) *Lancet* **347**, 1017-1021.

80. Neose Technologies, Inc. (Nasdaq: NTEC),Horsham, PA, USA, press release, 6 May 1997.

81. Glaxo Wellcome (Nasdaq: GLX) London, UK, press release, 27 Oct., 1998.

82. SYNSORB Biotech, Inc. (Nasdaq: SYBBF, TSE: SYB) Calgary, AB, Canada, press release, 3 June, 1996.

83. SYNSORB Biotech, Inc. (Nasdaq: SYBBF, TSE: SYB) Calgary, AB, Canada, press release, 9 September, 1997.

84. SYNSORB Biotech, Inc. (Nasdaq: SYBBF, TSE: SYB) Calgary, AB, Canada, press release, 2 December, 1997.

85. Biomira Inc. (Nasdaq: BIOMF, TSE: BRA) Edmonton, AB, Canada, press release, 30 November, 1998.

86. Shaw, D. J. (1980) in *Introduction to Colloid and Surface Chemistry, 3rd Ed.* Butterworths, Toronto, ON.

87. Hiemenz, P. C. (1986) in *Principles of Colloid and Surface Chemistry, 2nd Ed.* Dekker, New York, NY.

88. Grossman, P. D., and Colburn, J. C. (1992) in *Capillary Electrophoresis: Theory and Practice*, Academic Press, San Diego, CA.

89. Beckman Instruments, Inc. (1991) in *Introduction to Capillary Electrophoresis* (part number 360643), pp. 4-8, , CA.

90. Oda, R. P., and Landers, J. P. (1997) in *Handbook of Capillary Electrophoresis, 2nd Ed.* (Landers, J. P. ed.) pp. 7-10, CRC Press, Boca Raton.

91. Helmholtz, H. Z. (1879) *Annal. Phys. Chem.* **7**, 337.

92. Terabe, S. T., Otsuka, K., Ichikawa, K., Tsuchiya, A., and Ando, T. (1984) *Anal. Chem.* **56**, 111-113.

93. Terabe, S. T., Otsuka, K., Ando, T. (1985) *Anal. Chem.* **57**, 834-841.

94. Terabe, S. T. (1991) in *Micellar Electrokinetic Chromatography*, pp.1-7, Beckman Instruments, Inc., CA.

95. Szoko, E. (1997) *Electrophoresis* **18**, 74-81.

96. Nishi, H. (1997) *J. Chromatogr. A* **780**, 243-264.

97. Nishi, H., and Terabe, S. T. (1996) *J. Chromatogr. A* **735**, 3-27.

98. Sadecka, J., Polonsky, J., and Shintani, H. (1994) *Pharmazie* **49**, 631-641.

99. Oefner, P. J., and Chiesa, C. (1994) *Glycobiology* **4**, 397-412.

100. Yang, L., and Lee, C. S. (1997) *J. Chromatogr. A* **780**, 207-218.

101. Calbiochem-Novabiochem Corp. (1998) Glycobiology catalogue, pp. *x*, La Jolla, CA.

102. Böeseken, J. (1949) *Adv. Carbohydr. Chem.* **4**, 189-210.

103. Weigel, H. (1963) *Adv. Carbohydr. Chem.* **18**, 61-97.

104. Hoffstetter-Kuhn, S., Paulus, A., Gassmann, E., and Widmer, H. M. (1991) *Anal. Chem.* **63**, 1541-1547.

105. Huang, X., Gordon, M. J., and Zare, R. N. (1988) *Anal. Chem.* **60**, 377-380.

106. Walbroehl, Y., and Jorgenson, J. W (1984) *J. Chromatogr.* **315**, 135-143.

107. Gilman, S. D., and Ewing, A. G. (1995) *Anal. Chem.* **67**, 58-64.

108. Nann, A., Silvestri, I., and Simon, W. (1993) *Anal. Chem.* **65**, 1662-1667.

109. Waldron, K. C., and Dovichi, N. J. (1992) *Anal. Chem.* **64**, 1396-1399.

110. Dovichi, N. J., and Cheng, Y.F. (1988) *Abstr. Pap. Am. Chem. S.* **195**, 36-ANYL. Part 1.

111. Cheng, Y. F., and Dovichi, N. J. (1988) *Science* **242**, 562-564.

112. Craig, D. B., Arriaga, E., Wong, J. C. Y., Lu, H., and Dovichi, N. J. (1998) *Anal. Chem.* **70**, 39A-43A.

113. Zhang, Y., Le, X., Dovichi, N. J., Compston, C. A., Palcic, M. M., Diedrich, P., and Hindsgaul, O. (1995) *Anal. Biochem.* **227**, 368-376.

114. Stults, C. L., Sullivan, M. T., Macher, B. A., Johnston, R. F., and Stack, R. J. (1994) *Anal. Biochem.* **219**, 61-70.

115. Nakamura, M., and Sweeley, C. C. (1987) *Anal. Biochem.* **166**, 230-234.

116. Stults, C. L., and Macher, B. A. (1990) *Arch. Biochem. Biophys.* **280**, 20-26.

Chapter Two

The Biosynthesis of Lewis X in *Helicobacter Pylori*

A version of this chapter has been published.

Chan, N. W. C., Stangier, K., Sherburne, R., Taylor, D. E., Zhang, Y., Dovichi, N. J., and Palcic, M. M. (1995) *Glycobiology* **5**, 683-688.

Acknowledgments: I would like to thank Dr. O. Hindsgaul (University of Alberta) for providing the synthetic acceptors and GDP-fucose, Dr. A. Otter (University of Alberta) for obtaining the NMR spectra and Dr. S. Forsberg (Complex Carbohydrate Research Center, University of Georgia) for methylation analysis. I would also like to thank Drs. R. Sherburne and D. E. Taylor (University of Alberta) for providing *H. pylori* cells and immunoassay results and Dr. Y. Zhang (University of Alberta) for obtaining the electropherograms for this chapter.

2.1 Introduction

Bacteria have long been recognized as bearing oligosaccharides on their cell surfaces similar to those found on mammalian cells. These include A, B and H blood group structures (1), the H-Type I determinant (αFuc(1→2)βGal(1→3)GlcNAc-) (2) and Lewis^x structures (3). While the mammalian glycosyltransferases that synthesize these structures are well characterized (4, 5), little is known about the corresponding bacterial enzymes. The recent report of the Lewis^x structure (βGal(1→4)[αFuc(1→3)]βGlcNAc-) on O antigens of *Helicobacter pylori* (3), a human pathogen associated with gastritis, gastric and duodenal ulcers and gastric adenocarcinoma (6), prompted our investigation into its biosynthesis. In mammals, this structure is found on glycoproteins and glycolipids, where it is a stage-specific embryonic antigen (SSEA-1) and a tumour-associated marker (7-9). The Lewis^x structure has also been found in a lower eukaryote, in the surface antigen from the eggs of the parasitic worm, *Schistosoma mansoni*, where it has been shown to play a signaling role in the interaction of the parasite with its human host (10).

In mammals, the Lewis^x structure is synthesized by the strictly sequential addition of galactose from UDP-galactose to GlcNAc, catalyzed by a β1,4 galactosyltransferase, followed by the transfer of fucose from GDP-Fuc to the disaccharide βGal(1→4)GlcNAc (LacNAc) by an α1,3 fucosyltransferase. We demonstrate that the synthesis of Lewis^x occurs in an analogous fashion in *Helicobacter pylori* and provide a preliminary kinetic characterization of the glycosyltransferases involved.

The findings of Chan *et al.* (11) were the first report of Lewis^x biosynthesis in *Helicobacter pylori*. The investigation of the glycosyltransferases in *H. pylori* was made possible by the availability of the sensitive CE-LIF technique as well as several synthetic substrates. CE-LIF facilitated the discovery of an unusual glycosyltransferase in a strain of *H. pylori* reported here which was later demonstrated by Monteiro and coworkers (12) to be an α1,6 glucosyltransferase.

2.2 Experimental Section

2.2.1 Materials

βGlcNAc-O-$(CH_2)_8$COOMe, βGal(1→4)βGlcNAc-O-$(CH_2)_8$COOMe, βGal (1→3)βGlcNAc-O-$(CH_2)_8$COOMe (Lewis^c), βGlcNAc-O-$(CH_2)_8$CONHCH$_2$CH$_2$NH-tetramethylrhodamine (TMR), βGal(1→4)βGlcNAc-O-$(CH_2)_8$CONHCH$_2$CH$_2$NH-TMR and βGal(1→3)βGlcNAc-O-$(CH_2)_8$CO-NHCH$_2$CH$_2$NH-TMR were provided by Dr. O. Hindsgaul, Department of Chemistry, University of Alberta. GDP-fucose was synthesized by the method of Gokhale *et al.* (13), GDP-[1-^{3}H]fucose (5.1 Ci/mmol) and UDP-[6-^{3}H]galactose (15 Ci/mmol] were from American Radiolabeled Chemicals Inc. (St. Louis, MO). The antibodies used were mouse isotype IgM anti-human CD15 MAB from Cederlane Laboratories which have documented specificity for (βGal(1→4)[αFuc(1→3)]βGlcNAc(1→3)βGal(1→4)Glc) Lacto-*N*-fucopentaose III (LNFP III) also called hapten X and Lewis^x (14). Anti-Le^a MAB purchased from Synaff-Chembiomed is specific for βGal(1→3)[αFuc(1→4)]βGlcNAc (Lewis^a) and anti-Le^b MAB specific for αFuc(1→2)βGal(1→3)[αFuc(1→4)]βGlcNAc (Lewis^b). Brain heart infusion agar and Mueller Hinton agar were both purchased from Oxoid (Basingstoke, U.K.). Sep-Pak Plus C-18 reverse phase cartridges were obtained from Waters (Mississauga, Ont.), and were conditioned before use by washing with 10 ml of HPLC grade methanol and 20 ml of Milli-Q water. Methyl silicone capillary column from Quadrex Corporation. Protein concentrations were estimated with a Bio-Rad protein assay kit which is based on the method described by Bradford (15), with bovine serum albumin as a standard. All other chemicals were of reagent grade.

2.2.2 Cell Growth and Immuno-electron Microscopy

Helicobacter pylori strains UA 861, UA 802 and UA 1182 were isolated from endoscopic biopsy specimens obtained from patients attending the University of Alberta Hospital using methods described previously by Taylor *et al.* (16, 17). *H. pylori* strains were grown on brain heart infusion agar containing 5% yeast extract, 5% bovine serum with 15 µg/ml vancomycin and 15 µl/ml amphotericin. Cultures were incubated with 5% carbon dioxide, 5% hydrogen and the balance nitrogen at 37°C. Control cultures of *Campylobacter fetus* and *Campylobacter jejuni* were grown on Mueller Hinton agar and incubated in 5% carbon dioxide at 37°C. Each petri dish contained approximately 2.5 x 10^9 colony forming units (c.f.u.).

Campylobacter coli, Campylobacter fetus and *H. pylori* whole cells were removed from agar plates and suspended in PBS, pH 7.3. The whole cell suspensions were then centrifuged using a Clinical Centrifuge (International Equipment Co. model CL) and washed twice with PBS. Bacterial suspensions were then adsorbed onto formvar coated electron microscope grids by floating the grid on a drop of suspension, transferred to the primary MAB's and incubated. Samples were blocked with 1% bovine serum albumin and further incubated with goat anti-mouse IgM 10 nm colloidal gold conjugate (EY Labs.), washed in distilled water and examined unstained. Positive labeling was determined by the presence of gold particles on unfixed and unstained *H. pylori* cells. Images were recorded on Kodak #4489 electron microscope film using a Philips model 410 transmission electron microscope.

2.2.3 Enzyme Extract Preparation

Cells were removed from the Petri dishes by washing with 2 ml of 20 mM HEPES buffer, pH 7.0 and centrifuging at 3,000 *g* for 10 minutes at 4°C. The supernatant (2 ml) was removed and saved for assays of secreted enzymes. The cell pellet was resuspended in 4 ml of 20 mM HEPES buffer, pH 7.0, and disrupted by sonication for 5 x 15 sec using a microprobe tip. Cells were spun at 3,000 *g* for 10 min and the supernatant (4 ml) retained for analysis of soluble enzymes. The pellet was resuspended in 1 ml of 20 mM HEPES, pH 7.0, containing 20 mM $MnCl_2$, 0.2% bovine serum albumin and 0.2% Triton X-100. The suspension was vortexed for 5 min, centrifuged for 10 min at 3,000 *g* and the supernatant (1 ml) set aside for assays for membrane-bound enzymes. All enzyme activities were stable in all of the extracts for 7 days when stored at 4°C.

2.2.4 Activity Screening

α1,3 and α1,4 fucosyltransferase activities were assayed by incubating 24 µl of extract at 37°C for 90 min with 450 µM acceptor, 50 µM GDP-fucose, 45,000 d.p.m. GDP-[^{3}H]fucose, 20 mM HEPES buffer, pH 7.0, 20 mM $MnCl_2$ and 0.2% bovine serum albumin in a total volume of 40 µl. For α1,3 fucosyltransferase activity βGal(1→4)βGlcNAc-O-$(CH_2)_8$COOMe was used as an acceptor, while for α1,4 fucosyltransferase activity βGal(1→3)βGlcNAc-O-$(CH_2)_8$COOMe was used as an acceptor. After incubation, the reaction mixtures were loaded onto Sep-Pak Plus C-18 cartridges, the cartridges were washed with 50 ml of water to remove unreacted donor and then products were eluted with 3.5 ml of methanol and quantitated by

counting in 10 ml of Ecolite (+) cocktail in a Beckman LS 1801 scintillation counter (18). A milliunit of enzyme activity is defined here as the amount that catalyzes the conversion of 1 nmol of acceptor to product per min under the standard screening conditions.

β1,4 Galactosyltransferase activity was estimated by incubating 10 µl of the various extracts at 37°C for 90 min with 372 µM βGlcNAc-O-$(CH_2)_8$COOMe, 182 µM UDP-galactose, 80,000 d.p.m. UDP-[^{3}H]Gal, 77 mM sodium cacodylate buffer, pH 7.4, 8 mM $MnCl_2$ and 0.25 M NaCl in a total volume of 55 µl. Radiolabeled product was isolated and quantitated as described previously for the fucosyltransferase assays. A milliunit of enzyme activity is the amount that catalyzes the conversion of 1 nmol of acceptor to product per min under the standard screening conditions. Negative control utilizing uninoculated plates, *Campylobacter fetus*, *Campylobacter jejuni* or *Escherichia coli* cells were carried out in an analogous fashion for both enzyme activities.

2.2.5 Kinetic Characterizations

Kinetic evaluations were carried out in duplicate on the membrane-associated fractions (Triton X-100 detergent extracts). The K_m^{app} for βGal(1→4)βGlcNAc-O-$(CH_2)_8$COOMe was estimated using six different concentrations of acceptor ranging from 14 to 450 µM in 40 µl incubation mixtures as described under activity screening (section **2.2.4**). GDP-fucose concentrations were kept constant at 50 µM. The K_m^{app} for GDP-fucose was estimated using six concentrations of donor ranging from 7 to 225 µM at 450 µM of βGal(1→4)βGlcNAc-O-$(CH_2)_8$COOMe, except for UA 1182 ,

in which case a donor concentration range of 1-56 μM was used. Data were fitted to the Michaelis-Menten equation by non-linear regression, with the Sigma Plot program.

Galactosyltransferase kinetics to estimate the K_m^{app} of acceptor used βGlcNAc-O-$(CH_2)_8$COOMe (12-372 μM) with 182 μM UDP-galactose in a total of 55 μl with buffer components and enzyme volumes similar to those described under activity screening (section **2.2.4**). For donor kinetics, 6-200 μM UDP-galactose were used at an acceptor concentration of 510 μM.

2.2.6 Capillary Electrophoresis

For fucosyltransferase reactions, the incubation mixtures contained 33 μl of the membrane-associated extract from UA 802 or UA 861, 28 μM LacNAc-TMR and 50 μM GDP-fucose in a total volume of 40 μl of 20 mM HEPES buffer, pH 7.0, containing 20 mM $MnCl_2$ and 0.2% BSA. After incubation at 37°C for 3 hr, the samples were applied to Sep-Pak Plus C-18 cartridges which were then washed with 30 ml of water, then product was eluted in 3.5 ml of HPLC grade methanol. Samples were diluted (1:2) with running buffer (10 mM disodium hydrogen phosphate, 10 mM borate, 10 mM SDS and 10 mM phenylboronic acid, pH 9.0) and 13 pl were injected onto a 42 cm capillary electrophoresis column at 1 kV for 5 s (19, 20). Species eluted from the column were detected by laser-induced fluorescence. For galactosyltransferase reactions, 15 μl of the Triton X-100 extract were incubated for 3 hr at 37°C with 182 μM GlcNAc-TMR, 182 μM UDP-galactose in 245 mM NaCl, 8 mM $MnCl_2$ in a total volume of 55 μl of 77 mM sodium cacodylate buffer, pH 7.4.

Products were isolated and analyzed by capillary electrophoresis at 400 V/cm as described above for the fucosyltransferases.

2.2.7 Preparative Syntheses

To 1.5 ml microfuge tubes were added 0.5 mg of acceptor (βGal(1$\rightarrow$4)βGlcNAc-O-$(CH_2)_8$COOMe or βGlcNAc-O-$(CH_2)_8$COOMe), 1.5 equivalents of GDP-fucose or UDP-galactose and between 0.25 to 1.0 ml of the Triton X-100 extract from all three stains (0.4 milliunits). The reaction was allowed to proceed for 48 hr at ambient temperature and was monitored by TLC using CH_2Cl_2/MeOH (4:1) as the eluent with product detection by spraying with sulfuric acid (5%) and charring. Unreacted starting material and products were isolated by applying the reaction mixture to Sep-Pak Plus C-18 cartridges, washing with 30 ml of water to remove unreacted donor, enzyme and buffer components, and then eluting with 10 ml of methanol. Triton X-100 was removed by passing the sample through Iatrobeads (bed volume 3 ml in a Pasteur pipette) equilibrated with CH_2Cl_2/MeOH (4:1). Solvent was removed by lyophilization and the sample dissolved in 100% D_2O for analysis by ^{1}H-NMR spectroscopy on a Varian Unity 500 spectrometer operating at 500 MHz. Chemical shifts were measured using acetone as an external standard (2.225 p.p.m.) at 30°C.

2.2.8 Methylation Analysis

Samples were subjected to methylation analysis (21, 22) using the Hakomori procedure (23). In this procedure, the permethylated oligosaccharide obtained during

the Hakomori methylation is subjected to sequential hydrolysis (2 N trifluoroacetic acid, 100°C, 2 hr), *N*-acetylation (methanol, pyridine/acetic anhydride), hydrolysis (2 N TFA, 121°C, 2 hr), and reduction with sodium borodeuteride. The resulting partially-methylated alditols are then acetylated and analyzed by gas liquid chromatography-mass spectrometry (GC-MS) (electron impact) using a 50 m methyl silicone capillary column. Scans are compiled at a rate of 1 scan per sec over a m/z range of 40-500 amu.

2.3 Results and Discussion

2.3.1 Detection of Lewis^x on *H. pylori* Cell Surface

Three different strains of *Helicobacter pylori* (UA 861, UA 1182 and UA 802) were isolated from endoscopic biopsy specimens and screened for enzyme activity. These strains all produce Lewis^x on their surfaces as detected with specific antibodies to Le^x in immuno-electron microscopy and ELISA, although for UA 802 Lewis^x is found on only 13% of the cells surveyed (Taylor, D. E., unpublished). Transmission electron microscopy and immuno-gold labeling of UA 1182 *H. pylori* cells treated with anti-CD15 MAB antibody shows strong reactivity to the cell and flagella sheath and no binding to flagella structures (**Fig. 2.1**). *H. pylori* whole cells were negative for binding of anti-Le^a MAB and anti-Le^b MAB in both immuno-electron microscopy and ELISA. Whole cells of *Campylobacter coli* and *Campylobacter fetus* were negative for immuno-gold labeling with anti-Le^a, anti-Le^b and anti-Le^x MABs.

2.3.2 Fucosyltransferase and Galactosyltransferase Activities

α1,3 Fucosyltransferase activity was quantitated using βGal(1→4)βGlcNAc-O$(CH_2)_8$COOMe as an acceptor and GDP-fucose as the donor. For strain UA 861, most of the activity was detected in the Triton X-100 extracts, while activity was found in all fractions for UA 802 and UA 1182 extracts (**Table 2.1**). UA 802 and 1182 had similar enzyme activity levels in all fractions, consistently higher than that found in membrane-bound in UA 861 cells. No α1,4 fucosyltransferase activity was found in any of the strains using βGal(1→3)βGlcNAc-O$(CH_2)_8$COOMe as an

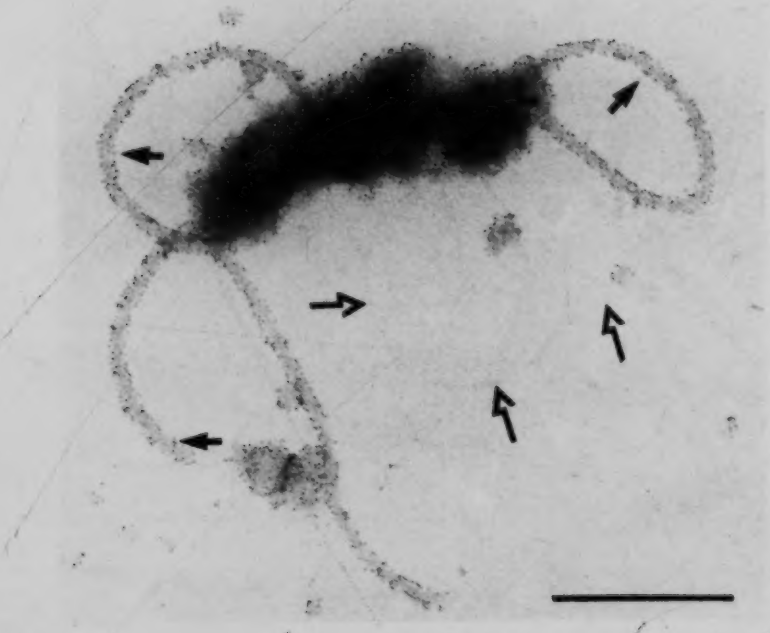

Figure 2.1 Transmission electron micrograph of unstained, unfixed *H. pylori* strain UA 1182 incubated with anti-human CD15 IgM MAB and goat anti-mouses IgM-colloidal gold 10 nm particles. Positive labelling is determined by the presence of gold particles (solid arrows) on the cell and flagella sheath. The absence of particles on the unsheathed flagellum (open arrows) indicates no binding of CD15 to flagellar structures. The scale bar represents 1.0 μm.

acceptor. While the levels of activity were similar in different extracts of UA 802 and UA 1182, they were highly variable and occasionally undetectable in extracts from UA 861 cells. Neither α1,3 nor α1,4 fucosyltransferase activity was present in *Campylobacter fetus*, *Campylobacter jejuni* or *Escherichia coli* cells grown on the same media as all strains of *H. pylori*.

The β1,4 galactosyltransferase activity was the highest in the Triton X-100 extracts in all of the strains, suggesting that it is a membrane-bound enzyme (**Table 2.1**). The highest level of activity was found in *H. pylori* strain UA 1182 (10 milliunits per 2.5 x 10^9 c.f.u.), and no activity was observed in *Campylobacter fetus*, *Campylobacter jejuni* or *Escherichia coli*.

2.3.3 Detection of Lewis^x and a New Product by CE-LIF

Preliminary characterization of the reaction products was achieved by capillary electrophoresis with laser induced fluorescence detection using acceptors labeled with tetramethylrhodamine (TMR) (19, 20). The electropherograms from these mixtures are shown in **Fig. 2.2**. For UA 861 and UA 802, incubation mixtures containing GDP-fucose and LacNAc-TMR both gave a new peak in the electropherogram, which was not present in negative controls, with the same elution time as a synthetic reference sample of Lewis^x-TMR (**Figs. 2.2b** and **2.2e**). The extract from UA 802 incubated with UDP-galactose and GlcNAc-TMR gave a new peak with the same elution time as a LacNAc-TMR standard (**Fig. 2.2d**). For UA 861, the only new peak that had a longer elution time was shown (see section **2.3.4**) to be the α1→6 isomer (**Fig. 2.2c**).

Table 2.1 Cellular distribution of galactosyltransferase and fucosyltransferase activities in *H. pylori* extracts.

Strain	Fucosyltransferase (milliunits)[a]			Galactosyltransferase (milliunits)		
	secreted	soluble	membrane bound	secreted	soluble	membrane bound
UA 861	8.0×10^{-4}	1.7×10^{-3}	0.01 (1.4×10^{-3})[b]	2.6×10^{-2}	1.4×10^{-2}	1.0[c] (0.20)
UA 802	1.4	1.6	0.41 (0.41)	7.3×10^{-2}	5.3×10^{-2}	4.0 (4.0)
UA 1182	0.93	2.3	0.57 (1.9)	0.47	1.5	10 (31)

[a] All activities are from the extractions of one Petri dish containing 2.5×10^9 c.f.u. The volumes of the extracts were 2 ml for secreted, 4 ml for soluble and 1 ml for membrane bound.

[b] Specific activities (mU/mg protein), determined for membrane-bound enzymes only, are given in parentheses.

[c] α1,6 Galactosyltransferase activity (a recent report (12) suggests an α1,6 glucosyltransferase).

2.3.4 Identification of the New Product by ^{1}H-NMR and Methylation Analysis

Capillary electrophoresis suggested that di- and trisaccharides had been produced by galactosyltransferases and fucosyltransferases in the extracts. Structural characterization of the products of these reactions was achieved by preparative incubation, isolation and analysis by ^{1}H-NMR spectroscopy. **Fig. 2.3** shows the partial NMR spectrum of the product obtained from an incubation of UA 1182 and UDP-galactose with βGlcNAc-OR as an acceptor (upper panel). A new glycosidic linkage with a β-configuration is evident from the H-1 doublet (J = 7.7 Hz) at δ 4.50 p.p.m. consistent with the formation of LacNAc-OR. A conversion in excess of 95% was achieved. A similar spectrum was obtained from the UA 802 incubations, although only 52% of the acceptor was converted to product (data not shown). The product from UA 861 incubations was shown by methylation analysis to be αGal(1→6)GlcNAc- (24), the α-anomeric configuration being evident from a doublet ($J_{1,2}$ = 3.7 Hz) at δ 5.02 p.p.m. in the ^{1}H-NMR spectrum (data not shown). A portion of the product from UA 861 incubations was subjected to the methylation analysis (21, 22) using the Hakomori procedure (23). The resulting partially-methylated alditol acetates were then analyzed by gas liquid chromatography-mass spectrometry (GC-MS). Two derivatives were observed, 2,3,4,6-tetra-*O*-methyl-1,5-di-*O*-acetyl galactitol and *N*-acetyl-*N*-methyl-1,5,6-tri-*O*-acetyl-3,4-di-*O*-methyl glucosaminitol, in a 1:1 ratio. The first product is derived from terminal (unsubstituted) galactose, and the second from 6-*O*-substituted *N*-acetylglucosamine. The only possible oligosaccharide yielding these derivatives in the observed ratio would be Gal(1→6)GlcNAc. No other derivatives were observed.

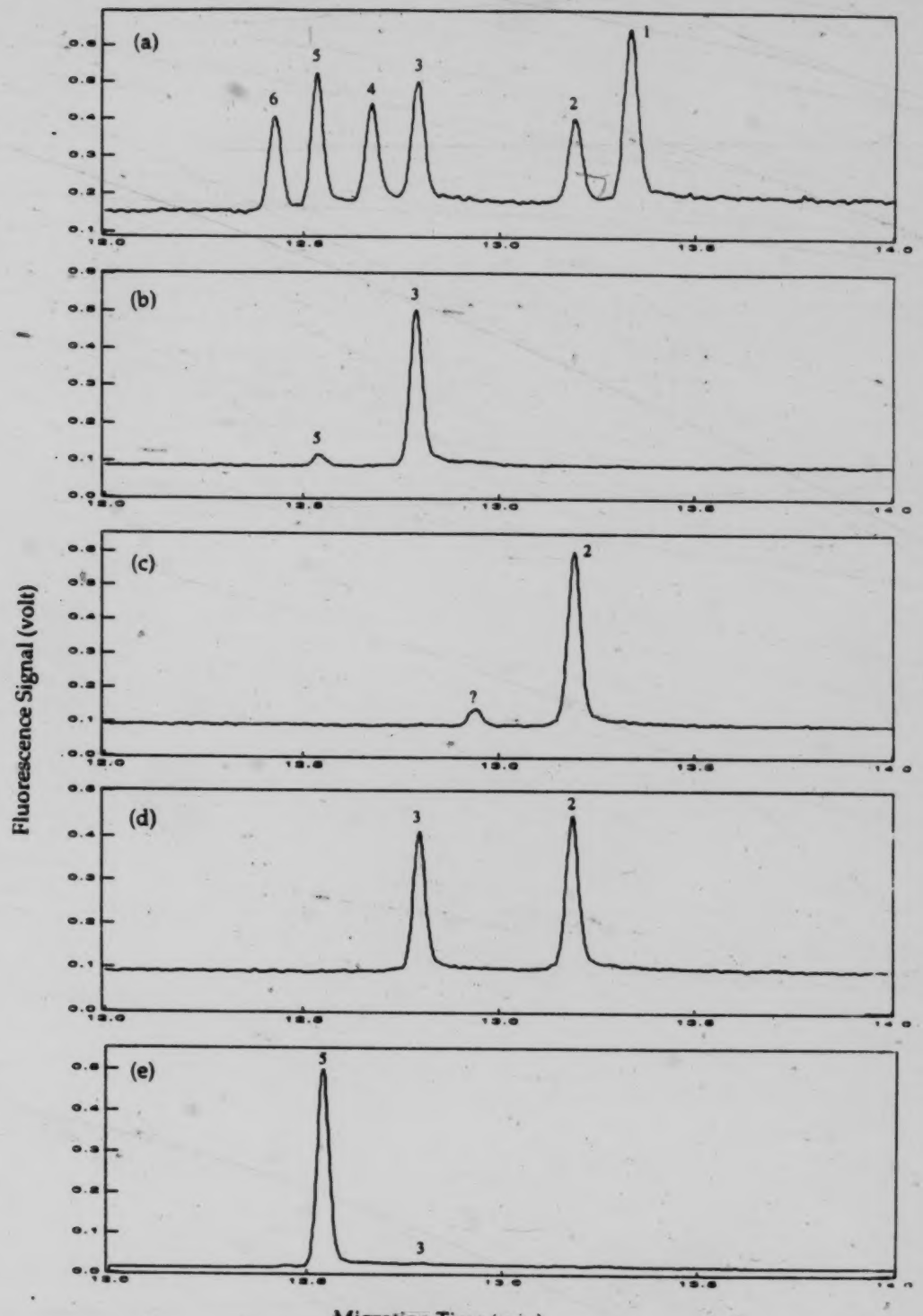
(a)
6
5
4
3
2
1
(b)
5
3
(c)
?
2
(d)
3
2
(e)
5
3
Fluorescence Signal (volt)
Migration Time (min)

Figure 2.2 Analysis of reaction mixtures from *H. pylori* UA 861 and UA 802 incubations by capillary zone electrophoresis with laser-induced fluorescence detection.

(a) Baseline separation of five standard TMR oligosaccharides found in mammalian metabolism (6, 7), the linker arm-TMR (**1**), βGlcNAc- (**2**), LacNAcβ- (**3**), αFuc(1→2)βGal(1→4)βGlcNAc- (**4**), β Gal(1→4)[αFuc(1→3)]βGlcNAc- (**5**), αFuc(1→2)βGal(1→4)[αFuc(1→3)]βGlcNAc- (**6**). The capillary was 42 cm long (10 μm i.d.) and the samples were injected onto the electrophoresis column at 1 kV for 5 s. The running buffer was 10 mM in disodium hydrogen phosphate, borate, phenylboronic acid and SDS at pH 9.0; the running voltage was 400 V/cm.

(b) Electropherogram showing the reaction product from an incubation containing LacNAc-TMR (peak 3) and GDP-fucose with the Triton X-100 extract from *H. pylori* strain UA 861. Peak 5 corresponds to Lewis^x (βGal(1→4)[αFuc(1→3)]βGlcNAc-TMR) formed.

(c) Electropherogram showing the product obtained from incubations containing βGlcNAc-TMR (peak 2) and UDP-galactose with an extract of *H. pylori* strain UA 861. Subsequent methylation analysis confirmed the unidentified peak to be αGal(1→6)βGlcNAc-TMR.

(d) LacNAc-TMR product (peak 3) formed in incubations of GlcNAc-TMR (peak 2) and the donor UDP-galactose with an extract from *H. pylori* strain UA 802.

(e) Quantitative formation of Lewis^x (peak 5) by an extract of *H. pylori* strain UA 802 using LacNAc-TMR as the acceptor and GDP-fucose as the donor.

The identification of an unusual α1,6 galactosyltransferase by CE-LIF and methylation prompted further investigation of the lipopolysaccharide chains on cell surface of *H. pylori* UA861. A recent report on the detection of glucosylated *N*-acetyllactosamine O-antigen chain in the lipopolysaccharide from *H. pylori* UA861 suggested this unusual enzyme is likely to be an α1,6 glucosyltransferase rather than a galactosyltransferase (12). This discrepancy arises because of the use of UDP-galactose as the donor in the reaction. UDP-[^{3}H]glucose was not tested as a donor because the presence of an α1,6 glucosyltransferase was not expected in the cell extract. The bacterium may have both α1,6 glucosyltransferase and α1,6 galactosyltransferase activities *in vivo*. However, direct evidence awaits the cloning and subsequent characterization of the postulated enzymes.

2.3.5 Identification of Lewis^x by ^{1}H NMR

The product of the fucosyltransferase reaction from UA 802 is shown in the lower panel of **Fig. 2.3**. A new anomeric signal for H-1 (J = 4.0 Hz) at δ 5.12 p.p.m. is seen in the spectrum along with the characteristic quartet of H-5 (Fuc) which appears at the unique upfield shift of δ 4.84 p.p.m. (25) identical with the authentic standard of the Lewis^x trisaccharide (26). This is consistent with complete conversion of LacNAc to Lewis^x in these preparations. An identical spectrum was obtained for UA 1182 extracts. However, in this case, there was 78% conversion of the disaccharide acceptor to the trisaccharide product.

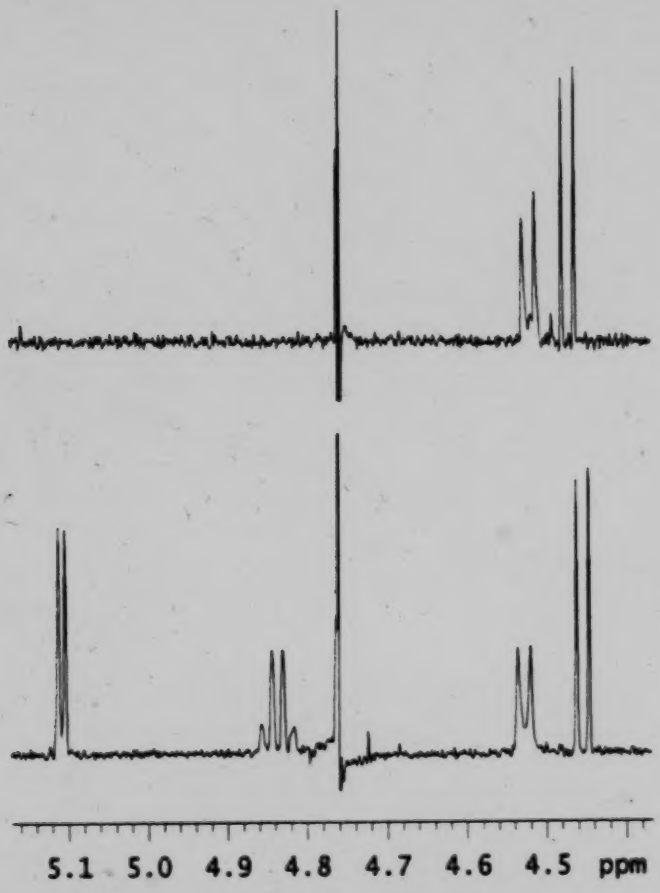

Figure 2.3 Partial 500 MHz ^{1}H NMR spectra of reaction products.

Upper panel: βGal(1→4)βGlcNAc-O(CH_2)$_8$COOMe (LacNAc-OR) obtained from incubations of GlcNAc-OR and UDP-galactose with extracts from UA 1182 cells. The H-1 signal for βGlcNAc is at 4.5 p.p.m. and H-1 of the βGal residue is near 4.5 p.p.m.

Lower panel: Lewis^x product isolated from incubations containing LacNAc-OR and GDP-fucose with a Triton X-100 extract from UA 802 cells. The signal for H-1 of the αFuc unit is at 5.12 p.p.m., and the quartet for H-5 of fucose at 4.84 p.p.m.

2.3.6 Biosynthetic Pathway of Lewis^x in *H. pylori*

The biosynthesis of Lewis^x in *Helicobacter pylori* most likely proceeds as outlined in **Scheme 2.1**. GlcNAc-OR is converted to LacNAc-OR by a β1,4 galactosyltransferase in UA 802 and UA 1182 using UDP-galactose as donor. For UA 861 insufficient β1,4 galactosyltransferase activity is present in the extracts to demonstrate this conversion, and only the α1→6 product has been isolated. UA 861, UA 802 and UA 1182 all convert LacNAc to Lewis^x through fucosyltransferases which use GDP-fucose as a donor substrate. Insufficient activity was present to confirm Lewis^x by NMR in UA 861 extracts. However, capillary electropherograms of reaction mixtures are consistent with Lewis^x formation. Extracts from UA 1182 and UA 802 did not transfer fucose from GDP-fucose to the monosaccharide, GlcNAc-OR, confirming that the biosynthesis of Lewis^x in *Helicobacter pylori* is strictly ordered i.e. galactosylation is followed by fucosylation, as in mammalian biosynthesis. Since the acceptors used in this study are synthetic, then while it could not be shown here that fucose is transferred to GlcNAc-OR, this may be possible, *in vivo*, where transfer would be to a natural acceptor.

2.3.7 Kinetic Variation in Different Strains of *H. pylori*

Preliminary characterizations of the enzymes revealed that K_m^{app} values for both donors and acceptors varied between strains (**Table 2.2**). In the case of the fucosyltransferases, the K_m^{app} values for the acceptor, LacNAc, range from 45 to 350 μM, and for the donor, GDP-fucose, from 17 to 140 μM. Similarly, for galactosyltransferases, the acceptor K_m^{app} values were 191 and 414 μM and the donor

K_m^{app} values were 28 and 102 μM. The crude extracts may contain more than one form of α1,3 fucosyltransferase and β1,4 galactosyltransferase. However, the absence of biphasic kinetics suggests that if multiple forms are present, they are kinetically indistinguishable.

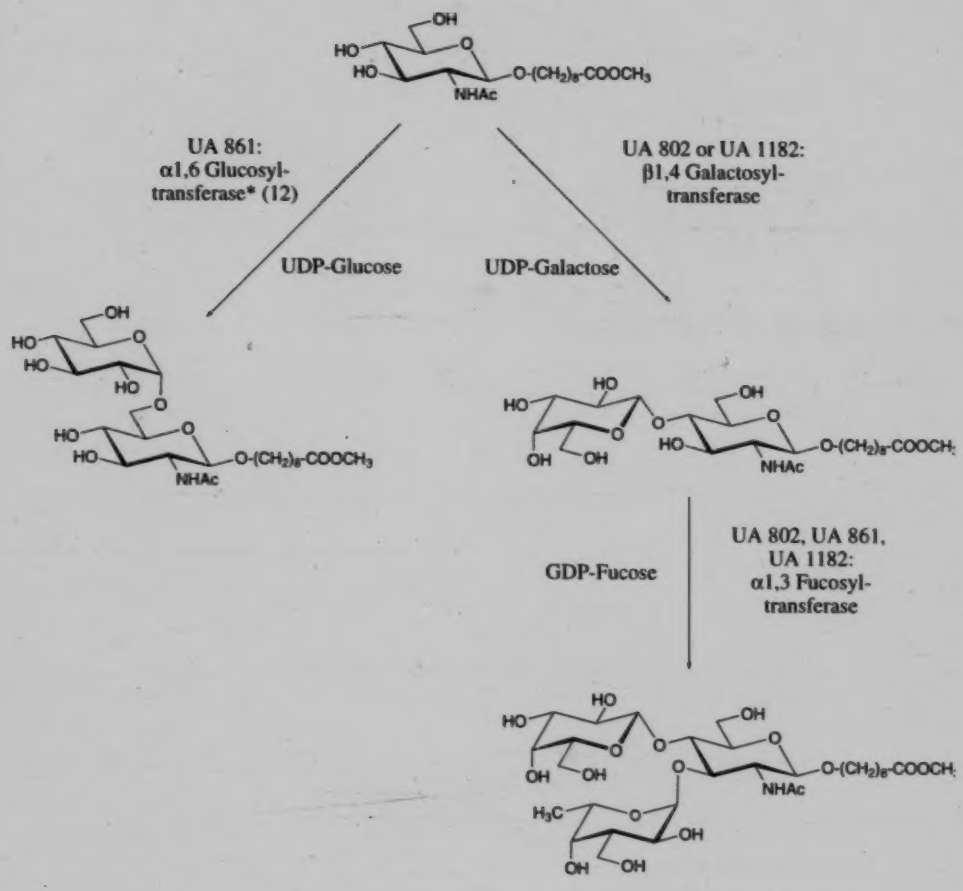

Scheme 2.1 Biosynthesis of Lewis^x in *H. pylori*. Galactosylation of GlcNAc is catalyzed by a β1,4 galactosyltransferase in *H. pylori* strains UA 802 and UA 1182 using the donor, UDP-galactose. Insufficient β1,4 activity is found in UA 861, where the major product detected is αGlc1→6GlcNAc (12). In all three strains, fucosylation of the disaccharide, LacNAc, is catalyzed by α1,3 fucosyltransferase which transfers fucose from GDP-fucose to yield Lewis^x.

Table 2.2 K_m^{app} values for the substrates of the Membrane Bound Glycosyltransferases from *Helicobacter pylori* strains

Strain	Substrates			
	LacNAc-OR[a] (μM)	GDP-Fuc (μM)	GlcNAc-OR (μM)	UDP-Gal (μM)
UA 861	180 ± 20[c]	30 ± 6	—[b]	—[b]
UA 802	45 ± 3	140 ± 20	190 ± 20	28 ± 2
UA 1182	350 ± 30	17 ± 2	410 ± 20	102 ± 7

[a] R = $(CH_2)_8COOMe$.

[b] Only α1,6 activity quantitated.

[c] K_m^{app} values were mean ± S.D. (n=2) from SigmaPlot.

2.4 Conclusions

Radiochemical assays can be used to screen the activities of glycosyltransferases from *Helicobacter pylori* extracts. The biosynthesis of Lewis^x in these strains of *H. pylori* was determined by CE-LIF which facilitated separation and detection of low levels of products resulting from low activities of glycosyltransferases in the extracts, or by ^{1}H-NMR after a preparative synthesis. The compound produced in the mixture of UA 802 incubated with GlcNAc and UDP-galactose was identified as αGal(1→6)GlcNAc by both ^{1}H NMR and methylation analysis. This unusual enzyme was thought to be an α1,6 galactosyltransferase because UDP-galactose was used in the reaction mixture and was transferred to the acceptor. The structural results obtained from studies on the intact lipopolysaccharide of *H. pylori* UA861 suggested that the product was likely αGlc(1→6)GlcNAc formed by an α1,6 glucosyltransferase rather than by an α1,6 galactosyltransferase (12). It is uncertain whether *H. pylori* UA861 have both enzymes *in vivo*, however, cloning and subsequent characterization would provide direct evidence of the postulated enzymes.

The biochemical basis for the different cellular distributions, levels of activity and kinetic properties of the enzymes in the three strains of *Helicobacter pylori* is unclear. Either different protein sequences or post-translationally modified proteins might be involved. Diversity at the genome level has been demonstrated for different strains of *H. pylori* (16). The isolation of homogeneous enzymes, sequencing and cloning of the galactosyltransferases and fucosyltransferases will provide insights into their differential properties. A comparison with the sequences of mammalian glycosyltransferases will be of particular interest.

2.5 References

1. Springer, G. F., Williamson, P., and Brandes, W. C. (1961) *J. Exp. Med.* **113**, 1077-1093.
2. Sashkov, A. S., Vinogradov, E. V., Knirel, Y. A., Nifant'ev, N. E., Kochetkov, N. K., Dabrowski, J., Kholodkova, E. V., and Stanislavsky, E. S. (1993) *Carbohydr. Res.* **241**, 177-188.
3. Aspinall, G. O., Monteiro, M. A., Pang, H., Walsh, E. J., and Moran A. P. (1994) *Carbohydr. Lett.* **1**, 151-156.
4. Schachter, H. (1991) *Current Biology* **1**, 755-765.
5. Kleene, R., and Berger, E. G. (1993) *Biochim. Biophys. Acta.* **1154**, 283-325.
6. Moran, A. P., Helander, I. M., and Kosunen, T. U. (1992) *J. Bacteriol.* **174**, 1370-1377.
7. Hakomori, S. (1989 *Adv. Cancer Res.* **52**, 257-331.
8. Muramatsu, T. (1988) *Biochimie* **70**, 1587-1596.
9. Feizi, T. (1985) *Nature* **314**, 53-57.
10. Velupillai, P., and Harn, D. A. (1994) *Proc. Natl. Acad. Sci. USA*, **91**, 18-22.
11. Chan, N. W. C., Stangier, K., Sherburne, R., Taylor, D. E., Zhang, Y., Dovichi, N. J., and Palcic, M. M. (1995) *Glycobiology* **5**, 683-688.
12. Monteiro, M. A., Rasko, D., Taylor, D. E., and Perry, M. B. (1998) *Glycobiology* **8**, 107-112.
13. Gokhale, U. B., Hindsgaul, O., and Palcic, M. M. (1990) *Can. J. Chem.* **68**, 1063-1071.

14. Larsen, E., Palabrica, T., Sajer, S., Gilbert, G. E., Wagner, D. D., Furie, B. C., and Furie, B. (1990) *Cell* **63**, 467-474.

15. Bradford, M. (1976) *Anal. Biochem.* **72**, 248-254.

16. Taylor, D. E., Hargreaves, J. A., Ng, L. K., Sherbaniuk, R. W., and Jewell, L. D. (1988) *Am. J. Clin. Pathol.* **87**, 49-54.

17. Taylor, D. E., Eaton, M., Chang, N., and Salama, S. M. (1992) *J. Bacteriol.* **174**, 6800-6806.

18. Palcic, M. M., Heerze, L. D., Pierce, M., and Hindsgaul, O. (1988) *Glycoconjugate J.* **5**, 49-63.

19. Zhao, J. Y., Dovichi, N. D., Hindsgaul, O., Gosselin, S., and Palcic, M. M. (1994) *Glycobiology* **4**, 239-242.

20. Zhang, Y., Le, X., Dovichi, N. J., Compston, C. S., Palcic, M. M., Diedrich, P., and Hindsgaul, O. (1995) *Anal. Biochem.* **227**, 368-376.

21. York, W. S., Darvill, A. G., McNeil, M., Stevenson, T. T., and Albeasheimo, P. (1985) *Methods Enzymol.* **118**, 3-40.

22. Stellner, K., Saito, H., and Hakomori, S-I. (1973) *Arch. Biochem. Biophys.* **155**, 464-472.

23. Hakomori, S. (1964) *J. Biochem.* **55**, 205-208.

24. Lindberg, B., and Lonngren, J. (1978) *Methods Enzymol.* **50**, 3-33.

25. Palcic, M. M., Venot, A. P., Ratcliffe, R. M., and Hindsgaul, O. (1989) *Carbohydr. Res.* **190**, 1-11.

26. Hindsgaul, O., Norberg, T., LePendu, J., and Lemieux, R. U. (1982) *Carbohydr. Res.* **109**, 109-142.

Chapter Three

Intracellular Glucosidase I Inhibition in Cultured Cells Measured by Capillary Electrophoresis with Laser-Induced Fluorescence Detection

---

A version of this chapter has been submitted for publication.

Chan, N. W. C., Arriaga, E., Dovichi, N. J., Srivastava, O. P., and Palcic, M. M. (1998) *Glycobiology*, submitted.

Acknowledgments: I thank Miss Xiaoling Puyang for maintaining the HT29 cell line, and Dr. Rakesh Bhatnagar for help in the confocal laser scanning microscopy.

3.1 Introduction

N-linked glycosylation of mammalian proteins in the lumen of endoplasmic reticulum is initiated by transfer of the $Glc_3Man_9GlcNAc_2$ unit from dolichol pyrophosphate to an asparagine residue on the protein (1). Further modification of this asparagine $Glc_3Man_9GlcNAc_2$-*N*-conjugate by the trimming enzyme, α-glucosidase I, involves removal of the terminal glucose unit (2). The resulting oligosaccharide is hydrolyzed by α-glucosidase II and different α-mannosidases prior to transferase-mediated addition of a variety of sugar units. The complex hybrid oligosaccharides thus formed are then transported to the plasmalemma for expression on the cell surface. Inhibition of α-glucosidase I prevents the removal of glucose residues during the normal processing of HIV gp-120 membrane protein and results in altered glycoproteins that have been implicated in breaking the virus replication cycle. Thus, α-glucosidase I is an important enzyme in this pathway, and has been studied intensively from the point of view that inhibitors may be potential anti-viral agents and thus aid in the treatment of HIV (3-12).

In conventional assay systems, measurement of the efficacy of an α-glucosidase I inhibitor usually requires two separate stages. Cultured cells are incubated with inhibitor in the presence of radiolabeled substrate, and sequestered radioactivity is measured after a predetermined period. Cells are then lysed and radiolabeled glycoproteins are collected. These are digested into fragments with enzymes such as pronase and endoglucosaminidase H (Endo-H). Separation of fragments is achieved by gel filtration, and since radioactivity present in different fractions can be attributed in part to α-glucosidase I activity, the degree of enzyme

inhibition can be assessed (8-11,13-17). The inhibitory potency of the compound towards the enzyme is also tested *in vitro* versus enzyme which has been partially purified, thereby providing a benchmark against which results obtained from intracellular studies might be compared (8,15-18). Since it may take several days to determine the effects of an inhibitor at a single concentration, estimation of IC_{50} values is a time-consuming and costly task.

A method that permits the rapid determination of inhibitor potencies by a non-radiochemical procedure would thus be advantageous, particularly if the degree of sensitivity could be maintained, or even exceeded. In the present study, the activity of α-glucosidase I has been examined in a human colon carcinoma HT29 cell line by capillary electrophoresis with laser-induced fluorescence detection (CE-LIF), which allows separation and quantification of metabolites in less than 15 minutes. The natural $Glc_3Man_9GlcNAc_2$ substrate was replaced with triglucose-TMR (TG-TMR), a truncated structure labeled with the fluorescent TMR molecule (19-21). TG-TMR is metabolized by α-glucosidase I to diglucose-TMR (DG-TMR), and thereafter by glucosidase II, first to monoglucose-TMR (MG-TMR) and finally to the linker-arm-TMR (HO-TMR) (**Scheme 3.1**). The TG-TMR substrate entered HT29 cells during incubation and its *in vivo* intracellular degradation was determined by this method. The potencies of two α-glucosidase I inhibitors, 1-deoxynojirimycin (1-dNJ) and castanospermine (CAST), were assessed as inhibitors of TG-TMR degradation in this intracellular assay. Their IC_{50} values were obtained and reflected the bioavailability of the inhibitor in the intracellular compartment where the enzyme is localized. In order to show that this application has the potential to be used to uncover new

compounds of therapeutic importance, a novel carbohydrate-based inhibitor was tested and the degree of enzyme inhibition was assessed.

The separation efficiency of CE provides improved peak resolution compared with existing gel filtration methods, leading to more accurate estimations of inhibitor potencies. With a detection limit of approximately 200 molecules, the use of CE-LIF allows analysis of enzyme activities in individual cultured cell (22). This method should be suitable for the assay of a variety of enzymes, and for examinations of enzyme inhibitors, in many different cell systems.

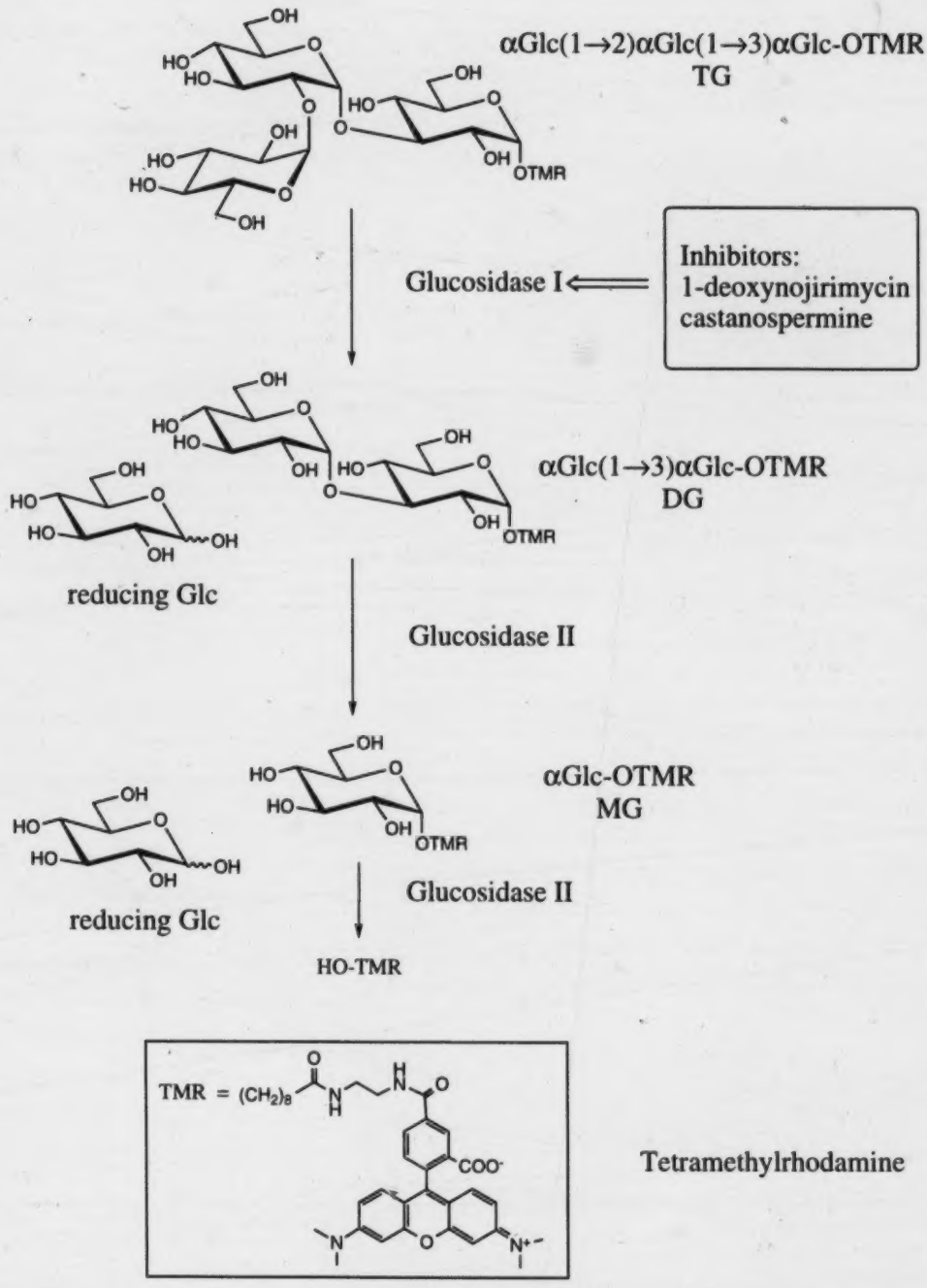

Scheme 3.1 Metabolism of TG-TMR by glucosidases to DG-, MG-, and HO-TMR.

3.2 Experimental Section

3.2.1 Materials

A human colon HT29 adenocarcinoma cell line was obtained from American Type Culture Collection (Rockville, MD). Dulbecco's modified Eagle's medium (D-MEM), fetal bovine serum, gentamicin, trypsin-EDTA, and Trypan-Blue dye were from Gibco BRL, (Gaithersburg, MD). Cells were grown in T25 culture flasks or Falcon tissue culture plates purchased from Becton Dickinson Labware (Lincoln Park, NJ). αGlc(1→2)αGlc(1→3)αGlc-*O*gr (TG), αGlc(1→3)αGlc-*O*gr (DG), αGlc-*O*gr (MG) were provided by Dr. O. Srivastava at the Carbohydrate Research Program, Alberta Research Council. DG-TMR, MG-TMR, and linker-arm-TMR were provided by Dr. O. Hindsgaul at the department of Chemistry, University of Alberta. The fluorescent probe, tetramethylrhodamine was purchased from Molecular Probes Inc. (Eugene, OR), and covalently linked to the oligosaccharides following the method described by Zhang *et al.* (21) with modifications. The micro glass homogenizers used were from Fisher Scientific (Nepean, ON). The Sep-Pak Plus C-18 reverse phase cartridges were obtained from Waters (Mississauga, ON), and were conditioned before use by washing with 5 ml of HPLC grade methanol and 10 ml of Milli-Q water. The MultiProbe 2001 confocal laser scanning microscope (CLSM) was purchased from Molecular Dynamics (Sunnyvale, CA). The covered glass-bottomed microwell dish used in cell culture for CLSM was from MatTek Corp. (Ashland, MA). Castanospermine, 1-deoxynojirimycin, and swainsonine were obtained from Boehringer Mannheim (Laval, QC). The Millex-GV filter units were from Millipore (Mississauga, ON). The capillary electrophoresis instrument was

constructed in the laboratory of Dr. N. J. Dovichi, Department of Chemistry, University of Alberta) and contained a He-Ne laser (543.5 nm) from Melles Griot (Victoria, B.C., Canada), and a Spellman High Voltage supply (Spellman High Voltage Electronic Corp., Plainview, NY). The analysis programs used in this chapter were Igor Pro, version 2.04 from WaveMetrics (Lake Oswego, OR), and GraphPad Prism, version 2.0 from GraphPad software Inc. (San Diego, CA).

3.2.2 Preparation of Ethylenediamine monoamides

Five mg αGlc(1→2)αGlc(1→3)αGlc-*O*gr (TG-*O*gr) was dissolved in 3 ml neat anhydrous ethylenediamine and the mixture was heated at 70°C for 50 hr in a screw-capped culture tube with a Teflon lined cap. After reaction, the tube was cooled in an ice bath and 5 ml cold water was added. The cooled solution was diluted with 20 ml water and loaded onto a Sep-Pak C-18 cartridge which was washed with 30 ml water. The aqueous flowthrough was loaded onto a fresh Sep-Pak cartridge which was also washed with 30 ml water. Product was eluted from each Sep-Pak by washing with 30 ml methanol, the eluates were combined, and the methanol was evaporated. The residue was dissolved in 10 ml water and re-isolated on a third, fresh Sep-Pak cartridge from which it was eluted with 30 ml methanol. The residue after evaporation was dissolved in 5 ml water and passed through a 0.2 μm filter and lyophilized. Reaction yield was 90%. Product was confirmed by ^{1}H NMR (Varian Inova 300, 300 MHz in D_2O) and electrospray ionization-mass spectrometry (ESI-MS).

3.2.3 Preparation of TG-TMR

Fluorescent labeling reaction was done by mixing 5 mg of 5-carboxytetramethylrhodamine succinimidyl ester in 250 µl dimethylformamide (DMF) and 4-5 mg of the above prepared ethylenediamine monoamide in 250 µl 0.185 M $NaHCO_3$, pH 8.5. After 4 hr, the reaction mixture was diluted with 5 ml water and applied to a DEAE-A25 column (Cl^- form, 0.8 x 5 cm) and about 50 ml water was passed through the column until the eluate was colourless. The brilliant red product was isolated from the washed Sep-Pak C-18 adsorption as described in **section 3.2.2**. The residue in methanol was dissolved in a solvent mixture of ethylacetate:methanol:water (3:2:1) and loaded onto an Iatrobead column (2.5 x 30 cm). The R_f of TG-TMR in the solvent system was 0.21; fractions containing TG-TMR were pooled and solvent was evaporated. The red residue was dissolved in water and re-isolated on a Sep-Pak C-18 cartridge, passed through a 0.2 µm filter, and lyophilized. Product yields were in the range of 70%. The product was confirmed by ^1H NMR (Varian Inova 300, 300 MHz in CD_3OD) and electrospray ionization-mass spectrometry (ESI-MS).

3.2.4 Culture of HT29 cells

A human colon HT29 adenocarcinoma cell line, was grown in T25 culture flasks or 24-well Falcon tissue culture plates in D-MEM supplemented with 10% fetal bovine serum and 40 µg/ml gentamicin, at 37°C and in an atmosphere of 5% CO_2/air. Cells were grown to 80% confluence (2-3 days) prior to assay. Incubations were initiated by adding culture medium containing 25 µM TG-OTMR (19, 20) to the

cells. After an 18 hr incubation in a culture flask, 50 ml of sterile phosphate-buffered saline (PBS) were added to the flask and cells were soaked for 5 minutes. Cells were then washed four times with 5 ml PBS. 1 ml Trypsin-EDTA, (0.05%(w/v) trypsin, 0.53 mM EDTA) was added to the flask, and when cells had been coated evenly, the trypsin solution was aspirated. Cells were then incubated at 37°C for 6 minutes and were dislodged from the flask in 1 ml PBS. A 50 µl aliquant of cells was mixed with 450 µl Trypan-Blue dye and cells were counted and their viability assessed in a haemocytometer. A 100 µl cell pellet was obtained by centrifuging the remaining cell suspension at 500 *g* for 4 minutes. The pellet was resuspended in 400 µl water and homogenized gently once every 15 minutes at 0°C over a 1.5 hr period in a micro glass homogenizer. The homogenate was loaded onto a conditioned Sep-Pak Plus C-18 reverse phase cartridge (23), washed with 20 ml water, and the TMR labeled oligosaccharides were eluted with 3 ml HPLC-grade methanol. The solvent was evaporated and the sample dissolved in water and lyophilized to reduce the volume to less than 20 µl. The cell medium, as well as washings (pre- and post-trypsinization) were also loaded onto Sep-Pak Plus C-18 cartridges prior to analysis by CE-LIF.

3.2.5 Confocal Laser Scanning Microscopic Image of HT29 Cells Incubated with TG-TMR

Cells were grown in a covered glass-bottomed microwell dish, incubated with substrate, washed, and images were obtained with a MultiProbe 2001 confocal laser scanning microscope. The excitation source was a 4 mW, 568 nm Argon-Krypton laser.

3.2.6 Inhibition Assays with 1-Deoxynojirimycin and Castanospermine

Cells were grown in separate wells in a 24-well plate (1.5 ml well volume). Castanospermine (Boehringer Mannheim; 300 nM to 1 mM) or 1-deoxynojirimycin (Boehringer Mannheim; 100 nM to 10 mM) were added to wells 24 hr prior to incubation with TMR-labeled substrate. Following the 24 hr inhibitor preincubation period, medium was aspirated from wells and was replaced with fresh medium containing the appropriate concentration of inhibitor, as well as the TG-TMR substrate which had been filtered through a Millex-GV filter. Cells were then incubated at 37°C for a further 18 hr. The α-mannosidase II inhibitor, swainsonine (2, 16, 24-26), was used as a negative control. Cells were washed and trypsinized, as described above, prior to analysis by CE-LIF. To determine the inhibitory effect of the novel inhibitor, 1,5-trans-*C*-glucoside (27), a concentration of 5 mM was used in the medium during pretreatment and incubation with substrate as described above. All the inhibitors used in this chapter are shown in **Fig. 3.1**.

3.2.7 Sample Preparation for Analysis by Capillary Electrophoresis with Laser-Induced Fluorescence Detection

Appropriate amounts (typically 15-20 µl) of water were added to lyophilized samples such that each injection volume (13 pl) contained the equivalent of the volume of one cell. The CE running buffer contained 10 mM disodium hydrogen phosphate (dibasic), 10 mM phenylboronic acid, 10 mM SDS, and 10 mM sodium borate at pH 9.3. A capillary electrophoresis system equipped with post-column laser-induced fluorescence detection (20, 21) was used for separation and analysis of

oligosaccharides. Separation was done in a fused silica capillary (60 cm x 10 μm i.d.) with an electric field of 400 V/cm. A 5 mW He-Ne laser with a wavelength of 543.5 nm was used to excite the TMR molecules. Sample was introduced into the capillary electrokinetically by applying a potential of 1 kV for 5 seconds. All separations were performed at ambient temperature, without temperature control. The instrument had an injected (13 pl) detection limit of 200 rhodamine 6G molecules, as determined by Knoll's method (28).

3.2.8 Data Analysis

The area under each peak was determined with the graphing and data analysis program, Igor Pro, version 2.04. The sum of the areas under the hydrolyzed product peaks was divided by the total area to calculate the degree of hydrolysis in each case. The degree of hydrolysis at each inhibitor concentration was then compared with that in the control to obtain the % inhibition. These values were plotted against inhibitor concentrations (log scale) in the cell medium, and IC_{50} values were obtained by nonlinear regression analysis of the data with GraphPad Prism, version 2.0.

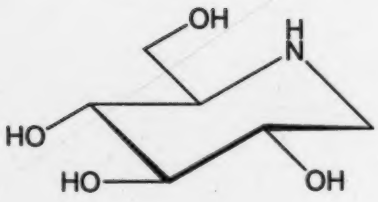

1-deoxynojirimycin

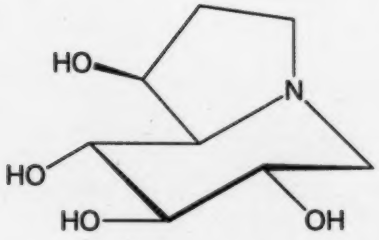

castanospermine

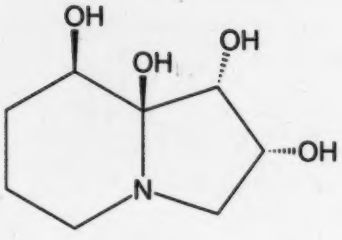

Swainsonine

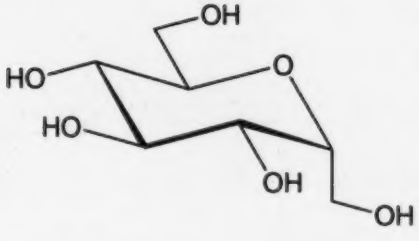

1,5-trans-*C*-glucoside

Figure 3.1 Structures of inhibitors used in experiments described in this chapter.

3.3 Results and Discussion

3.3.1 ^{1}H NMR and ESI-MS characterization of TG-TMR

Characterization of TG-TMR was done by ^{1}H NMR in CD_3OD using a Varian Inova 300 MHz spectrometer. **Fig. 3.2A** shows the partial 300 MHz spectrum of the anomeric region of TG-TMR. The H-1 signals for three αGlc are at 5.34, 4.99, 4.74 p.p.m. The broad band at around 4.85 p.p.m. is the residue of the D_2O suppression. **Fig. 3.2B** shows the partial spectrum of the aromatic protons of TG-TMR. All nine aromatic proton signals are at δ 8.50 (one H), 8.04 (one H), 7.36 (one H), 7.24 (two H), 7.00 (two H), and 6.91 (two H). The molecular mass of TG-TMR ($C_{54}H_{74}N_4O_{21}$, exact mass = 1114.5) determined by ESI-MS was 1115.5 $(M+H)^+$, and 1137.5 $(M+Na)^+$.

3.3.2 Intracellular Localization of Fluorescent Substrate using Confocal Scanning Laser Microscopy

The TG-TMR substrate was seen by confocal microscopy (22) to have gained access to the cytoplasm and to have become concentrated within unidentified subcellular organelles of HT29 cells. **Fig. 3.3** shows a confocal laser scanning microscopic image of the HT29 colon carcinoma cells after incubation with TG-TMR and washing with phosphate-buffered saline. There was no detectable leakage of the fluorescent-tagged compound from the cells into the surrounding medium. Incubation of HT29 cells with DG-TMR resulted in complete removal of the disaccharide and formation of MG-TMR and HO-TMR products (**Fig. 3.4**), confirming the presence of glucosidases other than glucosidase I in the cells and

illustrating that the final products of TG-TMR metabolism would be MG-TMR and HO-TMR.

3.3.3 Detection of α-Glucosidase Products by CE-LIF

Separation by CE-LIF of labeled mono-, di-, and trisaccharides from HT29 cells incubated with fluorescent TG-TMR substrate is illustrated in an electropherogram (**Fig. 3.5**). The major peak (peak 1) was identified as TG-TMR, while peaks 2, 3 and 4 corresponded to DG-TMR, MG-TMR and HO-TMR, respectively. The average degree of hydrolysis of TG-TMR in these experiments was 20% ± 1.5% (n = 16). This electropherogram provides confirmation that the substrate was first converted to DG-TMR and then to MG- and HO-TMR. Shown in the insert to **Fig. 3.5** is the separation of a mixture of saccharide-TMR standards, each at 500 pM in an injected volume of 13 pl. Migration times varied slightly between runs due to factors such as temperature fluctuation, capillary condition and slight differences in buffer content affecting electroosmotic flow in the capillary. Thus, in each experiment, four samples were spiked with the four individual standards at final concentrations of 5 nM, this being adequate to increase peak height and area sufficiently to allow identification of peaks in a parallel, unspiked sample.

In order to check that the hydrolyzed products did not leak from the cells, the culture medium and washings were examined by CE-LIF. Analysis of the medium following incubation showed a single peak corresponding to TG-TMR, while fluorescence signals in the cell wash were not above background (**Fig. 3.6**).

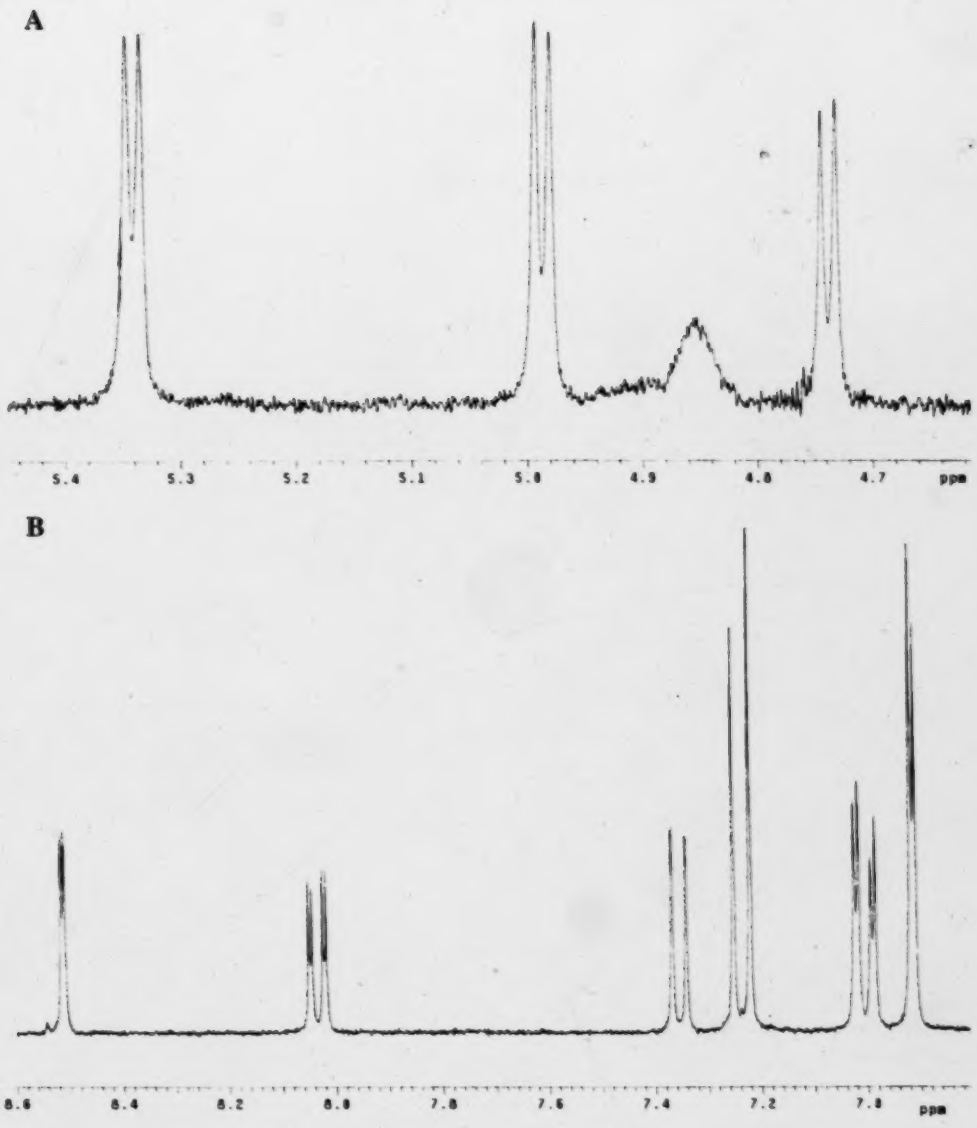

Figure 3.2 Partial 300 MHz ^{1}H NMR spectrum of TG-TMR in CD_3OD. The upper spectrum (**A**) shows the anomeric region of TG-TMR, three doublets are the H-1 protons of three αGlc residues. The lower spectrum (**B**) shows the nine aromatic protons of TG-TMR.

Figure 3.3 Confocal laser scanning microscopic image of HT29 cells incubated with TG-TMR. The image clearly shows the fluorescent signal derived from intracellular substrate (arrows). Fluorescence is associated with distinct subcellular organelles, but not the nucleus. The scale bar represents 10 μm.

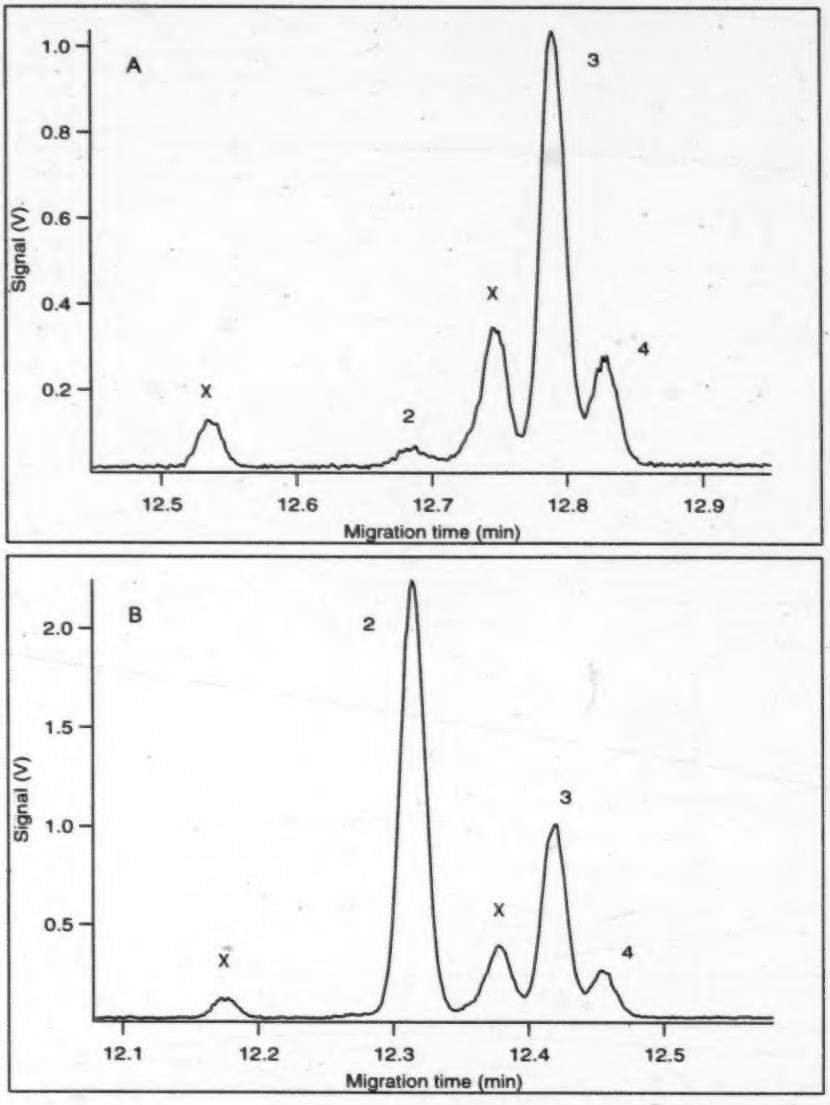

Figure 3.4 Diglucose-TMR incubation data: all the diglucose-TMR had converted to monoglucose-TMR and HO-TMR (**A**) confirmed by co-migration with 25 nM standard DG-TMR (**B**). Therefore, the cellular content of α-glucosidase II is higher than that of α-glucosidase I. Peak 2, DG-TMR; peak 3, MG-TMR; peak 4, HO-TMR; peaks X were unknown metabolic by-products.

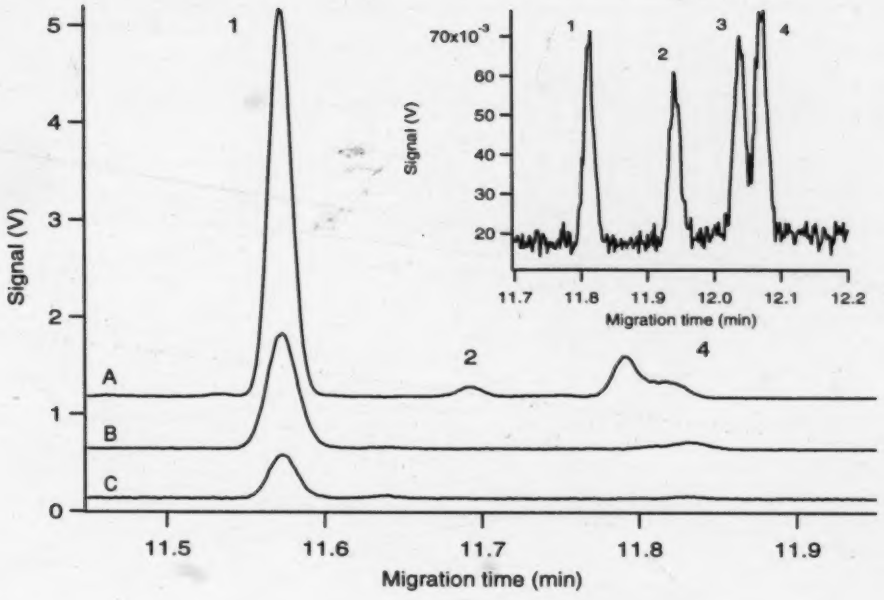

Figure 3.5 Electropherogram of TMR-labeled compounds obtained from CE separation of the contents of HT29 cells incubated with TG-TMR. Peak 1 is the substrate, TG-TMR, peak 2 is the product of glucosidase I activity, DG-TMR, and peaks 3 and 4 correspond to MG-TMR and HO-TMR, respectively, formed by subsequent removal of the remaining 2 glucose units by glucosidase II. Peaks were identified by demonstrating co-migration with individual standards. The insert shows an expanded portion of the CE separation of a sample of 4 authentic standards. Concentration of each standard was 500 pM, and the injected amount was 3,600 molecules per standard.

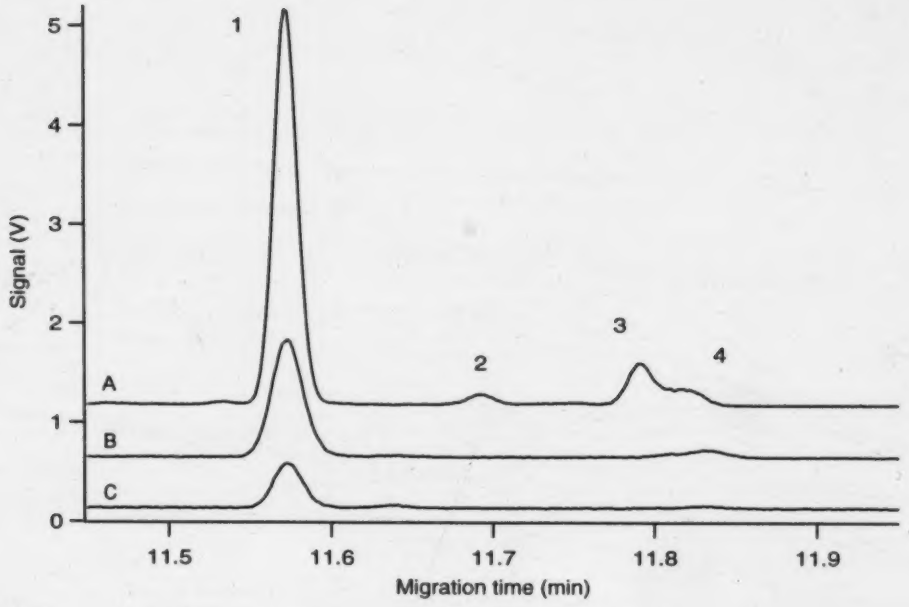

Figure 3.6 Electropherograms of TMR-labeled species obtained from CE separation of the contents of lysed HT29 cells (curve **A**), the cell medium (curve **B**), and the final PBS buffer wash of the HT29 cells (curve **C**). Electropherograms **A** and **B** were offset vertically for clarity.

HT29 cells incubated with inhibitors showed no changes in morphology or cell viability compared with control cells, indicating that at the concentrations used, inhibitors displayed no cytotoxicity.

3.3.4 Intracellular Inhibition of α-Glucosidase

Typical electropherograms obtained following treatment of HT29 cells with inhibitors showed that the inhibition of glucosidase I activity by CAST and 1-dNJ was concentration-dependent. For example, approximately 80% of enzyme activity was inhibited by 1 mM CAST compared with only 8% inhibition at 10 μM. Inhibition by 1-dNJ appeared to be less potent, since 3 mM inhibitor caused only 60% inhibition, and enzyme activity was unaffected by the inclusion of 6 μM 1-dNJ in the cell medium (**Fig. 3.7**).

No error bars are shown for each concentration on the IC_{50} plots due to the irreproducibility of the different cell passages, the plots were obtained from single set of data using a wide range of inhibitor concentrations. However, triplicates of each concentration were run and the error bars from each run were discernible.

Inhibitor IC_{50} values were determined by nonlinear regression to be 165 μM and 320 μM for CAST and 1-dNJ, respectively (**Fig. 3.8**). These values are comparable with those (53 μM and 306 μM) obtained in $B_{16}F_{10}$ mouse melanoma cells by a radiochemical method (8).

HT29 cells were also incubated with the α-mannosidase II inhibitor, swainsonine, as a negative control. At 1 mM, swainsonine was without effect on hydrolysis of TG-TMR by α-glucosidase I (**Fig. 3.9**).

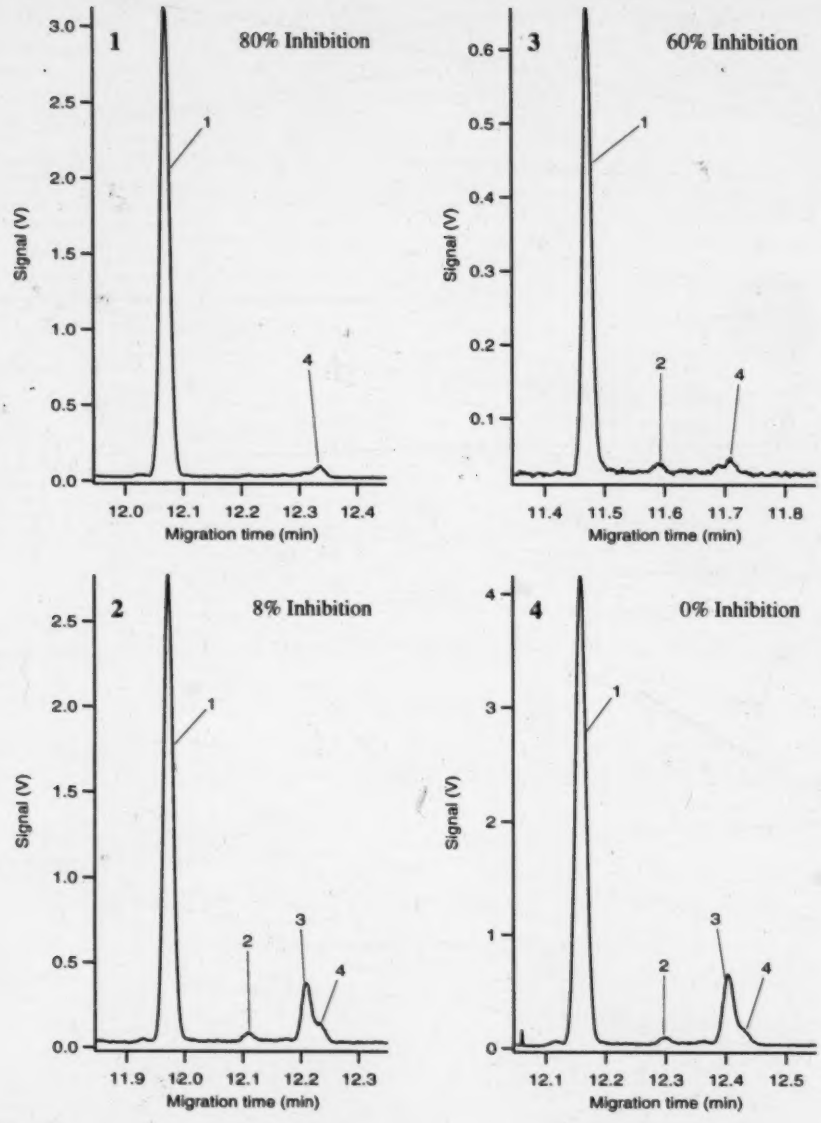

Figure 3.7 Electropherograms of HT29 cell contents after incubation with inhibitors followed by TG-TMR. Panels **1** and **2** show the effects of preincubating with 1 mM and 10 μM castanospermine, respectively. Panels **3** and **4** show effects of preincubating with 3 mM and 6 μM 1-deoxynojirimycin, respectively. Also shown is the degree of inhibition in each case, compared with controls.

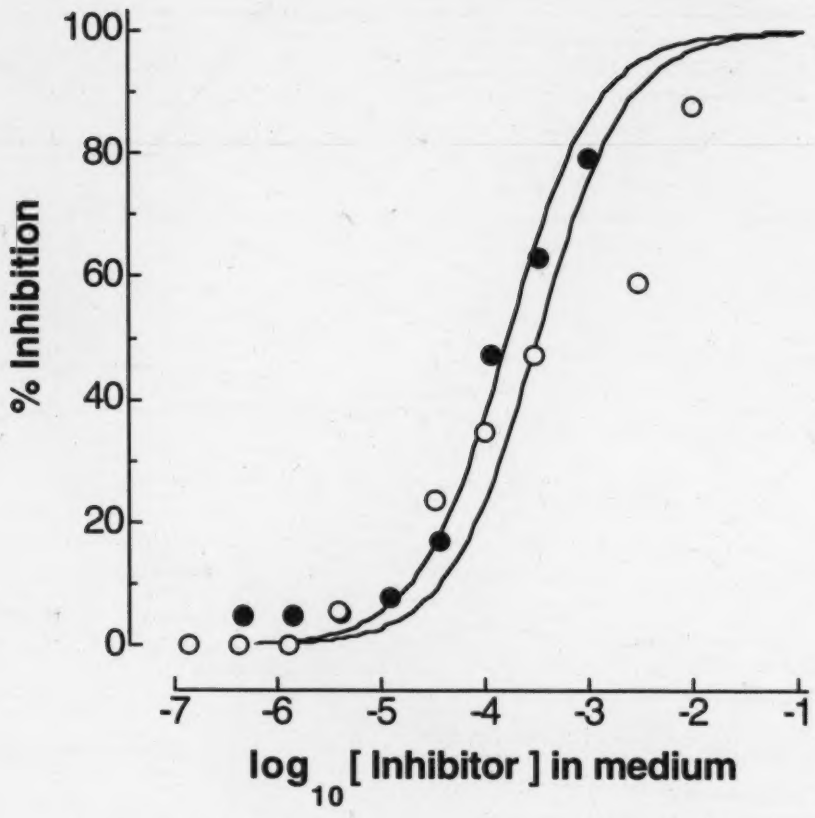

Figure 3.8 Inhibition of α-glucosidase I by a range of concentrations of 1-dNJ and CAST. Inhibition (%) was plotted against the logarithm of the concentration of the inhibitors in the cell medium. A sigmoid curve was fitted to the data by the nonlinear regression facility of GraphPad Prism, version 2.0. IC_{50} values were calculated to be 165 μM (CAST; ●) and 320 μM (1-dNJ; o). Triplicates were run for each concentration of inhibitor to obtain an average % inhibition. Due to the scale of the plot, the error bars are not visible. This set of data represents the inhibitory effects of 1-dNJ and CAST from only one passage of cells.

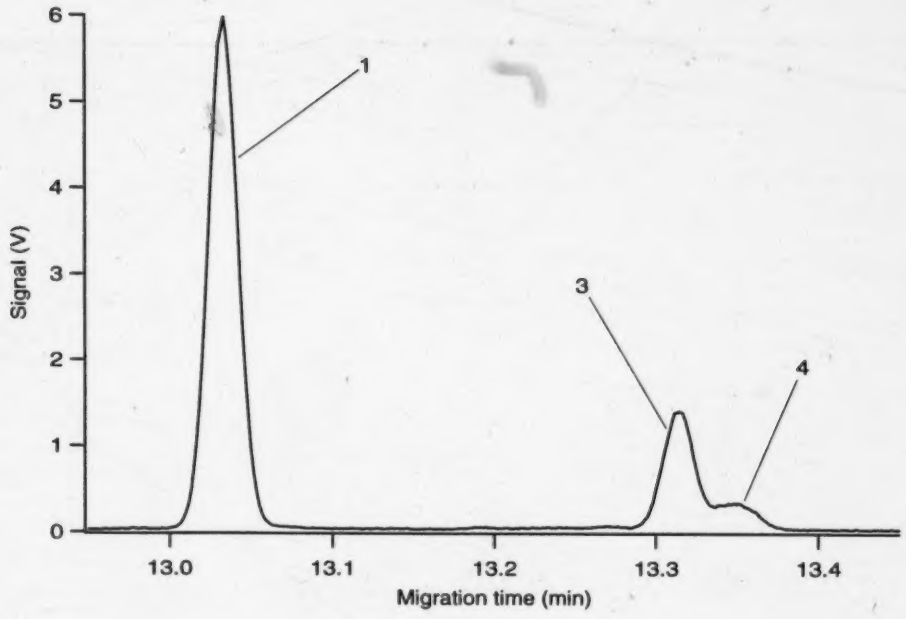

Figure 3.9 Electropherogram of HT29 cell contents after pretreatment with a mannosidase inhibitor, swainsonine, as negative control followed by TG-TMR incubation.

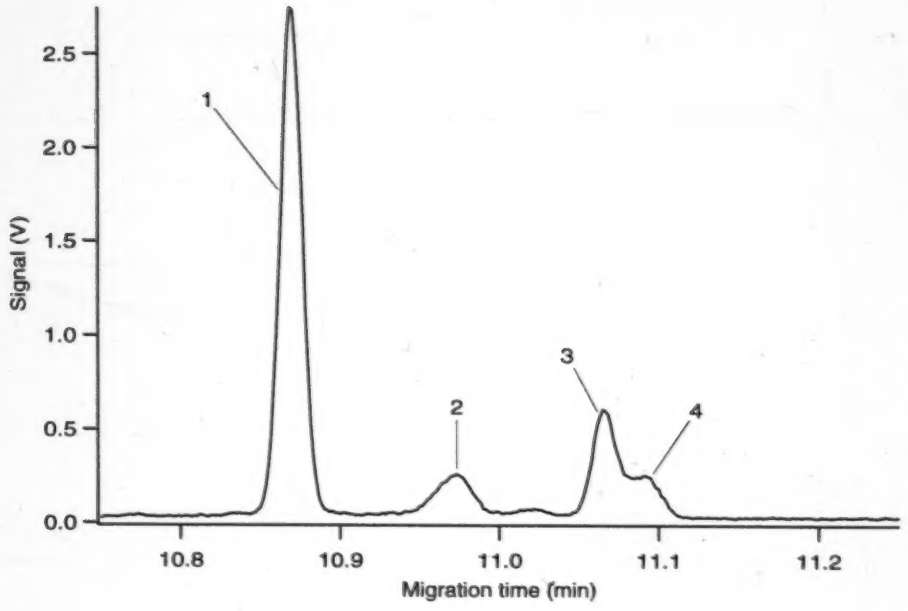

Figure 3.10 Electropherogram of HT29 cell contents after incubation with a novel carbohydrate-based inhibitor, 1,5-trans-*C*-glucoside (5 mM) followed by TG-TMR.

Fig. 3.10 shows electropherograms of HT29 cells after incubation with TG-TMR and 1,5-trans-*C*-glucoside. The compound showed 0% inhibition at a concentration of 5 mM and therefore, was not effective in terms of therapeutic importance.

1-Deoxynojirimycin was found to have an IC_{50} of 20 μM versus partially-purified glucosidase I from *S. cerevisiae* with radiolabelled [^{14}C] $Glc_3Man_9GlcNAc_2$ as substrate (17). Neverova and coworkers (29) reported IC_{50} values of 200 μM and 50 μM for 1-dNJ at substrate concentrations equal to 3 x K_m and 0.4 x K_m respectively, and with αGlc(1→2)αGlc(1→3)αGlc-O$(CH_2)_8COOCH_3$ as substrate. The inhibitor was reported to be even more potent versus a mammalian enzyme, displaying an IC_{50} of 3 μM versus glucosidase I isolated from calf liver, with $Glc_3Man_9GlcNAc_2$ as substrate (30). IC_{50} values reported here for inhibition of intracellular metabolism were significantly higher than those obtained versus purified glucosidase I enzymes, an observation similar to that of Kang and coworkers (8). The IC_{50} values of 1-dNJ and CAST versus enzyme isolated from porcine kidney were 77-fold and 500-fold lower, respectively, when compared with values versus enzyme in cultured $B_{16}F_{10}$ mouse melanoma cells (8). This might be attributed to poor accessibility of the inhibitors to the luminal space of the endoplasmic reticulum where glucosidase I is localized. The inhibitory potency of castanospermine presented here is a little higher than that of 1-deoxynojirimycin (165 μM vs. 320 μM), and agrees with reported values (7, 8). Crystal structures of 1-dNJ and CAST (31) suggest that the fixed positioning of the O-6 atom by the 5-membered ring closure in CAST might contribute to the observed increase in potency.

Inhibition of α-glucosidase I prevents the removal of glucose residues during the normal processing of HIV gp-120 membrane protein and results in altered glycoproteins that have been implicated in breaking the virus replication cycle. The inhibitors may thus have potential as anti-HIV therapeutic agents. The new potential inhibitor, 1,5-trans-*C*-glucoside was chosen based on the assumption that the *C*-glycoside was stable against hydrolysis similar to 1-dNJ and CAST. The estimated K_i value of 1,5-trans-*C*-glucose versus purified yeast α-glucosidase I was 200 μM, while no inhibition of purified yeast glucosidase II was seen (unpublished data). From the estimated K_i value, the compound would be considered as a potential inhibitor of similar potency to 1-dNJ and CAST. Results obtained from HT29 cells treated with 1,5-trans-*C*-glucoside (5 mM) showed that no inhibition of hydrolysis occurred, and the compound is thus unlikely to be of use as a pharmaceutical agent. The lack of inhibitory potency in this intracellular enzyme assay method suggested the compound was unable to penetrate the cell membrane or was not taken into the endoplasmic reticulum. Thus, the concentration of 1,5-trans-*C*-glucoside inside the cells was too low to inhibit the enzyme.

Many derivatives of 1-dNJ and CAST have been synthesized which are more potent inhibitors of glucosidases I and II than are the parent compounds, and which may have some efficacy as anti-HIV and anti-viral agents (7-11). Inhibitor potencies were assessed either by radioisotope labeling in cultured cells (8, 13), or radioactive immunoprecipitation followed by SDS-PAGE (10, 11). These procedures were time-consuming and provided poor resolution in most cases, even after re-chromatography of pooled fractions. The CE-LIF method described herein can be used to allow faster

and more precise comparisons of panels of inhibitor analogues. The simple 2-step fluorescent coupling reaction circumvents the necessity for radioactive substrates and allows a wider range of substrates to be examined. Separations are achieved within 15 minutes, and peak resolution and sensitivity are sufficiently high to allow single cell analysis. This method should prove sufficiently adaptable that many enzymes and enzyme inhibitors might be examined in a wide range of cell systems.

3.4 Conclusions

This chapter describes the development of an *in cella* enzyme microassay for α-glucosidase I which has a detection limit several orders of magnitude lower than existing radiochemical procedures. The assay used capillary electrophoresis with laser-induced fluorescence detection to monitor changes in the intracellular hydrolysis of a trisaccharide substrate labeled with a fluorescent tetramethylrhodamine (TMR) molecule. Following incubation of TG-TMR with a human colon adenocarcinoma cell line, hydrolysis products were separated by capillary electrophoresis and were quantified from the areas under the peaks of an electropherogram. IC_{50} values were obtained for the α-glucosidase I inhibitors, 1-deoxynojirimycin and castanospermine. The IC_{50} values determined in this manner reflect the amount of inhibitor that crossed the cell membrane and gained access to the target enzyme. This method was also used in the testing of a novel compound as a potential α-glucosidase I inhibitor, and results suggested that the molecule was unable to gain access to the intracellular enzyme. This technology provides a rapid and efficient method to evaluate the efficacy of inhibitors in cell systems, and is feasible for studies at the single cell level.

In the next chapter, this method was used to determine the intracellular inhibitory effect of a novel inhibitor towards blood group A-transferase in HT29 cells, illustrating the versatility of this technique in sample application.

3.5 References

1. Kornfeld, R., and Kornfeld, S. (1985) *Ann. Rev. Biochem.* **54**, 631-664.
2. Fuhrmann, U., Bause, E., and Ploegh, H. (1985) *Biochim. Biophys. Acta* **825**, 95-110.
3. Winchester, B., and Fleet, G. W. J. (1992) *Glycobiology* **2**, 199-210.
4. Sunkara, P. S., Bowlin, T. L., Liu, P. S., and Sjoerdsma, A. (1987) *Biochem. Biophys. Res. Commun.* **148**, 206-210.
5. Gruters, R. A., Neefjes, J. J., Tersmette, M., de Goede, R. E. Y., Tulp, A., Huisman, H. G., Miedema, F., and Pleogh H. L. (1987) *Nature* **330**, 74-77.
6. Walker, B. D., Kowalski, M., Goh, W. C., Kozarsky, K., Krieger, M., Rosen, C., Rohrschneider, L., Haseltine, W. A., and Sodroski, J. (1987) *Proc. Natl. Acad. Sci.* **84**, 8120-8124.
7. Tyms, A. S., Berrie, E. M., Ryder, T. A., Nash, R. J., Hegarty, M. P., Taylor, D. L., Mobberley, M. A., Davis, J. M., Bell, E. A., Jeffries, D. J., Taylor-Robinson, D., and Fellows, L. E. (1987) *Lancet* **1**, 1025-1026.
8. Kang, M. S., Liu, P. S., Bernotas, R. C., Harry, B. S., and Sunkara, P. S. (1995) *Glycobiology* **5**, 147-152.
9. Sunkara, P. S., Taylor, D. L., Kang, M. S., Bowlin, T. L., Liu, P. S., Tyms, A. S., and Sjoerdsma, A. (1989) *Lancet* **2**, 1206.
10. Tan, A., van den Broek, L., van Boeckel, S., Ploegh, H., and Bolscher, J. (1991) *J. Biol. Chem.* **266**, 14504-14510.
11. Karlsson, G. B., Butters, T. D., Dwek, R. A., and Platt, F. M. (1993) *J. Biol. Chem.* **268**, 570-576.

12. van den Broek, L. A. G. M., kat-van den Nieuwenhof, M. W. P., Butters, T. D., and van Boeckel, C. A. A. (1996) *J. Pharm. Pharmacol.* **48**, 172-178.

13. Szumilo, T., and Elbein, A. D. (1985) *Anal. Biochem.* **151**, 32-40.

14. Kaushal, G. P., and Elbein, A. D. (1994) *Methods Enzymol.* **230**, 316-329.

15. Kaushal, G. P., Pan, Y. T., Tropea J. E., Mitchell, M., Liu, P., and Elbein, A. D. (1988) *J. Biol. Chem.* **263**, 17278-17283.

16. Pan, Y. T., Hori, H., Saul, R., Sanford, B. A., Molyneux, R. J., and Elbein, A. D. (1983) *Biochemistry* **22**, 3975-3984.

17. Kilker, Jr. R. D., Saunier, B., Tkacz, J. S., and Herscovics, A. (1981) *J. Biol. Chem.* **256**, 5299-5303.

18. Saunier, B., Kilker, Jr. R. D., Tkacz, J. S., Quaroni, A., and Herscovics, A. (1982) *J. Biol. Chem.* **257**, 14155-14161.

19. Scaman, C. H., Hindsgaul, O., Palcic, M. M., and Srivastava, O. P. (1996) *Carbohydr. Res.* **296**, 203-213.

20. Le, X., Scaman, C. H., Zhang, Y., Zhang, J., Dovichi, N. J., Hindsgaul, O., and Palcic, M. M. (1995) *J. Chromatogr. A* **716**, 215-220.

21. Zhang, Y., Le, X., Dovichi, N. J., Compston, C. A., Palcic, M. M., Diedrich, P., and Hindsgaul, O. (1995) *Anal. Biochem.* **227**, 368-376.

22. Krylov, S. N., Arriaga, E., Zhang, Z., Chan, N. W. C., Palcic, M. M, and Dovichi, N. J. (1998) *in preparation.*

23. Palcic, M. M., Heerze, L. D., Pierce, M., and Hindsgaul, O. (1988) *Glycoconjugate J.* **5**, 49-63.

24. Jacob, G. S. (1995) *Curr. Opin. Struct. Biol.* **5**, 605-611.

25. Olden, K., Breton, P., Grzegorzewski, K., Yasuda, Y., Gause, B. L., Oredipe, O. A., Newton, S. A., and White, S. L. (1991) *Pharmac. Ther.* **50**, 285-290.

26. Dennis, J. W., Koch, K., Beckner, D. (1989) *J. Natl. Cancer Inst.* **81**, 1028-1033.

27. Srivastava, O. P., Szweda, R., Smith, R. H., Ippolito, R. W., and Spohr, U. (1996) US patent 5,571,796.

28. Knoll, J. E. (1985) *J. Chromatogr. Sci.* **23**, 422-425.

29. Neverova, I., Scaman, C. H., Srivastava, O. P., Szweda, R., Vijay, I. K., and Palcic, M. M. (1994) *Anal. Biochem.* **222**, 190-195.

30. Hettkamp, H., Legler, G., and Bause, E. (1984) *Eur. J. Biochem.* **142**, 85-90.

31. Hempel, A., Camerman, N., Mastropaolo, D., and Camerman, A. (1993) *J. Med. Chem.* **36**, 4082-4086.

Chapter Four

First Demonstration of Intracellular Inhibition of a Glycosyltransferase

Acknowledgments: I would like to thank Drs. T. Lowary and O. Hindsgaul for the 3-amino-3-deoxy-[αFuc(1→2)]βGal-*O*octyl compound and Dr. S. Laferté for the [^{35}S]-Met radiolabeling experiment.

4.1 Introduction

In recent years, one of the main goals of the University of Alberta Glycobiology research group has been to develop specific glycosyltransferase inhibitors for use as therapeutic agents in the treatment of cancers, inflammation and viral infection (1-7). In the past decade, many research groups have studied aspects of glycosyltransferase chemistry such as key polar group mapping (8-10), active site mapping using photo-affinity labeling (11, 12), site-directed mutagenesis (13, 14), and enzyme kinetics (15, 16). Availability of a potent glycosyltransferase inhibitor would be an excellent starting point in the search for more effective and potent drugs.

The natural acceptor for the blood group A-transferase (α-3-*N*-Acetyl-D-galactosaminyl transferase, EC. 2.4.1.40) is αFuc(1→2)βGal(1→3/4)βGlcNAc-OR, where R can be a glycoprotein or a glycolipid. The minimum structural requirement for blood group A-transferase to recognize the acceptor is the H disaccharide, αFuc(1→2)βGal-OR (17, 18). The blood group A-transferase transfers *N*-acetyl-galactosamine (GalNAc) from UDP-GalNAc to the acceptor (αFuc(1→2)βGal) to form the blood group A antigen, αGalNAc(1→3)[αFuc(1→2)]βGal-OR (**Scheme 4.1**). Lowary and Hindsgaul (5) have reported that 3-amino-3-deoxy-[αFuc(1→2)]βGal-*O*-octyl (**Fig. 4.1**) is a potent inhibitor of human serum blood group A-transferase with a K_i value of 200 nM. This low K_i value means that this compound may be useful therapeutically. The mode of inhibition was not determined in the publication, only assumed to be competitive to estimate the K_i value. In collaboration with Dr. S. Laferté, Department of Chemistry, University of Saskatchewan, the inhibitor was tested for its ability to decrease cell surface A type II

structures. However, the compound had no efficacy in these studies (unpublished results). There was no detectable reduction in the amount of cell surface structures measured by an indirect fluorescence immunoassay. The explanation given then was that the positive charge on the amine moiety at physiological pH (pH 7.5), would prevent the molecule from crossing the cell membrane. Since the enzyme is located on the lumen of the Golgi apparatus, this compound would most likely be ineffective *in vivo*. This problem, where the inhibitor is effective *in vitro* and not effective *in vivo*, has been observed and is believed to be due to the poor stability and bioavailability (3). In this case, it was also suspected that turnover of glycoproteins on the cell membrane was sufficiently slow that no changes in cell surface structures were apparent with fluorescent antibody detection.

In the knowledge that 3-amino-3-deoxy-[αFuc(1→2)]βGal-*O*-octyl has the potential to inhibit the blood group A-tranferase at sub-micromolar concentrations, it was decided to test this compound in the HT29 cell line using CE-LIF. The donor of the HT29 cell line has been reported to be blood type-A^+ (19), which is useful because the intracellular inhibition assay was developed using this cell line, and the method for growing the cells and for testing inhibitors is relatively well established.

The inhibitory effect of 3-amino-3-deoxy-[αFuc(1→2)]βGal-*O*-octyl was assessed and an IC_{50} was obtained using the intracellular inhibition assay. 3-Amino-3-deoxy-[αFuc(1→2)]βGal-*O*-octyl was also tested as an inhibitor by measuring [^{35}S]-methionine incorporation into cell-associated HT29 glycoproteins to assess glycosylation changes.

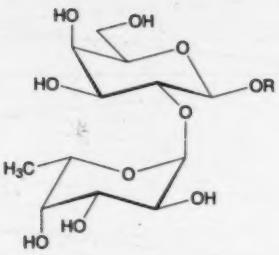

αFuc(1→2)βGal-OR

UDP-GalNAc

Blood Group A-transferase:
isolated cloned in *E. coli*
or intracellular in HT29 cells

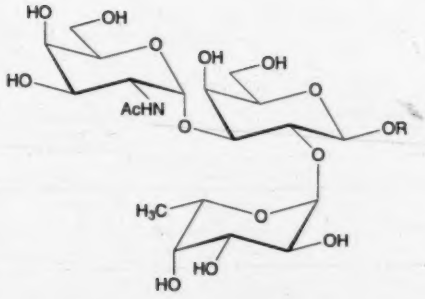

αGalNAc(1α→3)αFuc(1→2)βGal-OR

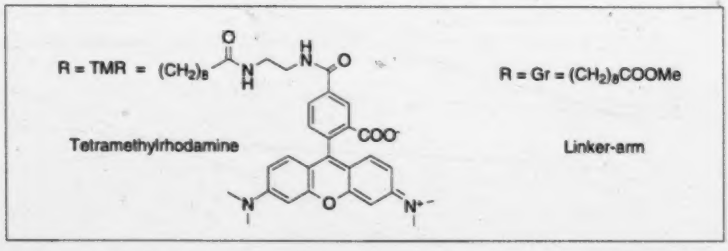

Scheme 4.1 Synthesis of A-trisaccharide from αFuc(1→2)βGal-*O*-octyl and UDP-GalNAc.

4.2 Experimental Section

4.2.1 Materials

A human colon HT29 adenocarcinoma cell line was obtained from the American Type Culture Collection (Rockville, MD). Dulbecco's modified Eagle's medium (D-MEM), fetal bovine serum, gentamicin, trypsin-EDTA, and Trypan-Blue dye were from Gibco BRL (Gaithersburg, MD). Cells were grown in Falcon 24-well tissue culture plates purchased from Becton Dickinson Labware (Lincoln Park, NJ). The cloned blood group A-transferase was provided by Dr. N. Seto at the Institute of Biological Science, National Research Council, and was isolated by Ms. C. Compston following the method of Seto *et al.* (15, 20). α Fuc(1→2)βGal-*O*-octyl, αFuc(1→2)βGal-TMR and 3-amino-3-deoxy-[αFuc(1→2)]βGal-*O*-octyl were provided by Dr. O. Hindsgaul, Department of Chemistry, University of Alberta. The fluorescent tag, tetramethylrhodamine (TMR) was purchased from Molecular Probes Inc. (Eugene, OR), and covalently linked to the oligosaccharides through an ethylenediamine linker using the method described previously in **sections 3.2.2 & 3.2.3**. The micro glass homogenizers used were from Fisher Scientific (Nepean, ON). The reverse-phase Sep-Pak Plus C-18 cartridges were obtained from Waters (Mississauga, ON), and were conditioned before use by washing with 5 ml of HPLC grade methanol followed by 10 ml of Mili-Q water (21). The Millex-GV filter units were from Millipore (Mississauga, ON). The capillary electrophoresis instrument (22) was the same as described in section **3.2.1**. The analysis programs were Igor Pro v.2.04 from WaveMetrics (Lake Oswego, OR) for obtaining integrals from electropherograms, and GraphPad Prism, version 2.0 from GraphPad software Inc.

(San Diego, CA) for obtaining the IC_{50} value. An Isotyping Kit from Bio-Rad Laboratories (Mississauga, ON) was used for MAB 8D5 isotyping. [^{35}S]-Methionine used in metabolic radiolabeling of HT29 cells was purchased from NEN (Calgary, AB). Protein A Sepharose-4B beads were from Pharmacia (Montreal, QC). Enlightning from NEN DuPont (Mississauga, ON) was used to visualize SDS-PAGE fluorograph.

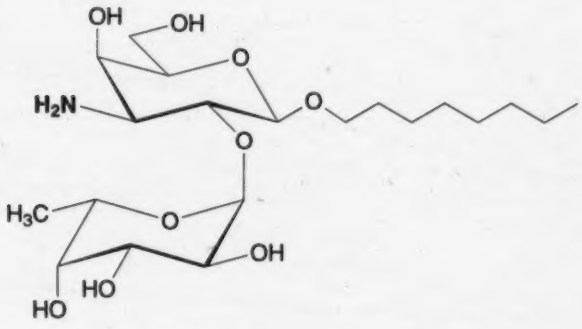

Figure 4.1 Structure of 3-amino-3-deoxy-[αFuc(1→2)]βGal-*O*-octyl.

4.2.2 Capillary Electrophoresis Assays for *In Vitro* Studies with Isolated Cloned Blood Group A-Transferase

The incubation mixture contained 15 μM αFuc(1→2)βGal-OTMR, 15 μM UDP-GalNAc, 0.31 mU isolated cloned blood group A-transferase in a total volume of 33 μl of 35 mM sodium cacodylate buffer, pH 7.0, containing 20 mM $MnCl_2$ and 1 mg/ml BSA. The inhibition assay tubes were incubated at 37°C in the presence of 15 μM or 30 μM 3-amino-3-deoxy-[αFuc(1→2)]βGal-*O*-octyl. After incubation for 30 minutes, an aliquant (10 μl) of the sample was applied to a Sep-Pak Plus C-18

cartridge, the sample was washed with 20 ml of water, then product as well as any unreacted acceptor was eluted with 4 ml HPLC grade methanol. The sample was lyophilized and 151.5 µl water were added to the dried sample so that the concentration of TMR stock was 1 µM. 10 µl of this solution were added to 190 µl of capillary electrophoresis running buffer (10 mM sodium phosphate, dibasic, 10 mM sodium borate, 10 mM sodium dodecyl sulfate, 10 mM phenylboronic acid, pH 9.3). Products were separated and analyzed by capillary electrophoresis with laser induced fluorescence detection, by injecting 13 pl onto a capillary column (60 cm long) at 1 kV for 5 s.

4.2.3 Detection of Intracellular A-Transferase Activity in HT29 Cells

A human adenocarcinoma HT29 cell line was grown to 60% confluence in 24-well Falcon tissue culture plates (1.5 ml well volume) in Dulbecco's modified Eagle's medium supplemented with 10% fetal bovine serum and 40 µg/ml gentamicin, at 37°C and in an atmosphere of 5% CO_2/air. Incubations were initiated by adding 0.5 ml culture medium containing 25 or 100 µM αFuc(1→2)βGal-OTMR to the cells. After 18 hr or 2 days incubation, cells were washed five times with 1 ml PBS. Cells were trypsinized and were dislodged from wells in 1 ml PBS. Cell pellets were resuspended in 450 µl water and 50 µl CE running buffer and homogenized gently at 0°C, once every 15 minutes for 1.5 hr in a micro glass homogenizer. The homogenate was loaded onto a conditioned reverse-phase Sep-Pak Plus C-18 cartridge, the sample was washed with 20 ml water, and the TMR labeled oligosaccharides were eluted with 4 ml HPLC grade methanol. The solvent was evaporated under vacuum and the

sample dissolved in water and lyophilized to reduce the volume to less than 20 µl, to facilitate analysis by CE. The solution preparation for CE separation was similar to that described in **section 3.2.7**.

4.2.4 Intracellular Inhibition Assays with 3-Amino-3-Deoxy-[αFuc(1→2)]βGal-*O*-Octyl by CE-LIF

HT29 cells were grown in separated wells in a 24-well plate. 3-Amino-3-deoxy-[αFuc(1→2)]βGal-*O*-Octyl (1 µM to 10 mM) was added to the wells 24 hours prior to incubation with TMR-labeled substrate. Following the 24 hr inhibitor preincubation period, medium was aspirated from the wells and was replaced with fresh medium containing the appropriate concentration of inhibitor, as well as the αFuc(1→2)βGal-OTMR substrate at 100 µM, which had been filtered through a Millex-GV filter. Cells were then incubated at 37°C for a further 48 hr. Cells were washed and trypsinized, as described in **section 4.2.3**, prior to analysis by CE-LIF. The preparation for analysis by CE-LIF was as described in **section 3.2.7**. The experiments were done in one passage of cells due to the irreproducibility during cell passages as described in **section 3.3.4**. CE-LIF detection was done in triplicates and errors were obtained.

4.2.5 Data Analysis

The area under each peak was determined with the graphing and data analysis program, Igor Pro. The area under the product peak was divided by the total area to calculate the degree of biosynthesis of the blood group A antigen in each case. The

degree of blood group A antigen biosynthesis at each inhibitor concentration was then compared with that in the control to obtain the % inhibition. Values were plotted against inhibitor concentrations (log scale) in the cell medium, and IC_{50} values were obtained by nonlinear regression analysis of the data with GraphPad Prism, version 2.0.

4.2.6 Intracellular Inhibition Assay with 3-Amino-3-Deoxy-[αFuc(1→2)]βGal-*O*-Octyl by [^{35}S]-Methionine Radiolabeling

4.2.6.1 Preparation of Monoclonal Antibodies

The isolation of MAB 3A7, 7A8 and 11D4 has been described elsewhere (23, 24). Monoclonal antibody 8D5 was isolated (25) following immunization of mice with 100 μg of HT29 plasma membranes emulsified with Freund's complete adjuvant. The hybridoma secreting MAB 8D5 was injected intraperitoneally into Balb/c mice for the production of ascitic fluid which was subsequently used for enzyme-linked immunosorbent assay (ELISA) and immunoprecipitation analyses, in **sections 4.2.6.2 & 4.2.6.4**. Isotyping of MAb 8D5 was carried out using the Isotyping Kit according to manufacturer's instructions. The MAB 8D5 was found to be of the IgG_1 subclass. The antibodies used were: MAB 3A7 exclusive for blood group A or B on type II chain, MAB 8D5 for blood group A on type I and II chains, MAB 11D4 for blood group A exclusively on type II chain, and MAB 7A8 for the epitope on the α3 chain of α3β1 integrin. MAB 7A8 was used as a control to ensure that the inhibitor did not inhibit protein synthesis, since α3β1 integrin is the major glycoprotein detected by anti-A and anti-A/B monoclonal antibodies.

4.2.6.2 Preparation of BSA-Glycan Conjugates

BSA-glycan conjugates were prepared and used as described previously (23). The incorporation of carbohydrates on each BSA-glycan conjugate was as follows (where n = number of oligosaccharide coupled per mole of BSA): H type 2-BSA (n=19); A disaccharide-BSA (n=17); A type 2-BSA (n=57); A type 1-BSA (n=13); A type 4-BSA (n=17); A type 6-BSA (n=13); B disaccharide-BSA (n=19); B type 2-BSA (n=18); B type 4-BSA (n=14); B type 5-BSA (n=15). Because of the different levels of incorporated oligosaccharide chains per BSA molecule, all BSA-glycan conjugates were diluted to a standard concentration of 50 nmol oligosaccharide/ml. ELISA were carried out as described by Laferté *et al.* and Prokopishyn *et al.* (23, 24) using 100 µl aliquots of the BSA-glycan conjugates.

4.2.6.3 Metabolic Labeling of Cells

HT29 cells were plated in 24-well tissue culture plates and grown overnight until the cells were healthy and at 30% confluence. The medium was aspirated and fresh medium was added to the control cells, while medium containing 3-Amino-3-deoxy-αFuc(1→2)βGal-*O*-Octyl (0.1 or 0.5 mM) was added to inhibitor-tested cells, and the cells were further incubated for 24 hr. Following incubation, the medium was aspirated, and cells were washed twice with PBS. The cells were then incubated at 37°C for 24 hr in 1 ml of methionine-free DMEM medium supplemented with 10% of normal concentration of methionine, 10% FBS and 70 µCi/ml [^{35}S]-methionine (800 Ci/mmol). The wells were washed three times in PBS and the cells solubilized on ice for 1 hr in 1 ml buffer containing 50 mM Tris-HCl, pH 8.0, 0.15 M NaCl, 1 mM

benzamidine, 1%(v/v) Triton X-100, 1%(w/v) deoxycholate, 0.02%(w/v) sodium azide. Cell debris was removed by centrifugation at 22,500 *g* for 15 minutes.

4.2.6.4 Immunoprecipitation and SDS-PAGE Detection

[^{35}S]-Methionine-labeled cell lysates (10-20 x 10^6 cpm) were incubated overnight at 4°C with 3 µl normal mouse serum or ascitic fluid prepared from anti-A or anti-A/B monoclonal antibodies. Protein A Sepharose-4B beads (100 µl of a 1:1 suspension) were added and the suspension rocked gently at 4°C for 1 hr. The beads were washed once with immunoprecipitation (IP) buffer (50 mM Tris-HCl pH 8.0, 1 mM PMSF, 1 mM benzamidine, 1% deoxycholate, 1% Triton X-100, 0.02% sodium azide), twice with IP buffer containing 0.5 M NaCl, twice with IP buffer containing 0.1% SDS and finally once with IP buffer. The immunoprecipitated proteins were then eluted by boiling for 5 min in SDS-PAGE sample buffer (0.125 M Tris-HCl pH 6.8, 2% SDS, 2% 2-mercaptoethanol, 10% glycerol) and analyzed by SDS-PAGE. The SDS-PAGE was performed as described by Laemmli (26) using 6.0% polyacrylamide gels. [^{35}S]-Methionine labeled proteins separated by SDS-PAGE were visualized by fluorography (27) using Enlightning.

4.3 Results And Discussion

4.3.1 *In Vitro* Inhibition of Isolated Cloned A-Transferase by 3-Amino-3-Deoxy-[αFuc(1→2)]βGal-*O*-Octyl

The degree of conversion to the product, αGalNAc(1→3)[αFuc(1→2)]βGal-OTMR, in the control was 80% after incubation for 30 minutes (**Fig. 4.2A**). Product was confirmed by co-migration with the standard produced by enzymatic synthesis. The conversion was reduced to 75% and 50% with 15 μM and 30 μM 3-amino-3-deoxy-[αFuc(1→2)]βGal-*O*-octyl, respectively (**Fig. 4.2B & C**), corresponding to 6.3% and 38% inhibition of the reaction at the 2 different concentrations of inhibitor. Therefore, the inhibition of cloned blood group A-transferase by 3-amino-3-deoxy-[αFuc(1→2)]βGal-*O*-octyl was concentration-dependent. It was then necessary to show that inhibition of A-transferase in HT29 cells was also concentration-dependent. The degradation product (peak 3) formed in much higher amount in **Fig. 4.2C** was due to the higher concentration of substrate, inhibited from forming A-trisaccharide, available in the reaction mixture.

4.3.2 Detection of A-Transferase Product by CE-LIF after Uptake of A-Transferase Substrate

The uptake experiment was done at a substrate concentration of 25 μM and with an 18 hr incubation, with HT29 cells growing to approximately 70% confluence, as described in **section 3.2.4**. However, under these conditions, no product was detected inside the cell. **Fig. 4.3** compares electropherograms for the

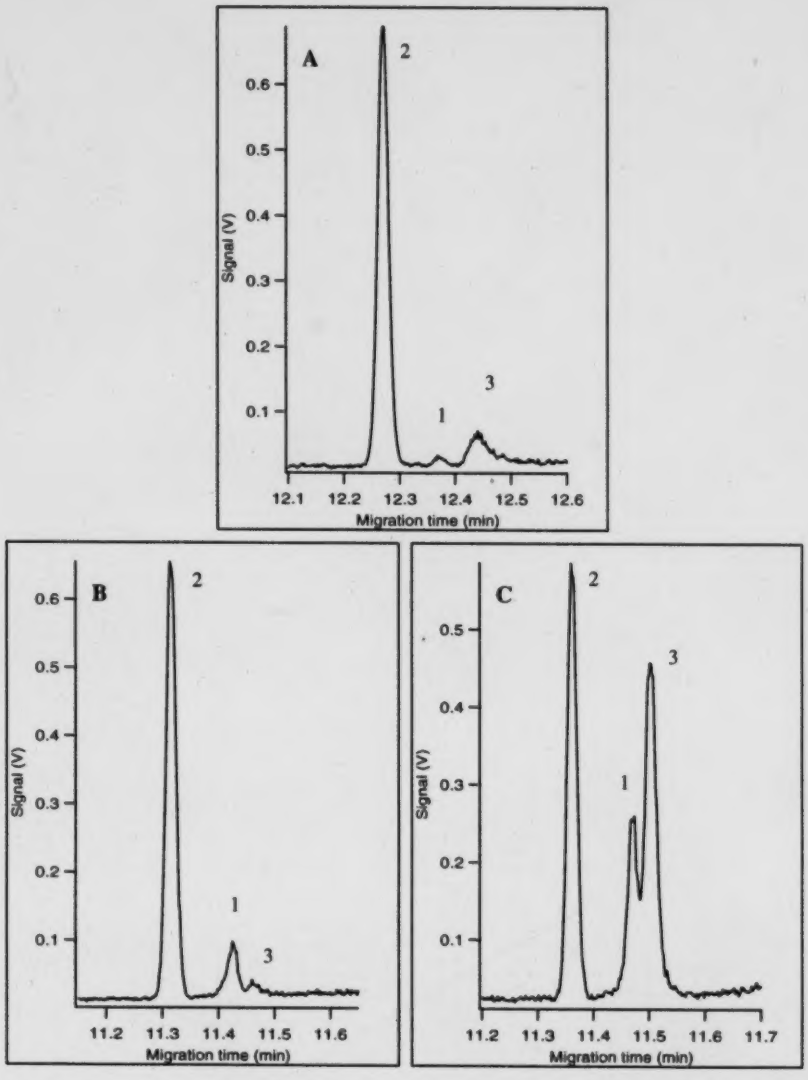

Figure 4.2 Electropherograms of αFuc(1→2)βGal-OTMR after incubation with isolated cloned blood group A-transferase and the inhibitory effects of 3-amino-3-deoxy-[αFuc(1→2)]βGal-*O*-octyl. Panel **A** shows the control reaction; peak 1 is the substrate, peak 2 is the product at 80% conversion, and peak 3 is a degradation product of αFuc(1→2)βGal-OTMR. Panels **B** and **C** show the effects of incubating with 15 μM and 30 μM 3-amino-3-deoxy -[αFuc(1→2)]βGal-*O*-octyl.

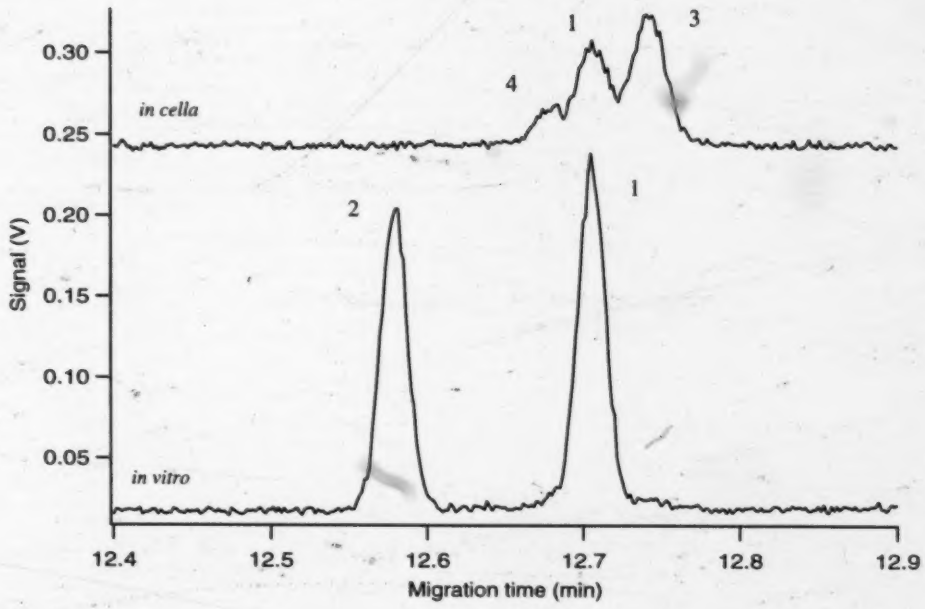

Figure 4.3 Capillary electropherograms of the *in vitro* incubation experiment and the intracellular uptake experiment (18 hr incubation). Product (peak 2) was not detected in the cell extract. Peaks 3 & 4 were metabolic by-products formed in whole cells that did not co-migrate with any TMR labeled standards available. Peak 1 on both electropherograms was the substrate, αFuc(1→2)βGal-OTMR.

enzymatic product from the *in vitro* experiment with the cell extract from the uptake experiment.

Peak 1 was confirmed as the substrate by co-migration studies with standard compounds. Peaks 3 & 4 were assumed to be by-products of the intracellular uptake because they were not found in the *in vitro* experiments. These peaks did not co-migrate with any of the TMR labeled standards available. The product (peak 2) was not found within this cell extract.

The lack of product formed by blood group A-transferase within the cells was assumed to be due to the poor bioavailability of substrate within the cell, and particularly at the site of the enzyme, in the lumen of the Golgi. Therefore, experimental conditions were altered in an attempt to increase substrate concentration within the cells. First, the concentration of the substrate was increased to 100 μM from 25 μM in the cell culture medium. Alternatively, the incubation time was increased to 2 days from 18 hr. Finally, both conditions were combined and product was obtained with 100 μM αFuc(1→2)βGal-OTMR in the medium and an incubation time of 2 days.

In **Fig. 4.4**, peak 2 was confirmed by co-migration as the product, αGalNAc (1→3)[αFuc(1→2)]βGal-OTMR. Another unknown peak (peak 5) had a lower migration time than had been observed in previous intracellular inhibition assays. The presence of this peak was not consistent in all experiments (occurring in anout 20% of the incubations), perhaps due to the fact that cells change its physiological characteristics according to the growing environment. For this reason, it was not

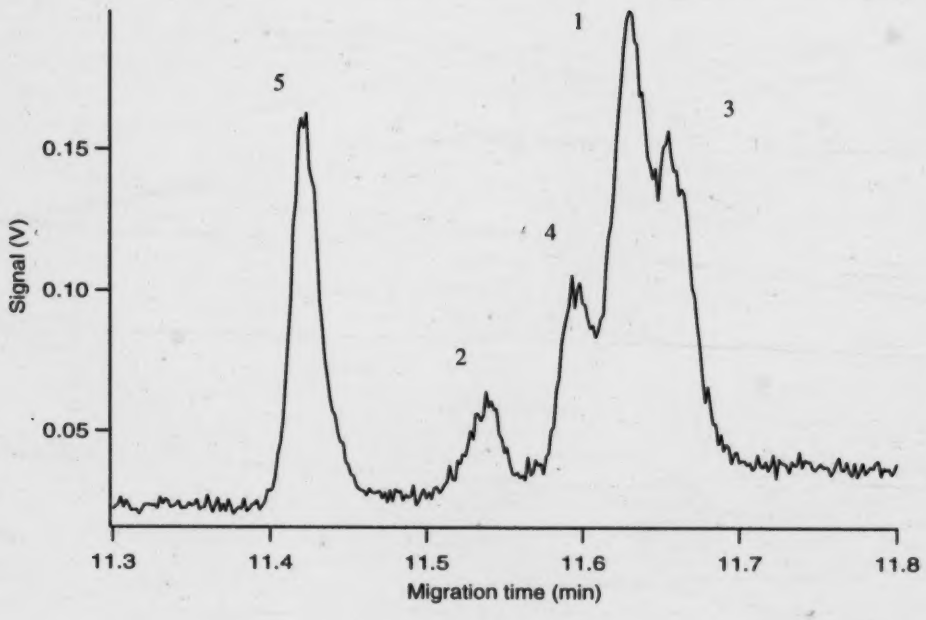

Figure 4.4 Electropherogram of FucGal-OTMR and its metabolites following incubation of HT29 cells for 2 days with 100 μM substrate. Peak 1 was identified as the substrate, αFuc(1→2)βGal-OTMR; peak 2 was the blood group A-transferase product, αGalNAc(1→3)[αFuc(1→2)]βGal-OTMR; peaks 3-5 were unknown metabolites which were formed during the incubation.

surprising to detect a variety of metabolites in cell extracts from different experiments.

4.3.3 Intracellular Inhibition of A-transferase in HT29 Cells

In **Fig. 4.5**, panel **A** shows an electropherogram of FucGal-OTMR following incubation with HT29 cells (control). Peak 1 was the substrate, peaks 3 & 4 were by-products, and peak 2 was the blood group A-transferase product, confirmed by co-migration. The areas under peak 2 and peaks 1, 3, and 4 were calculated by integration. The degree of conversion to the product was then calculated by dividing the area of peak 2 by the sum of all peaks. The average degree of conversion of FucGal to GalNAcFucGal in this experiment was 9.7% ± 0.42% (n = 7).

Electropherograms obtained following treatment of HT29 cells with 3-amino-3-deoxy-[αFuc(1→2)]βGal-*O*-octyl showed that the intracellular inhibition of blood group A-transferase was concentration-dependent. Panels **B** and **C** show electropherograms obtained following treatment of HT29 cells with inhibitor concentrations of 45 μM and 400 μM, respectively. Approximately 70% inhibition of enzyme activity was observed at 400 μM 3-amino-3-deoxy-[αFuc(1→2)]βGal-*O*-octyl, compared with 22% at 45 μM of the inhibitor (**Figs. 4.5B & C**).

HT29 cells incubated with the inhibitor at these concentrations showed no changes in morphology or cell viability compared with control cells, indicating that at the concentrations used, the inhibitor showed no apparent cytotoxicity.

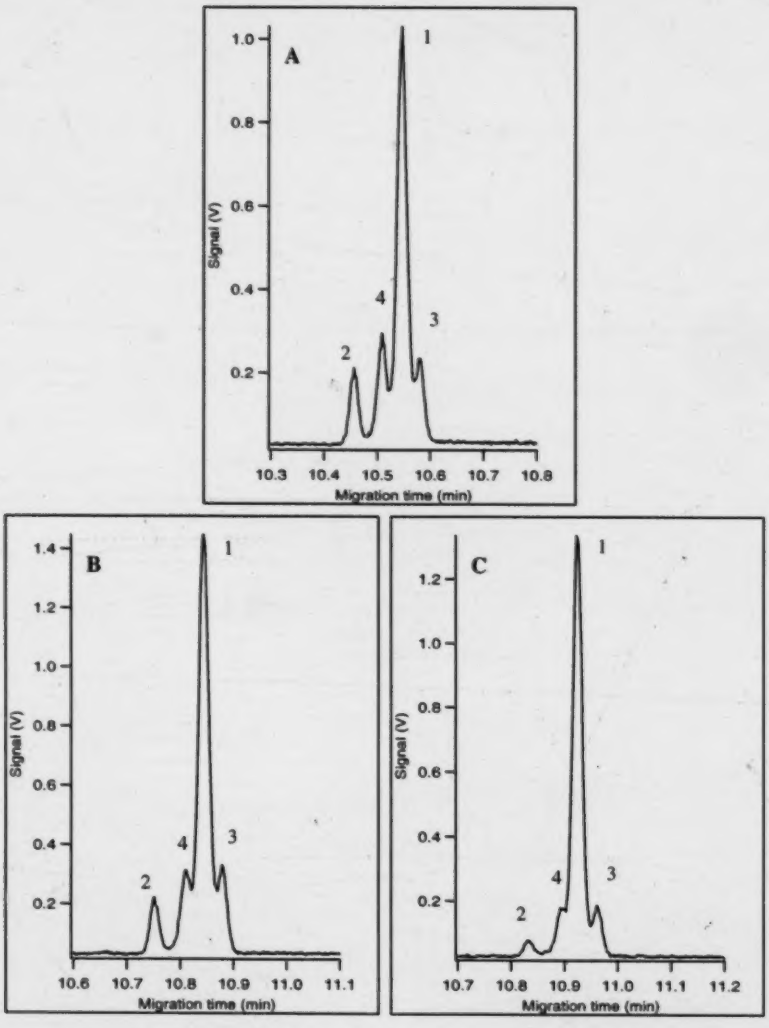

Figure 4.5 Electropherograms of HT29 cell contents after incubation with 3-amino-3-deoxy-[αFuc(1→2)]βGal-*O*-octyl followed by αFuc(1→2)βGal-OTMR. Panel **A** shows the control cell extract; peak 1 is the substrate, peak 2 is the product at 10% conversion, and peaks 3 & 4 are metabolic by-products. Panels **B** and **C** show the effects on metabolite levels of preincubating with 45 μM and 400 μM 3-amino-3-deoxy-[αFuc(1→2)]βGal-*O*-octyl, respectively.

4.3.4 Determination of The Intracellular IC_{50} Value for 3-Amino-3-Deoxy-[αFuc(1→2)]βGal-*O*-Octyl

In the experiment to determine the intracellular IC_{50} value for 3-amino-3-deoxy-[αFuc(1→2)]βGal-*O*-octyl, the concentrations used ranged from 1 μM to 10 mM in the cell medium. Cells grown in the presence of 3 mM and 10 mM 3-amino-3-deoxy-[αFuc(1→2)]βGal-*O*-octyl showed reduced viability (20%) after the incubation, compared with control cells, while cells that were treated with less than 3 mM 3-amino-3-deoxy-[αFuc(1→2)]βGal-*O*-octyl were >95% viable. Therefore, the cytotoxic level of the inhibitor on HT29 cells was reached at concentrations of 3 mM and above.

The IC_{50} value was found by linear regression (GraphPad Prism, version2.0) to be 282 μM for 3-amino-3-deoxy-[αFuc(1→2)]βGal-*O*-octyl (**Fig. 4.6**). This value was much higher than the K_i value (200 nM) reported by Lowary and Hindsgaul (5) using isolated serum enzyme, probably due to poor diffusion of the inhibitor into the cytoplasm, and therefore to the luminal space of the Golgi apparatus where blood group A-transferase is localized. Furthermore, the enzyme from HT29 cells was different kinetically from serum blood group A-transferase, as differences were seen between the K_m values obtained with the cloned blood group A-transferase (15 μM for FucGal-*O*-octyl, 13 μM for UDP-GalNAc) (15) and serum blood group A-transferase (5) (1.5 μM for FucGal-octyl). It is known that the K_m value of the donor is dependent upon the concentration of the acceptor in the reaction mixture, and vice-versa (15). In the intracellular inhibition assay, no UDP-GalNAc as donor was supplied to the cells. Presumably, then, there was endogenous donor present which

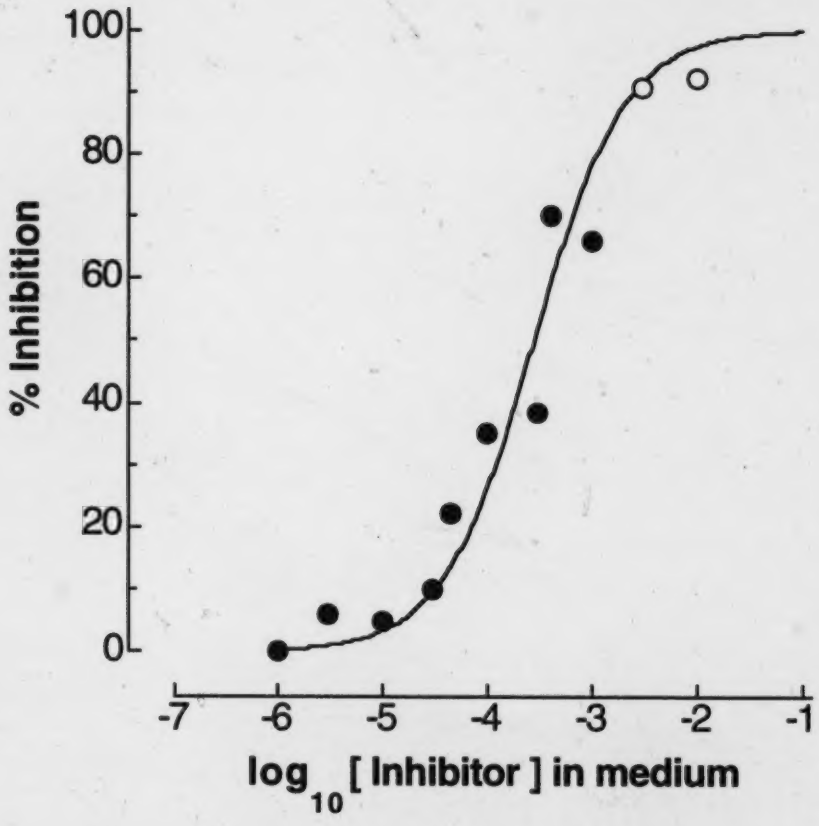

Figure 4.6 Inhibition of blood group A-transferase by a range of concentrations of 3-amino-3-deoxy-[αFuc(1→2)]βGal-*O*-octyl. Inhibition (%) was plotted against the logarithm of the concentration of inhibitor in the cell medium. Solid circles (●) represent concentrations of inhibitor used where cells were more than 90% viable, and open circles (O) represent concentrations of inhibitor at which viability was <20%. A sigmoid was fitted to the data by the nonlinear regression facility of GraphPad Prism, version 2.0. The IC_{50} value was calculated to be 282 μM. The error bars were not visible due to the scale of the plot.

allowed the reaction to take place. The endogenous substrate concentration was unknown during the incubation. Assuming that inhibition is competitive in nature, and since the IC_{50}, but not the K_i, is dependent upon substrate concentration, then it is not surprising that the IC_{50} determined in these experiments was substantially higher than the K_i value published by Lowary and Hindsgaul (5).

The inhibitory effect of 3-amino-3-deoxy-[αFuc(1→2)]βGal-*O*-octyl is concentration-dependent and reflects inhibition of the blood group A-transferase inside HT29 cells. It is not due to other non-enzymatic effects such as inhibition of fluorescent substrate from crossing cell membrane or prevention of αFuc(1→2)βGal-TMR uptake. The total fluorescent intensities extracted from HT29 cells after the incubation were consistent throughout the concentration range of inhibitor tested (see **Fig. 4.5**). Thus, 3-amino-3-deoxy-[αFuc(1→2)]βGal-*O*-octyl did not affect the uptake of substrate.

4.3.5 Inhibitory Effects of 3-Amino-3-Deoxy-[αFuc(1→2)]βGal-*O*-octyl on Glycosylation of Glycoproteins in HT29 cells

In addition to determining the kinetics of inhibition of A-transferase by 3-amino-3-deoxy-[αFuc(1→2)]βGal-*O*-octyl, its effect on terminal glycosylation of cell-associated glycoproteins with blood group A determinants were also examined. Thus monoclonal antibodies specific for blood group A determinant were used to immunoprecipitate metabolically-radiolabeled glycoproteins from the blood group A^+ human colon carcinoma cell line HT29 (19) cultured in the absence or presence of 3-amino-3-deoxy-[αFuc(1→2)]βGal-*O*-octyl. The antibodies used included MAB 11D4

which detects exclusively type 2 chain blood group A determinant (24), and MAB 3A7 which is specific for type 2 chain bearing either blood group A or B determinant (23). As shown in **Fig. 4.7** (lane **a**), immunoprecipitation of untreated [^{35}S]-labeled HT29 cell lysates with MABs 11D4 and 3A7 revealed a specific band of 140 kDa glycoprotein (gp140) not seen in the comparable normal mouse serum control lane. This result was consistent with previous studies (23, 24) which demonstrated that the major carrier of type 2 chain blood group A determinants in HT29 cells is a glycoprotein with an apparent mobility of 140 kDa, subsequently identified as α3β1 integrin. However, treatment of HT29 cells with 0.5 mM 3-amino-3-deoxy-αFuc(1→2)βGal-*O*-octyl prior to and during the period of metabolic labeling with [^{35}S]-methionine resulted in a significant decrease in the amount of gp140 immunoprecipitated with MABs 3A7 and 11D4 (**Fig. 4.7**, lane **c**). This effect was dependent on the concentration of 3-amino-3-deoxy-[αFuc(1→2)]βGal-*O*-octyl used since only minimal effects were observed in cells treated with only 0.1 mM inhibitor (**Fig. 4.7**, lane **b**).

MAB 8D5 (an antibody which detects blood group A determinant irrespective of chain type) was included in the study to rule out the possibility that the results obtained with 3-amino-3-deoxy-[αFuc(1→2)]βGal-*O*-octyl resulted from an indirect effect on enzymes involved in the biosynthesis of type 2 chains in HT29 cells. The specificity of MAB 8D5 was determined using a panel of BSA-glycan conjugates expressing blood group A or B determinants (**Table 4.1**). As is shown by ELISA in **Fig. 4.8**, MAB 8D5 detected blood group A determinant present on type 1, type 2, type 4 and type 6 chains. In contrast, MAB 8D5 did not detect A disaccharide, B

disaccharide or any of the BSA-glycan conjugates containing blood group B determinants. When this antibody was used in immuno-precipitation analyses of untreated and 3-amino-3-deoxy-[αFuc(1→2)]βGal-*O*-octyl-treated [^{35}S]-labeled HT29 cell lysates, the results obtained were identical to those seen with MABs 3A7 and 11D4 (**Fig. 4.7**).

In order to determine the inhibitory effect of 3-amino-3-deoxy-[αFuc(1→2)] βGal-*O*-octyl on the biosynthesis of blood group A determinants in HT29 cells was not the result of a general effect on protein synthesis, untreated and 3-amino-3-deoxy-[αFuc(1→2)]βGal-*O*-octyl-treated [^{35}S]-labeled cell lysates were immunoprecipitated with MAB 7A8. The MAB 7A8 is a monoclonal antibody which detects the polypeptide portion of α3 integrin subunit, one of the components of gp140. As shown in **Fig. 4.7**, similar amounts of α3β1 integrin were immunoprecipitated from untreated and treated HT29 cells, indicating that the inhibitor does not appear to affect protein synthesis.

Thus, these results indicate that at sufficiently high concentration, the level of inhibition of A-transferase obtained with 3-amino-3-deoxy-[αFuc(1→2)]βGal-*O*-octyl is accompanied by a markedly reduced level of blood group A determinants on gp140/α3β1 integrin, a major carrier of blood group A determinants in HT29 cells.

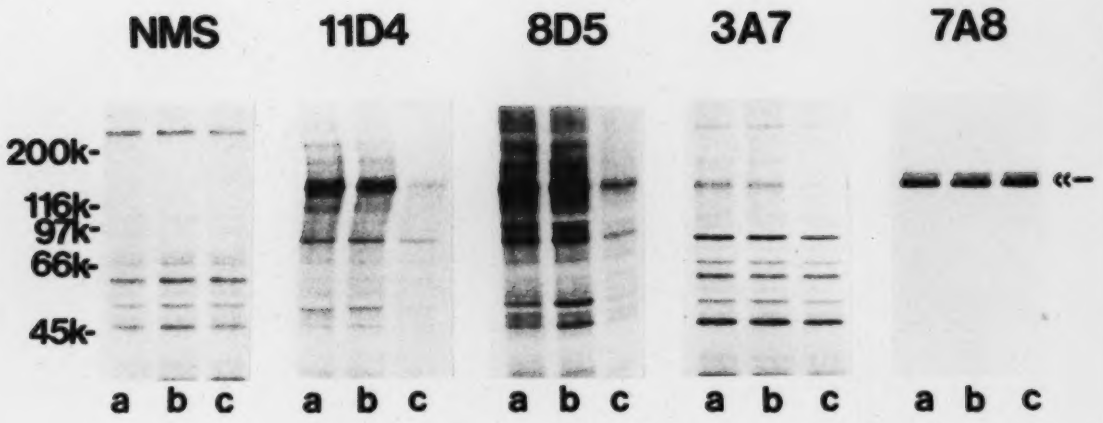

Figure 4.7 Effect of 3-amino-3-deoxy-[αFuc(1→2)]βGal-*O*-octyl on glycosylation of the cell-associated glycoprotein gp140/α3β1 integrin with blood group A determinants. HT29 cell monolayers radiolabeled for 18 hr with [^{35}S]-methionine in the absence (lane **a**) or presence of 0.1 mM (lane **b**) or 0.5 mM (lane **c**) $3NH_2$FucGal-*O*-octyl. Detergent-solubilized radiolabeled cell lysates were immunoprecipitated with either NMS or MABs 11D4 (anti-A type 2), 8D5 (anti-A), 3A7 (anti-A type 2 or B type 2), 7A8 (anti-α3 integrin subunit), as indicated above the figure. The immunoprecipitates were separated by 6% SDS-PAGE under reducing conditions, and bands visualized following fluorography and autoradiography. The numbers to the left of the figure indicate the sizes of molecular weight markers. The double arrowhead at the right of the figure indicates the position of gp140/α3β1 integrin, the major glycoprotein carrier of A type 2 determinants in HT29 cells (25).

Table 4.1 Structure of oligosaccharide moiety of BSA-glycan conjugates.

Name	Structure
H type II	αFuc(1→2)βGal(1→4)GlcNAc-BSA
A disaccharide	αGalNAc(1→3)Gal-BSA
A type 1	αGalNAc(1→3)[αFuc(1→2)]βGal(1→3)GlcNAc-BSA
A type 2	αGalNAc(1→3)[αFuc(1→2)]βGal(1→4)GlcNAc-BSA
A type 4	αGalNAc(1→3)[αFuc(1→2)]βGal(1→3)GalNAc-BSA
A type 6	αGalNAc(1→3)[αFuc(1→2)]βGal(1→4)Glc-BSA
B disaccharide	αGal(1→3)Gal-BSA
B type 2	αGal(1→3)[αFuc(1→2)]βGal(1→4)GlcNAc-BSA
B type 4	αGal(1→3)[αFuc(1→2)]βGal(1→3)GalNAc-BSA
B type 5	αGal(1→3)[αFuc(1→2)]βGal(1→3)Gal-BSA

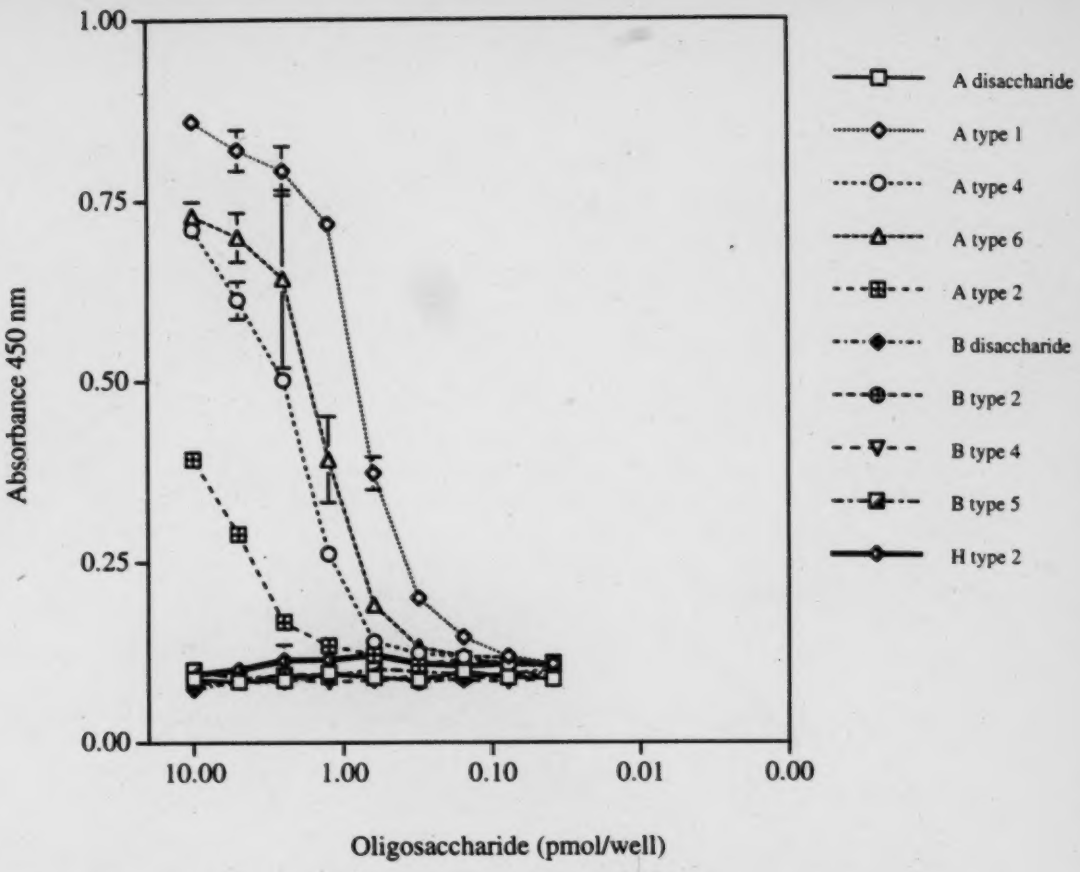

Figure 4.8 Solid-phase immunosorbent assay of BSA-glycan conjugates with MAB 8D5. Serial dilutions of BSA-glycan conjugates (10 to 0.01 pmol oligosaccharide/well), depicted in **Table 4.1**, were added in triplicate to a 96-well Immulon-2 plate and incubated overnight at 4°C. An enzyme-linked immunoassay (EIA) was carried out using MAB 8D5 (1:3000 dilution, 2 hr) followed by alkaline phosphatase-coupled goat anti-mouse Ig (1:3000, 1 hr). Colour development was monitores at 405 nm following addition of the substrate *p*-nitrophenyl phosphate. Each point on the graph represents the mean (with standard deviation). Note that for some of the data points, the standard deviation was not visible due to those values were lower than the graphic resolution.

4.4 Conclusions

An intracellular inhibition assay was developed to demonstrate the first *in cella* blood group A-transferase inhibition, in HT29 cells. The experiments clearly showed that the inhibitor, 3-amino-3-deoxy-[αFuc(1→2)]βGal-*O*-octyl was effective in decreasing intracellular enzyme activity. The inhibition was concentration-dependent and an intracellular IC_{50} (282 μM) was obtained for this inhibitor. This IC_{50} value determined may reflect the amount of inhibitor that crossed the cell membrane and was then localized in the same intracellular compartment as the target enzyme.

This intracellular inhibition assay is a very effective method in screening and determining the efficacy of potential drugs in cells and provides a benchmark for further testing of positive compounds, and therefore, a valuable contribution of interest to pharmaceutical companies. This assay method is a good intermediate to actual clinical tests because the choice of cell lines can provide a closer model to the tissue of interest than *in vitro* experiments. However one difficulty arising from using cells is the irreproducibility from one passage of cells to another (unknown peak 5, in **Fig. 4.4**, occurrence is only 20%). The inhibition assay would have to be done within the same passage of cells in order to avoid any misinterpretation of the results.

This is an ongoing project in which our collaborator, Dr. S. Laferté of the Department of Chemistry, University of Saskatchewan measured the effect in blood group A determinant formation in HT29 cells which occurs following treatment with 3-amino-3-deoxy-[αFuc(1→2)]βGal-*O*-octyl. Preliminary results have shown a decrease in blood group A antigen, but not on glycoprotein, formation in the [^{35}S]-

methionine incorporation experiment. Potential future studies using an indirect immuno-fluorescence detection assay may provide information on whether or not the inhibition of the blood group A-transferase by this inhibitor would lead to a decrease of cell surface carbohydrate structures.

4.5 References

1. Dennis, J. W., Laferté, S., Waghorns, C., Breitman, M. L., and Kerbel, R. S. (1987) *Science* **236**, 582-585.
2. Dennis, J. W. (1991) in *Cell Surface Carbohydrates and Cell Development* (Fukuda, M. ed.) pp. 161-194, CRC Press, Boca Raton.
3. Sears, P., and Wong, C.-H. (1998) *Cell. Mol. Life Sci.* **54**, 223-252.
4. Palcic, M. M., Heerze, L. D., Srivastava, O. P., and Hindsgaul, O. (1989) *J. Biol. Chem.* **264**, 17174-17181.
5. Lowary, T. L., and Hindsgaul, O. (1994) *Carbohydr. Res.* **251**, 33-67.
6. Lu P.-P., Hindsgaul, O., Compston, C. A., and Palcic, M. M. (1996) *Bioorg. Med. Chem.* **4**, 2011-2022.
7. Lu, P.-P., Hindsgaul, O., Li, H., and Palcic, M. M. (1997) *Carbohydr. Res.* **303**, 283-291.
8. Lemieux, R. U. (1985) in *Proc. VIIIth Int. Symp. Med. Chem.* pp. 329-351, Swedish Pharmaceutical Press, Stockholm 1.
9. Sujino, K., Malet, C., Hindsgaul, O., and Palcic, M. M. (1997) *Carbohydr. Res.* **305**, 433-442.
10. Gosselin, S., and Palcic, M. M. (1996) *Bioorg. Med. Chem.* **4**, 2023-2028.
11. Holmes, E. H. (1990) *J. Biol. Chem.* **265**, 13150-13156.
12. Sugumaran, G., Katsman, M., Sunthankar, P., and Drake, R. R. (1997) *J. Biol. Chem.* **272**, 14399-14403.
13. Datta, A. K., and Paulson, J. C. (1997) *Indian J. Biochem. Biophys.* **34**, 157-165.

14. Nagai, K., Ihara, Y., Wada, Y., and Taniguchi, N. (1997) *Glycobiology* **7**, 769-776.

15. Seto, N. O., Palcic, M. M., Compston, C. A., Li, H., Bundle, D. R., and Narang, S. A. (1997) *J. Biol. Chem.* **272**, 14133-14138.

16. Smith, S. L., Compston, C. A., Palcic, M. M., Bamford, M. J., Britten, C. J., and Field, R. A. (1997) *Biochem. Soc. Trans.* **25**, S630.

17. Watkins, W. M. (1980) in *Advances in Human Genetics* (Harris, H & Hirschhorn, K. eds.), pp. 1-136. Plenum Publishing Co, New York.

18. Watkins, W. M. (1991) *Pure Appl. Chem.* 62, 561-568.

19. Fogh, J., and Trempe, G. (1975) in *Human Tumor Cells In Vitro* (Fogh, J. ed.) pp. 115-159, Plenum Press, New York.

20. Seto, N. O. L., Palcic, M. M., Hindsgaul, O., Bundle, D. R., and Narang, S. A. (1995) *Eur. J. Biochem.* **234**, 323-328.

21. Palcic, M. M., Heerze, L. D., Pierce, M., and Hindsgaul, O. (1988) *Glycoconjugate J.* **5**, 49-63.

22. Zhang, Y., Le, X., Dovichi, N. J., Compston, C. A., Palcic, M. M., Diedrich, P., and Hindsgaul, O. (1995) *Anal. Biochem.* **227**, 368-376.

23. Laferté, S., Prokopishyn, N. L., Moyana, T., and Bird, R.P. (1995) *J. Cellular Biochem.* **57**, 101-119.

24. Prokopishyn, N. L., Puzon-McLaughlin, W., Takada, Y., and Laferté, S. (1999) *J. Cellular Biochem.* **72**, 189-209.

25. Laferté, S., and Loh, L.C. (1992) *Biochem. J.* **283**, 193-201.

26. Laemmli, U. K. (1970) *Nature* **227**, 680-685.

27. Bonner, W. M., and Laskey, R. A. (1974) *Eur. J. Biochem.* **46**, 83-88.

Chapter Five

Detection and Characterization of Novel Glycosyltransferases with CE-LIF

A portion of this chapter has been submitted for publication and filed for patent.

Wang, G., Boulton, P. G., Chan, N. W. C., Palcic, M. M., and Taylor, D. E. (1998) *J. Bacteriol. (Enzyme and Protein) submitted.*

I would like to thank Drs. D. E. Taylor, G. Wang, and Mr. P. Boulton in the Department of Medical Microbiology and Immunology, University of Alberta, and Dr. K. Sujino of the Department of Chemistry, U of A, for providing enzymatic reaction mixtures used in this chapter. I thank Dr. R. J. Jackson at the Cooperative Research Centre for Biological Control of Vertebrate Pest Population, Australia, who provide us with the novel cloned 2,3-sialyltransferase for syntheses. I would also like to thank Dr. O. Hindsgaul in the Department of Chemistry, U of A, for all synthetic acceptors, Dr. T. Kamata for synthesizing the 2,3 sialyl Lewis^a-TMR.

5.1 Introduction

This chapter is intended to illustrate the versatility of the capillary electrophoresis system equipped with laser-induced fluorescence detection. It was always a problem that the enzymatic reaction product(s) in standard Sep-Pak radiochemical assay (1) of novel glycosyltransferases could not be identified. The presence of glycosidases in enzyme preparations also posed a problem in degradation of substrate, therefore, lowering the substrate concentration in the reaction mixture. CE-LIF is able to circumvent these problems to some extent.

In radiochemical assays of glycosyltransferases (1), the reaction mixture typically contains hydrophobic acceptor and radiolabeled sugar-nucleotide donor, along with the enzyme in a suitable buffer solution. The enzyme catalyzes the transfer of radiolabeled monosaccharide from the nucleotide donor to the acceptor, at a particular -OH site, to form a new glycosidic linkage. After removing the unreacted, hydrophilic donor on a Sep-Pak Plus C-18 cartridge, the retained hydrophobic molecules (acceptor and enzymatic products) were eluted with methanol and subjected to scintillation counting. The decays per minute (d.p.m.) count was directly proportional to the enzyme activity. Due to the nature of the assay, the products were not separated from the unlabeled acceptor substrate, or from each other in cases where more than one product was formed. In cases where the identity of a new cloned enzyme was to be confirmed results from radiochemical assays did not permit unequivocal identification of the new enzyme. CE-LIF allows the separation of product(s) from the substrate and provides a means to identify the product by co-migration with existing standards.

Compare to our radiochemical assay for detection of glycosyltransferases, conventional assay methods such as HPLC (2, 3), TLC (4), and size-exclusion chromatography (5) can separate product(s) from the substrate. Major advantages of CE-LIF over these methods are the low detection limit (200 molecules) and sample concentration can be as low as 10^{-10} M (millimolar range in HPLC with UV detection), fast separation (less than 15 min), high separation efficiency (typically 10^6 theoretical plates), and eliminate the use of radioisotopes.

The combined chemical-enzymatic synthesis of oligosaccharides (6-12) has been used more extensively in recent times as a result of increased interest in the preparation of natural and unnatural carbohydrate structures in order to gain an increased understanding of their biological roles (13, 14). Demand for large-scale production of genetically-engineered mammalian glycosyltransferases (15-18) has increased because isolation from their host tissues, in which they are present in low amounts, is time-consuming and costly. Thus, the ability to engineer an enzyme that can compete with or exceed the ability of the mammalian glycosyltransferases to synthesize oligosaccharides is one from which great benefits might be gained. In today's genetically-engineered enzyme preparations, often cloned enzyme extracts are contaminated with hydrolyzing enzymes such as hexosaminidase or β-galactosidase. Substrates containing one of the structures, βGal(1→3)βGlcNAc-*O*-gr or βGal(1→4)βGlcNAc-*O*-gr, would be digested before detectable levels of product had been formed by the low level of cloned glycosyltransferase. CE-LIF not only provides an increased degree of sensitivity (comparable with that offered by

radiochemical assays), but the system also provides structural information with regard to the fate of the substrate during or after the reaction.

In this chapter, there are two examples of activity detection and characterization of such cloned enzymes; a *Helicobacter pylori* α1,2 fucosyltransferase (*HpfucT2 gene*) cloned in *E. coli* K38 (19), and a Brazilian myxoma viral α2,3 sialyltransferase infected into a European rabbit kidney RK_{13} cell line (20, 21). **Schemes 5.1** and **5.2** show a comparison between the mammalian and the cloned *Helicobacter pylori* α1,2 fucosyltransferases in the biosynthetic pathway of Lewis^y-OR and Lewis^b-OR, respectively. **Schemes 5.3** and **5.4** show a comparison between the mammalian and the Brazilian myxoma viral α2,3 sialyltransferases in the biosynthetic pathway of sialyl Lewis^x-OR and sialyl Lewis^a-OR, respectively. Radiochemical assay results obtained for both enzymes showed the transfer of the tritiated donor to the acceptor, but did not provide any structural and/or glycosidic linkage information. Using CE-LIF, the product of the reaction was separated from the starting material and was identified by co-migration and treatment of specific glycosidases.

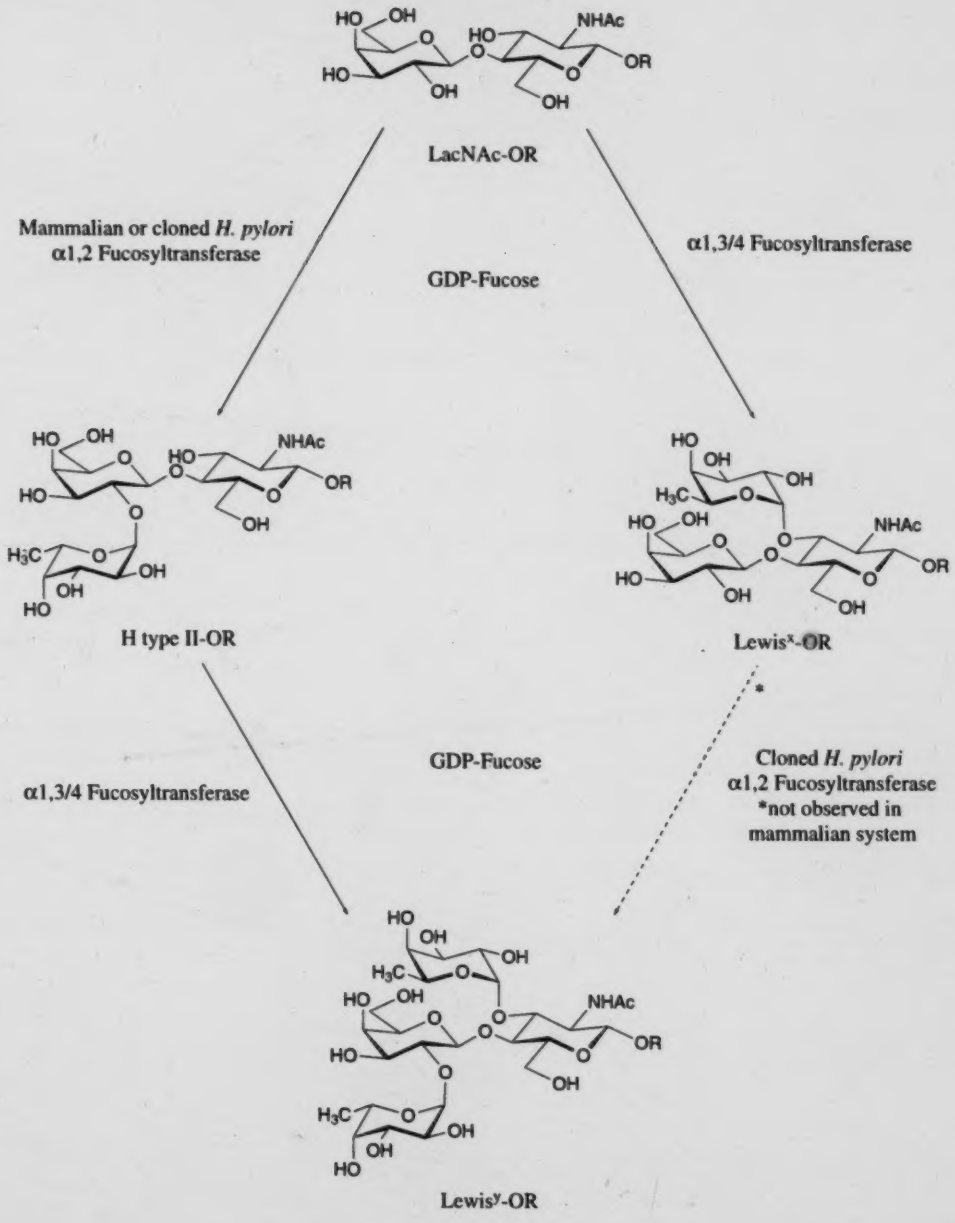

Scheme 5.1 Biosynthetic pathway of Lewis^y-OR involving α1,2 fucosyltransferase: comparison between the normal mammalian and the novel cloned *H. pylori* enzymes.

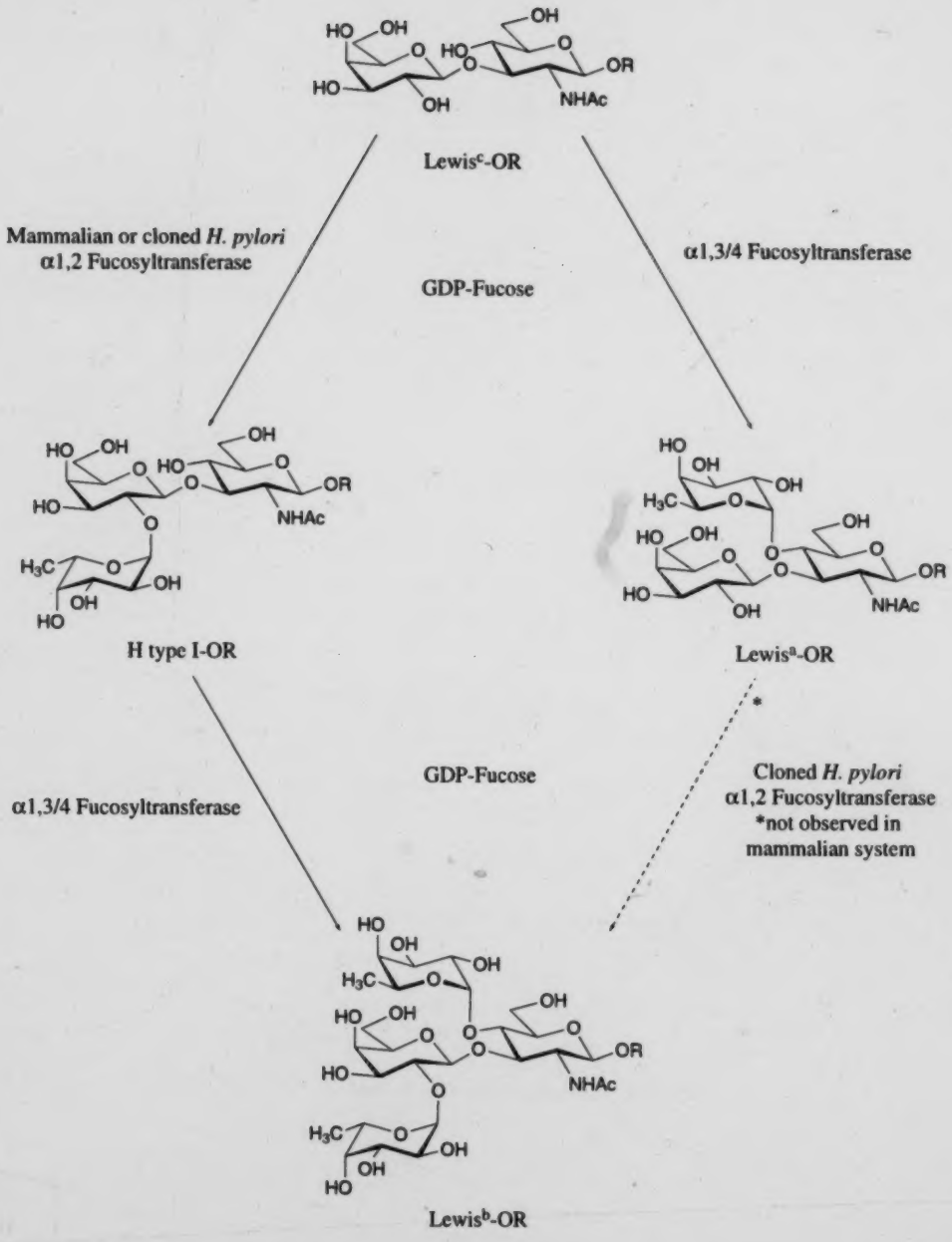

Scheme 5.2 Biosynthetic pathway of Lewis^b-OR involving α1,2 fucosyltransferase: comparison between the normal mammalian and the novel cloned *H. pylori* enzymes.

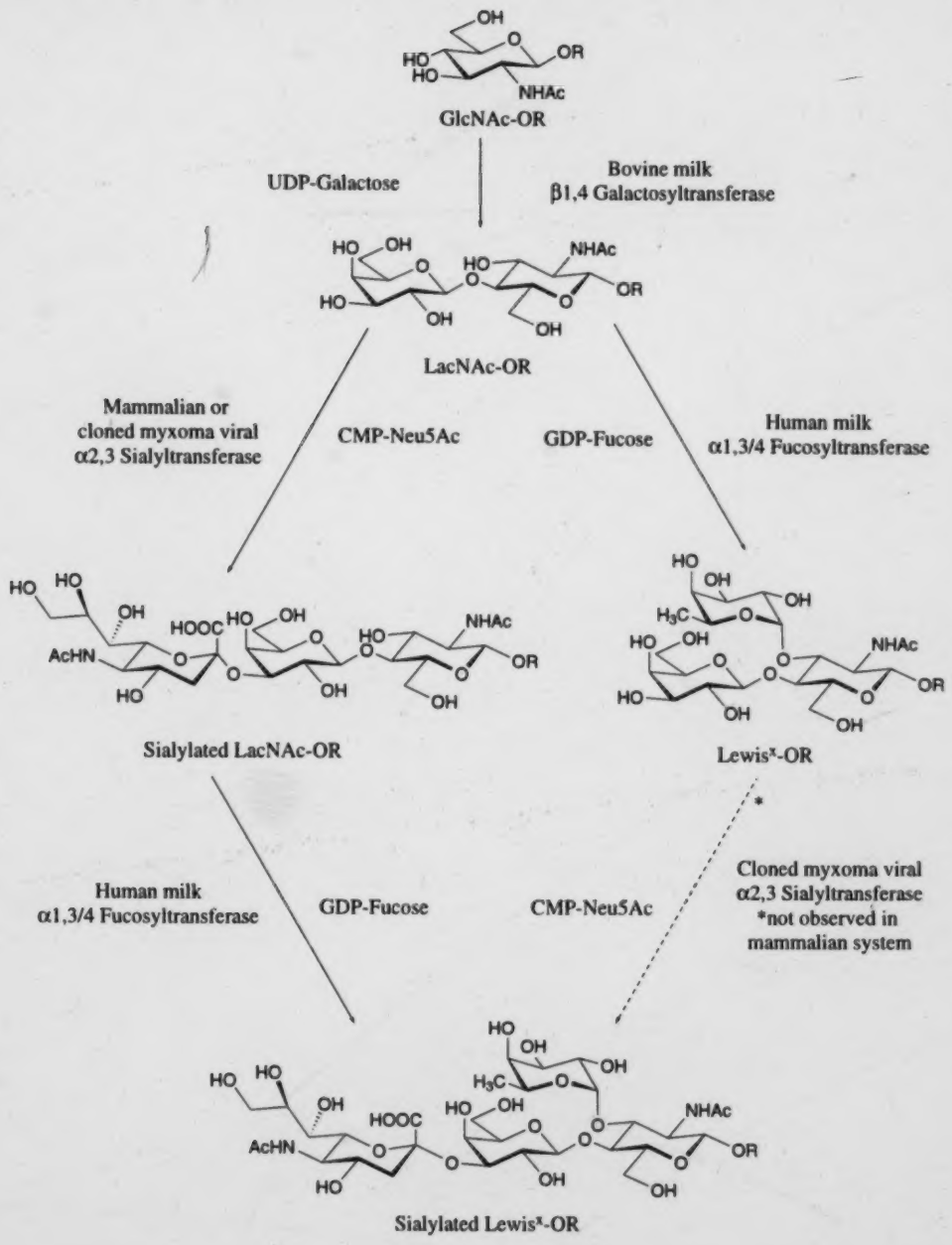

Scheme 5.3 Biosynthetic pathway of sialylated Lewis^x-OR involving α2,3 sialyltransferase: comparison between the normal mammalian and the novel myxoma viral enzymes.

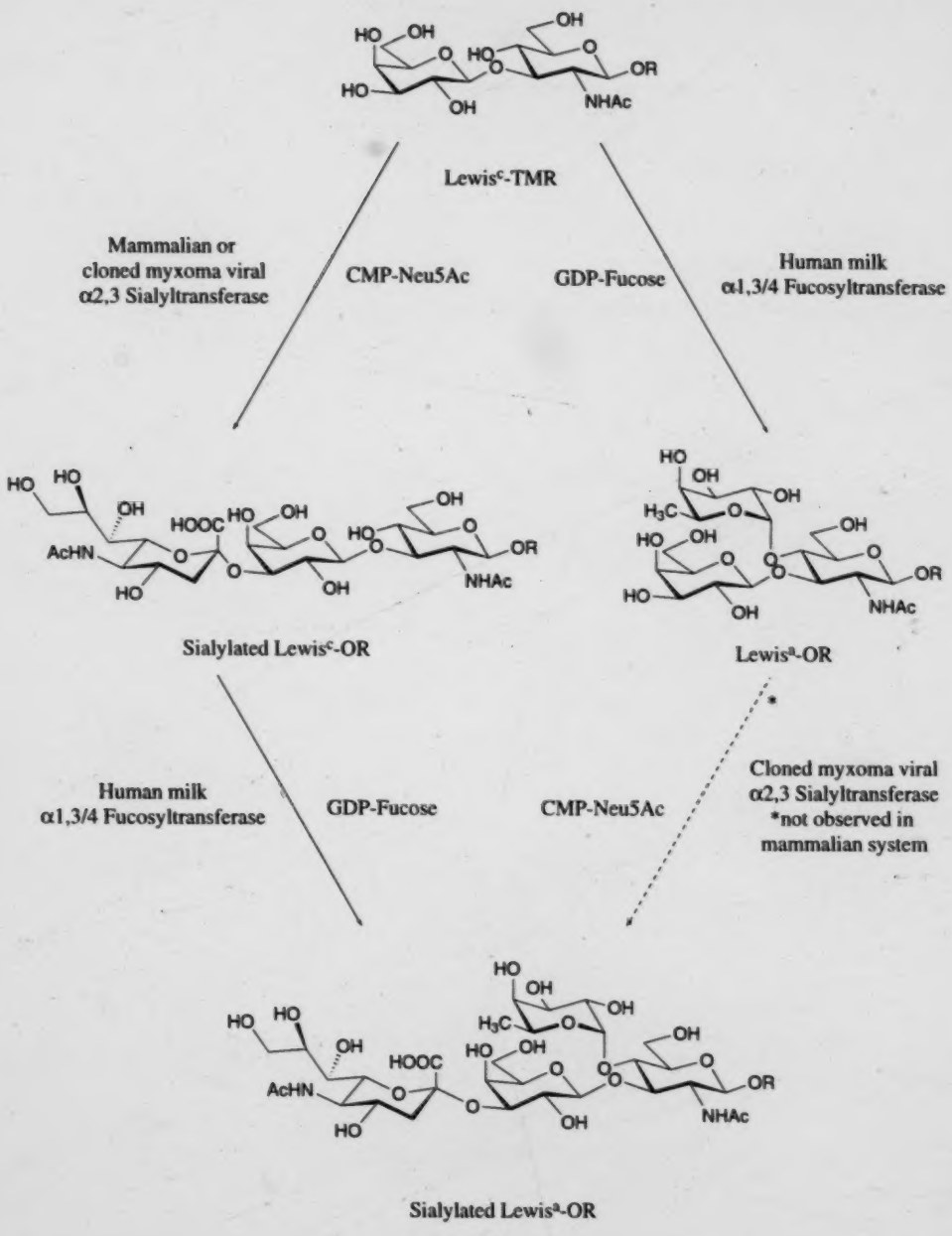

Scheme 5.4 Biosynthetic pathway of sialylated Lewis^a-OR involving α2,3 sialyltransferase: comparison between the normal mammalian and the novel myxoma viral enzymes.

5.2 Experimental Section

5.2.1 Materials

βGal(1→4)βGlcNAc-*O*-$(CH_2)_8$COOMe (LacNAc-gr), βGal(1→3)βGlcNAc-*O*-$(CH_2)_8$COOMe (Lewis^c-gr), αFuc(1→2)βGal(1→4)βGlcNAc-*O*-$(CH_2)_8$COOMe (H type II-gr), αFuc(1→2)βGal(1→3)βGlcNAc-*O*-$(CH_2)_8$COOMe (H type I-gr), βGal(1→4)[αFuc(1→3)]βGlcNAc-*O*-$(CH_2)_8$COOMe (Lewis^x-gr), β Gal(1→3)[αFuc(1→4)]βGlcNAc-*O*-$(CH_2)_8$COOMe (Lewis^a-gr), α Fuc(1→2)βGal(1→4)[αFuc(1→3)]βGlcNAc-*O*-$(CH_2)_8$COOMe (Lewis^y-gr), α Fuc(1→2)βGal(1→3)[αFuc(1→4)]βGlcNAc-*O*-$(CH_2)_8$COOMe (Lewis^b-gr), β Gal(1→4)βGlcNAc-*O*-$(CH_2)_8$CONHCH$_2$CH$_2$NH-TMR (TMR), βGal(1→3)βGlcNAc-*O*-TMR, αFuc(1→2)βGal(1→4)βGlcNAc-*O*-TMR, αFuc(1→2)βGal(1→3)βGlcNAc-*O*-TMR, βGal(1→4)[αFuc(1→3)]βGlcNAc-*O*-TMR, β Gal(1→3)[αFuc(1→4)]βGlcNAc-*O*-TMR, αFuc(1→2)βGal(1→4)[αFuc(1→3)]βGlcNAc-*O*-TMR, α Fuc(1→2)βGal(1→3)[αFuc(1→4)]βGlcNAc-*O*-TMR, αNeu5Ac(2→3)βGal(1→4)[αFuc(1→3)] βGlcNAc-*O*-TMR were provided by Dr. O. Hindsgaul, Department of Chemistry, University of Alberta. αNeu5Ac(2→3)βGal(1→3)[αFuc(1→4)]βGlcNAc-*O*-TMR was prepared enzymatically by Dr. T. Kamata in our laboratory. The fluorescent probe, *N*-hydroxysuccinimidyl ester derivative of tetramethylrhodamine (TMR) was purchased from Molecular Probes, Inc. (Eugene, OR), and covalently linked to the oligosaccharides following the method described by Zhang *et al.* with modifications (22). GDP-fucose was synthesized by the method of Gokhale *et al.* (23), GDP-[1-^{3}H]fucose (5.1 Ci/mmol) and CMP-[9-^{3}H]Neu5Ac (20 Ci/mmol) were from American Radiolabeled Chemicals Inc. (St. Louis, MO). To confirm the formation of the

products, neuraminidase (*Arthrobacter urefaciens*) was purchased from Sigma (Oakville, ON). Alkaline phosphatase was from Boehringer Mannheim (Montreal, QC). The European rabbit kidney cell line (*Oryctolagus cuniculus* kidney, RK_{13}) and Brazilian myxoma virus strain Lausanne (Lu) were purchased from the American Type Culture Collection (Rockville, MA). The PD-10 column was purchased from BioRad (Hercules, CA) and the HiTrap Blue Affinity chromatography column from Pharmacia (Piscataway, NJ). The reverse phase Sep-Pak C-18 cartridges were obtained from Waters (Mississauga, ON), and were conditioned before use by washing with 5 ml of HPLC grade methanol and 10 ml of Milli-Q water. Milliex-GV filters were from Millipore Corp. (Mississauga, ON). Ecolite (+) scintillation cocktail from ICN (Costa Mesa, CA) was used for liquid scintillation counting in all radiochemical assays. The capillary electrophoresis instrument (22, 24) used in these studies was that used for studies described in chapters 3 and 4. The analysis program used in these experiments was Igor Pro, version 2.04, from WaveMetrics (Lake Oswego, OR).

5.2.2 Characterization of *H. pylori* α1,2 Fucosyltransferase

5.2.2.1 Preparation of Extract Containing the Cloned α1,2 Fucosyltransferase

Details of over-expression and preparation of the *E. coli* cell lysate containing *Helicobacter pylori* α1,2 fucosyltransferase activity was published by Wang *et al.* (19). Briefly, *H. pylori* strain UA802 α1,2 fucosyltransferase protein was over-expressed in *E. coli* strain K38. The plasmid pGP1-2 which carries a T7 RNA polymerase, and which is under the control of a heat-inducible Plac promoter, was

used. *E. coli* K38 cells carrying the over-expressed α1,2 fucosyltransferasse protein were lysed in a French press (7000lb/in^2) at 4°C. The cytoplasmic fraction (supernatant) was obtained by ultracentrifugation. This supernatant was used for radiochemical and CE assays, and was found to be stable for no more than 30 minutes at a reaction temperature of 37°C.

5.2.2.2 Radiochemical Synthesis of α1,2 Fucosylated Products

α1,2 Fucosyltransferase activities were assayed by incubating 6.2 µl of extract (2.8 - 6.0 mg protein/ml extract) at 37°C for 20 minutes with 1.8 mM acceptor (Lewis^c-, Lewis^x-, LacNAc-, or Lewis^a-Ogr), 50 µM GDP-fucose, 38,000-47,800 d.p.m. GDP-[^{3}H]fucose in 20 mM HEPES buffer (pH 7.0), 20 mM $MnCl_2$, 100 mM NaCl, 35 mM $MgCl_2$, 1 mM ATP and 0.5%(w/v) BSA in a total volume of 20 µl. Following incubation, the reaction mixtures were diluted to 0.4 ml with water and then loaded onto Sep-Pak Plus C-18 cartridges. The cartridges were washed with 50 ml of water to remove unreacted donor, and products were eluted with 4 ml of methanol prior to quantification by counting in 10 ml of Ecolite (+) scintillation cocktail in a Beckman LS 1801 scintillation counter (1). The insertion of the plasmid (pGEM) itself into the *E.coli* K38 (pGP1-2) provide a negative control. A mU of enzyme activity is defined here as that amount that catalyses the conversion of one nanomole of acceptor to product per minute under the standard screening conditions.

5.2.2.3 α1,2 Fucosylated Product Analyses by Capillary Electrophoresis with Laser-Induced Fluorescence Detection

1.8 mM Fluorescent-labeled acceptor (LacNAc-, or Lewis^c-TMR), 1.8 mM GDP-fucose, 20 mM HEPES buffer (pH 7.0), 20 mM $MnCl_2$, 100 mM NaCl, 35 mM $MgCl_2$, 1 mM ATP and 0.2%(w/v) BSA were mixed in a total volume of 20 µl and incubated at 37°C for either 20 min or 18 hr. After each incubation period, an aliquot (2 µl, 0.9 nmol total TMR) of sample mixture was applied to Sep-Pak Plus C-18 cartridges which were washed with 15 ml of water, and product was eluted with 4 ml of HPLC grade methanol. Samples were lyophilized and water was added to the dried samples such that the concentration of TMR stock was 100 µM. This solution (1 µl) was mixed with capillary electrophoresis running buffer (10 mM disodium hydrogen phosphate, 10 mM sodium borate, 10 mM sodium dodecylsulphate, 10 mM phenyl boronic acid pH 9.3, 99 µl) and 13 pl were injected onto a capillary column (60 cm long x 10 µm i.d.) at 1 kV for 5 s (22, 24). The separation voltage was at 400 V/cm. In some experiments, lactose was added to the LacNAc-TMR reaction in order to inhibit the effect of β-galactosidase. The protein extract from the *E. coli* K38 clone containing the pGEM vector without *Hp fucT2* gene was used as negative control in all of the above reactions, for each acceptor tested.

5.2.3 Characterization of Brazilian Myxoma Viral α2,3 Sialyltransferase

5.2.3.1 Cell Extract Preparation Containing the myxoma viral α2,3 Sialyltransferase

The European rabbit kidney cell line (*Oryctolagus cuniculus* kidney, RK_{13}) was found to be susceptible to myxoma viral infection (20) and was therefore suitable for myxoma viral replication. RK_{13} cells which had no endogenous expression of eukaryotic α2,3 sialyltransferase were infected with Brazilian myxoma viral strain, Lausanne (Lu). The myxoma viral α2,3 sialyltransferase cell lysate was prepared by a method similar to that published in the International Patent Application Publication No. WO97/18302 (21). Cells were lysed and supernatant containing the expressed myxoma viral α2,3 sialyltransferase activity was obtained by centrifugation. The supernatant was applied to a 5 ml HiTrap Blue Affinity chromatography column and the α2,3 sialyltransferase was eluted in NaCl with stepwise increases in salt concentration (0.5, 1.0, 1.5, and 2.0 M). The α2,3 sialyltransferase was desalted by passing the eluent through a PD-10 column in column buffer (50 mM MES, pH 6.1, 0.1% Triton CF-54, 25% glycerol).

Total protein concentration was measured by the method of Bradford (25) with a Bio-Rad protein determination kit, with IgG as a protein standard.

5.2.3.2 Radiochemical Synthesis of Sialylated Lewis^x and Lewis^a

Acceptor (54 nmol), CMP-Neu5Ac (40 nmol), and CMP-[9-^{3}H]Neu5Ac (150,000-180,000 d.p.m.) were added to a mixture of cell lysate containing the cloned myxoma viral sialyltransferase (16 µl), in 50 mM MES, 0.1% Triton CF54, pH 7.0, in

a total volume of 50 µl. Reaction mixtures were incubated at 37°C for certain period of time, then loaded onto a Sep-Pak C-18 cartridge as described in **section 5.2.2.2**. The negative controls were European rabbit kidney cells (RK_{13}) which had not been infected with the myxoma virus and RK_{13} cells infected with the virus in which the α2,3 sialyltransferase gene-encoding region had been disrupted by the insertion of the *E. coli lacZ* gene. A mU of enzyme activity is the amount that catalyzes the conversion of one nanomole of acceptor to product per minute under standard screening conditions.

5.2.3.3 Confirmation of a 2,3 Linkage between Sialic Acid and Lewis^x or Lewis^a

Lewis^a- or Lewis^x-TMR (35 nmol) and CMP-Neu5Ac (200 nmol) were incubated with 4.9 µl viral cell lysate and 0.1 µl alkaline phosphatase solution (5 µl of alkaline phosphatase at 1000U/ml and 1 µl BSA solution at 100 mg/ml). After gentle rotation at room temperature (25°C) for 42 hr, additional alkaline phosphatase solution (0.2 µl) and 100 mM CMP-Neu5Ac solution (0.2 µl) were added to the mixture, which was incubated for a further 48 hr at room temperature. After 48 hr at r.t., the reaction temperature was elevated and maintained at 37°C for another 48 hr, the mixture was then loaded onto a Sep-Pak C-18 cartridge to work-up as described in section **5.2.2.3**. Water was added to dried-down eluate such that the concentration of TMR was approximately 100 µM. A 100 nM solution in CE running buffer was used for separation and analysis by CE-LIF (22, 24). A new product formed in the enzyme reaction had a migration time similar to that of authentic sialylated Lewis^x-TMR and sialylated Lewis^a-TMR.

5.2.3.4 Peak Identification Using a Neuraminidase

A 10 µl sample of the incubation mixture from **section 5.2.3.3**, containing 1 nmol total TMR-labeled compounds was mixed with 1 µl *Arthrobater urefaciens* neuraminidase (8.4 mU in 10 mM sodium phosphate, 0.025%(w/v) BSA, 0.05%(w/v) NaN_3, pH 7.0) and 20 µl sodium citrate, pH 5.0. The mixture was incubated with gentle rotation at 37°C for 72 hr. The mixture was then loaded onto a Sep-Pak Plus C-18 cartridge. A solution contains 100 nM of sample in CE running buffer was prepared for separation and detection with CE-LIF as described in **section 5.2.2.3**. The new product peak was converted back to the starting acceptor by treatment with neuraminidase

5.2.3.5 One-Pot Syntheses of Sialylated Lewis^x-TMR from GlcNAc-TMR & Sialylated Lewis^a-TMR from Lewis^c-TMR

For the multi-enzyme synthesis of Lewis^x-TMR from monosaccharide, GlcNAc-TMR (35 nmol), UDP-galactose (70 nmol), 0.5 µl isolated bovine milk β1,4 galactosyltransferase (0.3 mU), GDP-fucose (70 nmol), 0.5 µl isolated human milk α1,3/4 fucosyltransferase (0.03 mU), CMP-Neu5Ac (100 nmol) were incubated with 5.7 µl of concentrated viral cell lysate solution containing α2,3 sialyltransferase activity (0.1 mU). For synthesis of sialylated Lewis^a-TMR, Lewis^c-TMR (15 nmol), GDP-fucose (70 nmol), 0.5 µl isolated human milk α1,3/4 fucosyltransferase (0.03 mU; 26, 27), CMP-Neu5Ac (100 nmol), 0.1 µl of 1 M $MnCl_2$ and 0.1 µl alkaline phosphatase (10 mU Boehringer Mannheim) were incubated with 5.1 µl of

concentrated viral cell lysate solution containing α2,3 sialyltransferase activity (0.1 mU).

The samples were gently rotated at room temperature and at 1 day, 3 days, 1 month, and 2 months, aliquants were removed from the reaction mixtures and diluted with water. These samples were diluted with CE running buffer and injected into the CE instrument for separation and detection by LIF as describes in **section 5.2.2.3**. The reaction products were identified by comparison with the migration times of authentic standards. The area under each peak was determined with the graphing and data analysis program, Igor Pro version 2.04. The area of each product peak, biosynthesis by glycosyltransferases or biodegradation by glycosidases, was divided by the total area to calculate the degree of transfer in each case.

5.3 Results And Discussion

5.3.1 *Helicobacter pylori* α1,2 Fucosyltransferase Results

5.3.1.1 Radiochemical Synthesis of α1,2 Fucosylated Products

In radiochemical assays, 4 different acceptors were used to determine the degree of transfer of fucose by the cloned α1,2 fucosyltransferase. **Table 5.1** shows relative activities with each acceptor. Results revealed that the type I structures (Lewis^c-gr and Lewis^a-gr) were better acceptors having higher specific activities. The trisaccharides were acceptors for the cloned α1,2 fucosyltransferase when normally fucose would not be transferred to these trisaccharides (see **Schemes 5.1** and **5.2**). In the mammalian system, LacNAc-gr would be the best acceptor amongst those tested for the addition of fucose to the 2-OH position of galactose by α1,2 fucosyltransferase. Surprisingly, the cloned *H. pylori* α1,2 fucosyltransferase showed the lowest activity towards LacNAc-gr, whereas considerable activity was observed for the fucosylation of Lewis^x-gr (25-times higher).

5.3.1.2 Analysis of the α1,2 Fucosylation Products by Capillary Electrophoresis with Laser-Induced Fluorescence Detection

Incubation with LacNAc-TMR showed that it did not appear to be a good substrate for the α1,2 fucosyltransferase. However, the presence of β-galactosidase endogenous to the *E.coli* crude extract may have reduced the concentration of LacNAc in the reaction mixture quite substantially during the incubation period (**Fig. 5.1A**). The same problem may have occurred in the negative control in which only the pGEM plasmid was inserted (**Fig. 5.1B**). These observations were consistant with

Table 5.1 Relative *H. pylori* α1,2 fucosyltransferase activity with each acceptors.

Acceptor	Proposed product	Relative Activity[a]	Specific Activity (mU/mg)[b]
Lewis^c-gr	H Type I-gr	100%	0.309
LacNAc-gr	H Type II-gr	1.9%	0.006
Lewis^a-gr	Lewis^b-gr	97%	0.301
Lewis^x-gr	Lewis^y-gr	49%	0.150

[a] % Activity relative to that of Lewis^c-gr.

[b] A milliunit (mU) of the enzyme is expressed as the activity to convert 1 nmol of acceptor to product per minute. Specific activity was obtained by dividing the total activity (mU) by the total protein (mg) in the whole cell extract.

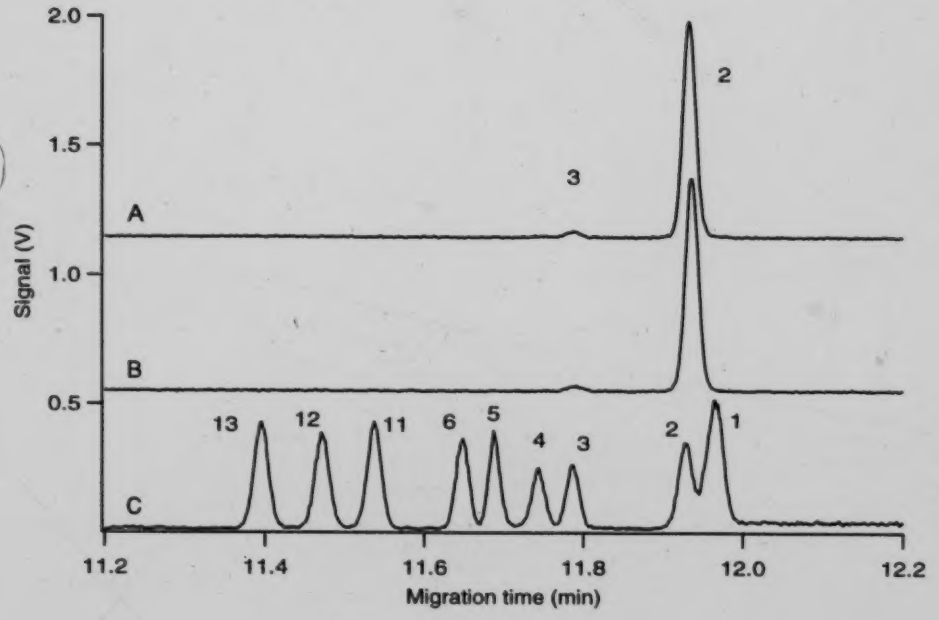

Figure 5.1 Analysis by CE-LIF of reaction mixtures from *E. coli* whole cell extract incubations. (**A**) Electropherogram showing the reaction of *H. pylori* α1,2 fucosyltransferase incubated with 1.8 mM LacNAc-TMR for overnight. (**B**) The negative control, *E.coli* inserted with the plasmid only, incubated with acceptor overnight. (**C**) Separation of 9 standard TMR oligosaccharides found in mammalian metabolism: linker arm- (**1**), GlcNAc- (**2**), LacNAc- (**3**), αFuc(1→2)βGal(1→4)βGlcNAc- (**4**), β Gal(1→4)[αFuc(1→3)]βGlcNAc- (**5**), αFuc(1→2)βGal(1→4)[αFuc(1→3)] βGlcNAc- (**6**), αNeu5Ac(2→6)LacNAc- (**11**), αNeu5Ac(2→3)LacNAc- (**12**), αNeu5Ac(2→3)Le^x-TMR (**13**). These electropherograms (**A** and **B**) were y-offset for clarity.

those from radiochemical assays where there was a very low degree of transfer with LacNAc-*O*gr. Therefore, it was decided to add different concentration of lactose (0.1, 0.5, 1 M) to the reaction mixtures, since lactose would compete with LacNAc for β-galactosidase. While this reduced degradation and allowed the concentration of LacNAc-TMR to stay relatively stable during the incubation, no H type II-TMR product could be detected (**Fig. 5.2**). This was probably due to the transfer of fucose to the 2-OH of Gal on lactose, rather than to LacNAc. The lactose added to the reaction mixture was not labelled with a chromophore. Thus, the product could not be observed with CE-LIF, and it was not possible to demonstrate this alternative reaction. This problem might be circumvented by adding a specific β-galactosidase inhibitor to the reaction mixture to ensure the stable concentration of LacNAc in the assay, without the possibility of fucose transfer to an alternative acceptor.

In the mammalian system, the biosynthetic pathway for type I structures begins with addition of fucose to Lewis^c by α1,2 fucosyltransferase to form H type I, followed by α1,3/4 fucosyltransferase to form Lewis^b. Synthesis of type II structures follows a similar pathway, from LacNAc to H type II, and then Lewis^y. If the 3-OH or 4-OH position of the GlcNAc residue is substituted by a fucose unit, α1,2 fucosyltransferase will not add the second fucose to the 2-OH of Gal. In the present experiments with cloned α1,2 FucT, Lewis^x-TMR was a better substrate than LacNAc-TMR. In the reaction mixture (**Fig. 5.3A**), we confirmed by comigration with standards that Lewis^y-TMR had been formed. There was no Lewis^y-TMR formed in the negative control (**Fig. 5.3B**).

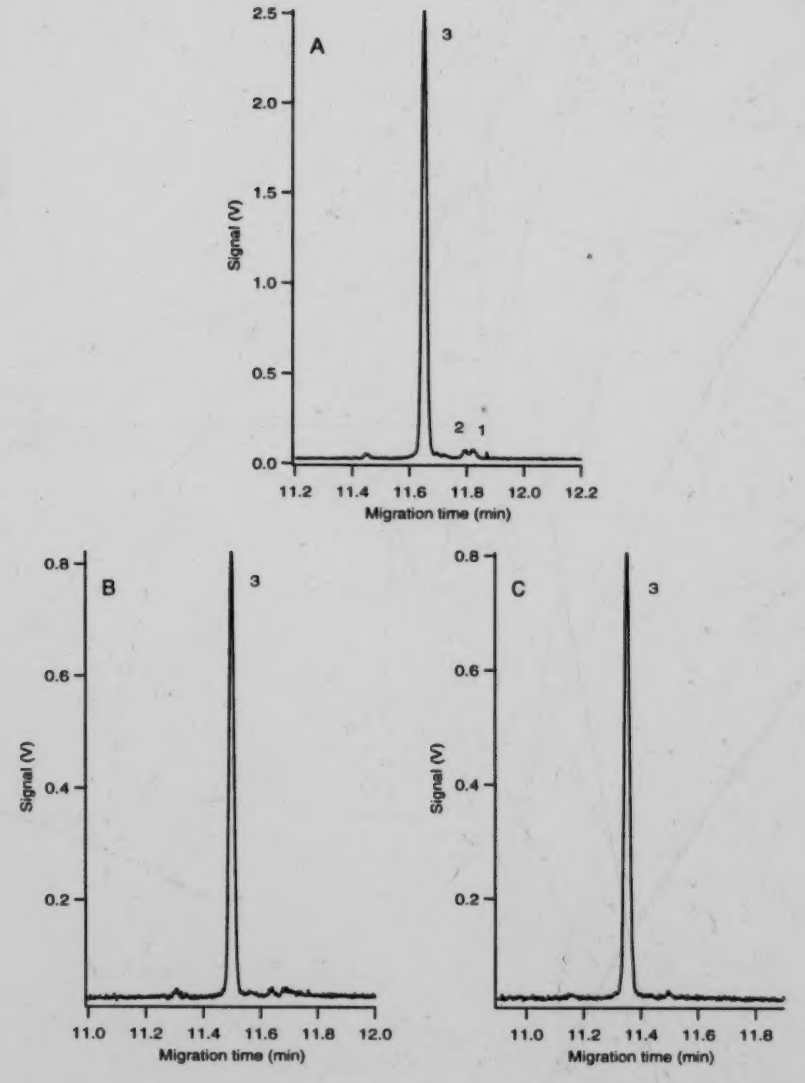

Figure 5.2 Analysis of reaction mixtures containing *H. pylori* α1,2 fucosyltransferase with 1.8 mM LacNAc and 0.1 M (**A**), 0.5 M (**B**) or 1.0 M (**C**) lactose. The peak identities are linker arm- (**1**), GlcNAc- (**2**), LacNAc-TMR (**3**).

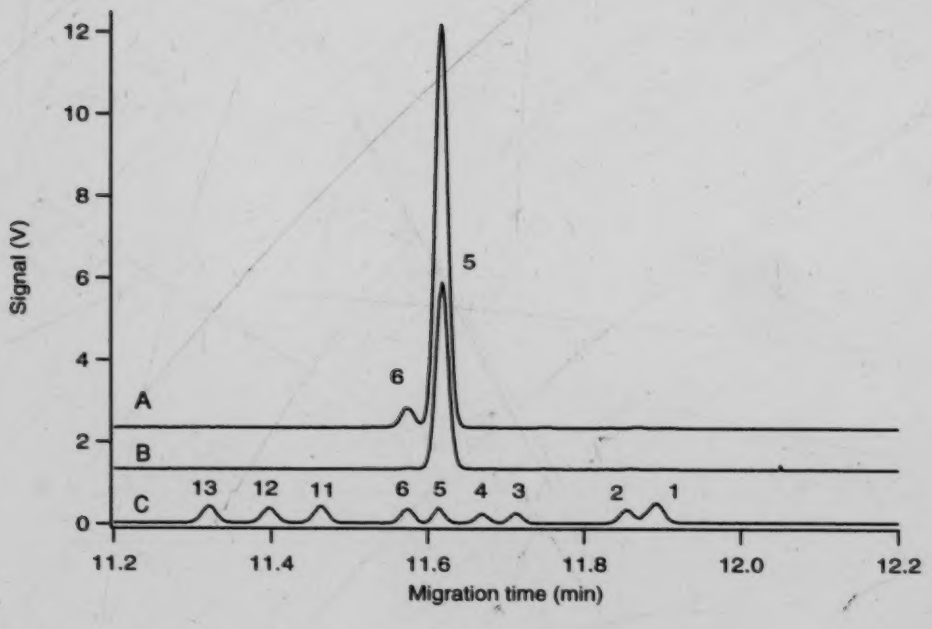

Figure 5.3 Analysis of reaction mixtures from the *E. coli* whole cell extract incubations by CE-LIF. (**A**) Electropherogram showing the reaction of *H. pylori* α1,2 fucosyltransferase incubated with 1.8 mM Le^x-TMR for overnight. (**B**) The negative control, *E.coli* inserted with the plasmid only, incubated with acceptor overnight. (**C**) Separation of 9 standard TMR oligosaccharides found in mammalian metabolism: linker arm- (**1**), GlcNAc- (**2**), LacNAc- (**3**), αFuc(1→2)βGal(1→4)βGlcNAc- (**4**), βGal(1→4)[αFuc(1→3)]βGlcNAc- (**5**), α Fuc(1→2)βGal(1→4)[αFuc(1→3)] βGlcNAc- (**6**), αNeu5Ac(2→6)LacNAc- (**11**), αNeu5Ac(2→3)LacNAc- (**12**), αNeu5Ac(2→3)βGal(1→4)[αFuc(1→3)]βGlcNAc-TMR (**1 3**). These electropherograms (**A** and **B**) were y-offset for clarity.

The enzyme recognized type I structures better than type II structures. The radiochemical assay results showed that the enzyme activities for type I acceptors were at least 2-fold higher than those for type II acceptors. The cloned enzyme also recognized the trisaccharide better than the disaccharide. Lewis^a-TMR (**Fig. 5.4A**) was a better substrate for the enzyme than the disaccharide (**Fig. 5.5A**) in the CE assay, though in the radiochemical assay, the relative activities were similar for both. A preliminary confirmation of the identity of the products was done by co-migration. The negative control showed no conversion of either substrate (**Figs. 5.4B** & **5.5B**).

In another assay tube (**Fig. 5.5C**), lactose (0.5 M) was added to the reaction mixture containing Lewis^c-TMR, under conditions similar to those in the LacNAc-TMR experiment. Results showed a decrease in the production of H Type I-TMR in this sample compared with that without lactose. As in the case with LacNAc-TMR, lactose was a competitive substrate in the reaction, resulting in a decrease in TMR product formation.

To confirm the identity of the enzyme products, standards of known concentration were added to the reaction mixtures and co-migration of the product with the standard was verified.

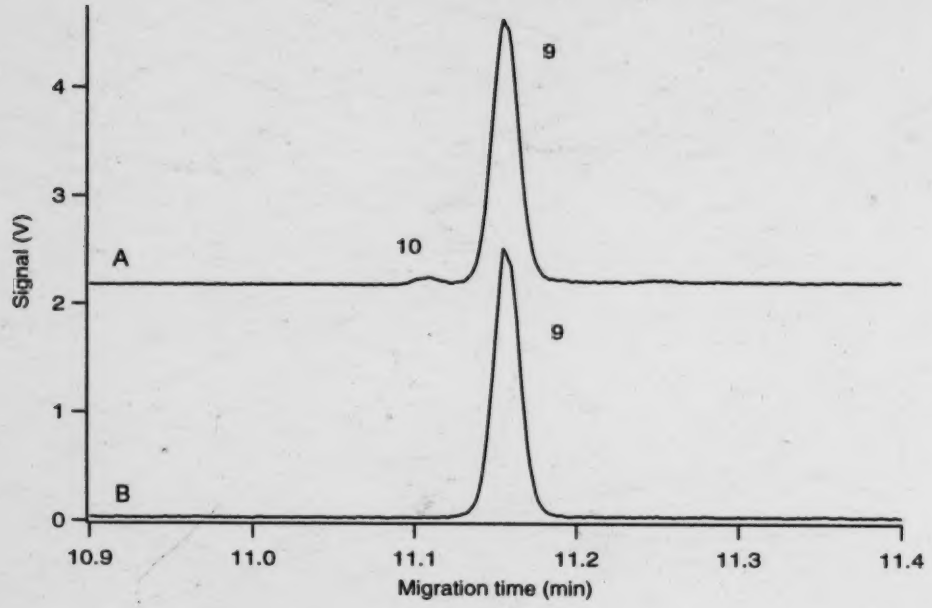

Figure 5.4 Analysis of Le^a-TMR reaction mixtures from the *E. coli* whole cell extract incubations by CE-LIF. (**A**) Electropherogram showing the reaction of *H. pylori* α1,2 fucosyltransferase incubated with 1.8 mM Le^a-TMR for 20 minutes. (**B**) The negative control, *E.coli* inserted with the plasmid only, incubated with acceptor for 20 minutes. The peak identifications are βGal(1→3)[αFuc(1→4)]βGlcNAc- (**9**), αFuc(1→2)βGal(1→3)[αFuc(1→4)]βGlcNAc-TMR (**10**). Electropherogram **A** was y-offset for clarity.

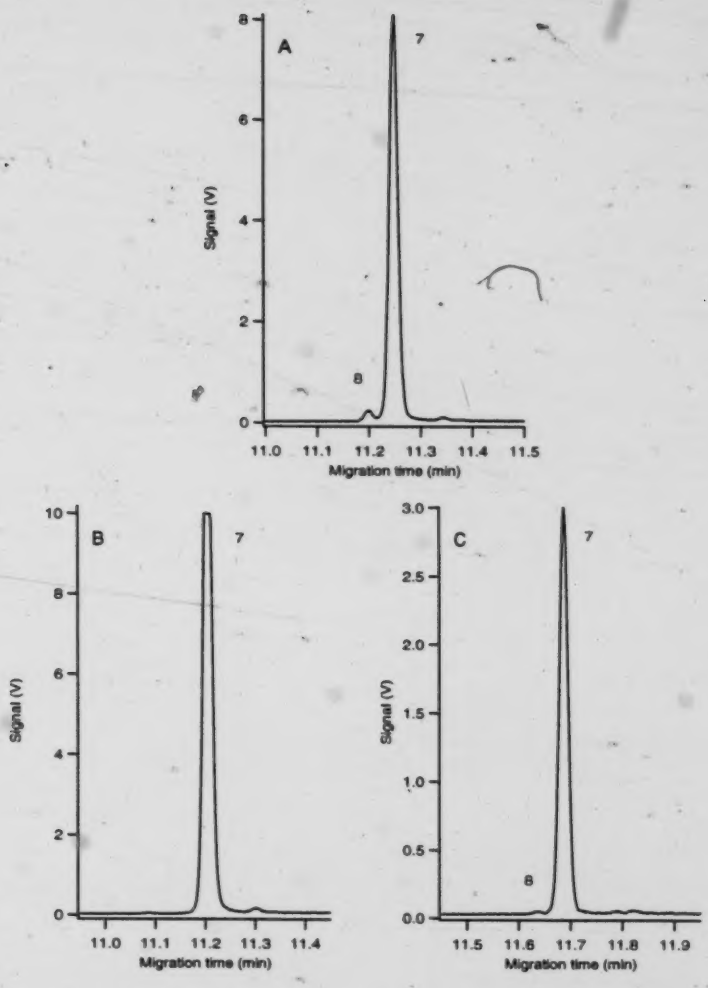

Figure 5.5 Analysis of Le^c-TMR reaction mixtures from the E. coli whole cell extract incubations by CE-LIF. (**A**) Electropherogram showing the reaction of *H. pylori* α1,2 fucosyltransferase incubated with 1.8 mM Le^c-TMR for 20 minutes. (**B**) The negative control, *E.coli* inserted with the plasmid only, incubated with acceptor for 20 minutes. (**C**) The *H. pylori* α1,2 fucosyltransferase incubated with 1.8 mM Le^c-TMR and 0.5 M lactose for 20 minutes. The peak identifications are βGal(1→3)βGlcNAc- (**7**), αFuc(1→2)βGal(1→3)βGlcNAc-TMR (**8**).

5.3.2 Brazilian Myxoma Viral α2,3 Sialyltansferase Results

5.3.2.1 Transfer of Sialic Acid to Lewis^a-gr and Lewis^x-gr

Results from radiochemical assays using Le^a-gr and Le^x-gr as acceptors for the myxoma viral α2,3 sialyltransferase showed that the enzyme used these trisaccharides as acceptors, a feature that was not found for any of the mammalian α2,3 sialyltransferase enzymes (**Schemes 5.3 & 5.4**). **Table 5.2** shows the results of these experiments, along with the possible products from the reaction. The enzyme had slightly higher affinity towards the Type I structures than the Type II structures. The K_m for Le^a-O-gr was 1.6 mM ± 0.1 mM (relative V_{max}/K_m was 0.03) and K_m for Le^x-O-gr was 9.5 mM ± 1.9 mM (relative V_{max}/K_m was 0.003) (Dr. K. Sujino, unpublished data).

5.3.2.2 Confirmation of the α2,3 Sialylated Le^x- and Le^a-TMR Products by CE-LIF

While radiochemical assay showed transfer of sialic acid to the 2 different trisaccharides, these results did not reveal the structural identities of the sialylated products. Using CE-LIF, products were separated from the starting material and identified by co-migration with standards and treatment with neuraminidase.

Fig. 5.6A shows the electropherograms obtained following incubation of the myxoma viral α2,3 sialyltransferase with Le^x-TMR and CMP-Neu5Ac. The two peaks were identified by co-migration with authentic standards as Le^x-TMR (peak 5) and α2,3 sialylated Le^x-TMR (peak 13). Similarly, **Fig. 5.6B** shows the

Table 5.2 Relative myxoma viral α2,3 sialyltransferase activity with Le^a- and Le^x-gr acceptors.

Acceptor	Possible Products[a]	Relative Rate of Transfer[b]	Specific Activity (μU/μg)[c]
$Lewis^a$-gr	αNeu5Ac(2→3)Le^a-gr and/or αNeu5Ac(2→6)Le^a-gr and/or αNeu5Ac(2→8)Le^a-gr	100%	0.59
$Lewis^x$-gr	αNeu5Ac(2→3)Le^x-gr and/or αNeu5Ac(2→6)Le^x-gr and/or αNeu5Ac(2→8)Le^x-gr	65%	0.39

[a] The exact structure of the product(s) could not be deduced from the radiochemical assay. The above proposed structures are commonly found in mammalian cells, any positions for the addition of Neu5Ac, other than 2-, 6-, 8-OH, are possible.

[b] % Activity relative to that of $Lewis^a$-gr.

[c] A microunit (μU) of the enzyme is expressed as that activity which convert 1 pmol of acceptor to product per minute. Specific activity was obtained by dividing the total activity (μU) by the total protein (μg) in the whole cell extract.

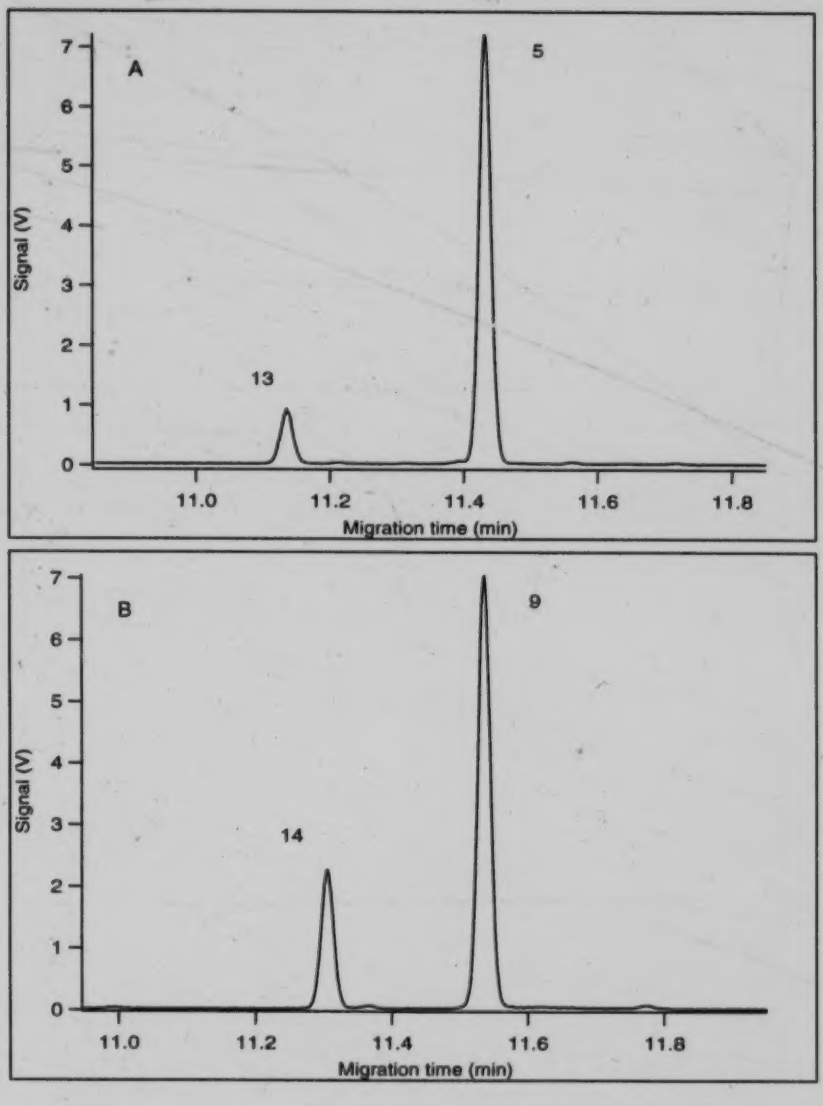

Figure 5.6 Analysis by CE-LIF of reaction mixtures from the myxoma virus enzyme extract incubations. Electropherograms show the reaction of α2,3 sialyltransferase incubated with Le^x-TMR (**A**) and with Le^a-TMR (**B**). The peak identifications are Le^x- (**5**), αNeu5Ac(2→3)Le^x- (**13**), Le^a- (**9**), and αNeu5Ac(2→3)Le^a-TMR (**14**), by co-migration.

electropherogram obtained following enzyme incubation with Le^a-TMR and CMP-Neu5Ac. The two peaks were also identified by co-migration with authentic standards , as Le^a-TMR (peak 9) and α2,3 sialylated Le^a-TMR (peak 14). As in the radiochemical assay results, these CE data also showed more αNeu5Ac(2→3)Le^a-TMR was formed than αNeu5Ac(2→3)Le^x-TMR. There were no other products formed under the described conditions. Therefore, the enzyme extract did not contain any hydrolyzing enzyme that would degrade the starting material.

The reaction mixtures were treated with neuraminidase to show that the new product in each of the two cases was the result of sialylation and not to addition of some other sugar unit present in the extract. In **Fig. 5.7A**, the electropherogram shows the result obtained following removal of the sialic acid moiety from α2,3 sialylated Le^x-TMR. The sample was compared with a set of authentic standards (**Fig. 5.7B**) and showed quantitative removal of α2,3 sialylated Le^x-TMR (see **Fig. 5.6A**). Similarly, sialic acid was removed completely from α2,3 sialylated Le^a-TMR after neuraminidase treatment (**Fig. 5.8A**).

5.3.2.3 Analysis of the One-Pot Syntheses

The ability to perform chemi-enzymatic synthesis in one container (one-pot synthesis) was desirable due to the convenience of one workup procedure to isolate all products after several synthetic steps. In the present experiments, the myxoma viral α2,3 sialyltransferase was useful in the production of αNeu5Ac(2→3)Le^x (potential anti-inflammatory) and αNeu5Ac(2→3)Le^a. It was reported that mammalian α2,3 sialyltransferase would not add a sialic acid moiety to an

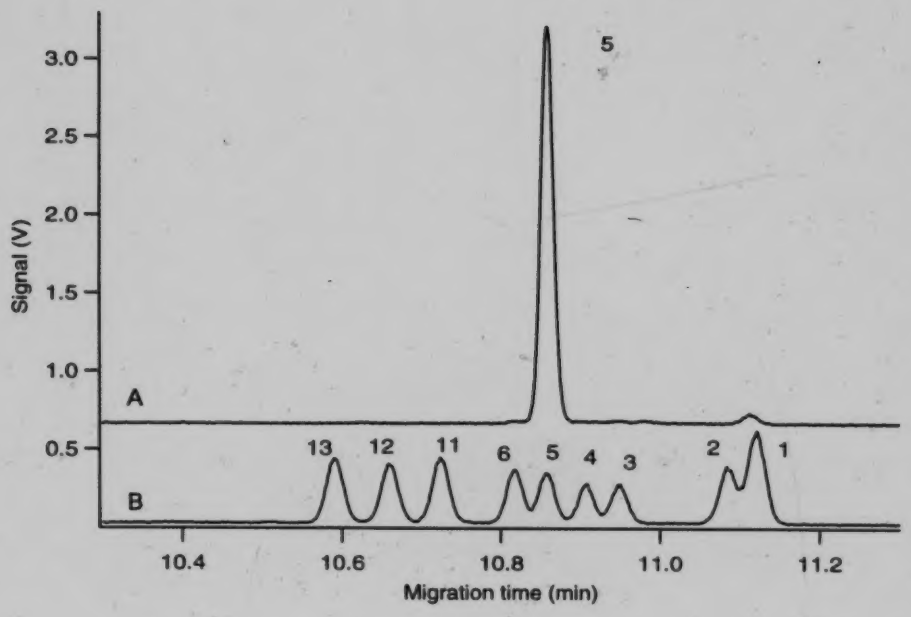

Figure 5.7 Analysis by CE-LIF of the Le^x-TMR reaction mixture from neuraminidase incubations. (**A**) Electropherogram showing the complete removal of αNeu5Ac(2→3)Le^x-TMR after incubation with neuraminidase for 72 hr. (**B**) Separation of nine standard TMR oligosaccharides found in mammalian metabolism: linker arm- (**1**), GlcNAc- (**2**), LacNAc- (**3**), αFuc(1→2)βGal(1→4)βGlcNAc- (**4**), βGal(1→4)[αFuc(1→3)]βGlcNAc- (**5**), α Fuc(1→2)βGal(1→4)[αFuc(1→3)] βGlcNAc- (**6**), αNeu5Ac(2→6)LacNAc- (**11**), αNeu5Ac(2→3)LacNAc- (**12**), αNeu5Ac(2→3)Le^x-TMR (**13**). Electropherogram **A** was y-offset for clarity.

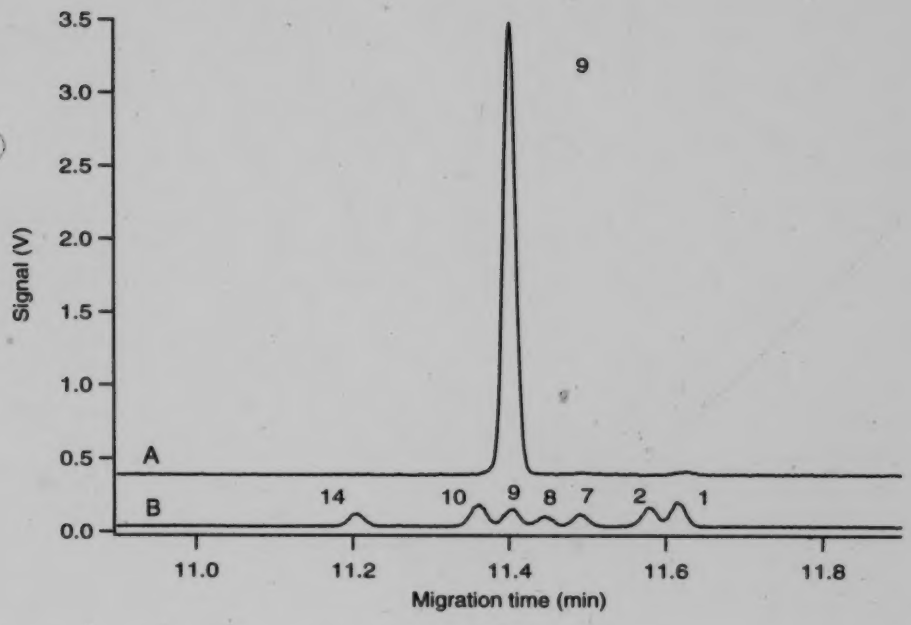

Figure 5.8 Analysis by CE-LIF of the Le^a-TMR reaction mixture from neuraminidase incubations. (**A**) Electropherogram showing the complete removal of αNeu5Ac(2→3)Le^a-TMR after the incubation with neuraminidase for 72 hr. (**B**) Separation of seven standard TMR oligosaccharides found in mammalian metabolism: linker arm- (**1**), GlcNAc- (**2**), Le^c- (**7**), αFuc(1→2)βGal(1→3)βGlcNAc- (**8**), βGal(1→3)[αFuc(1→4)]βGlcNAc- (**9**), αFuc(1→2)βGal(1→3)[αFuc(1→4)] βGlcNAc- (**10**), αNeu5Ac(2→3)Le^c-TMR (**14**). Electropherogram **A** was y-offset for clarity.

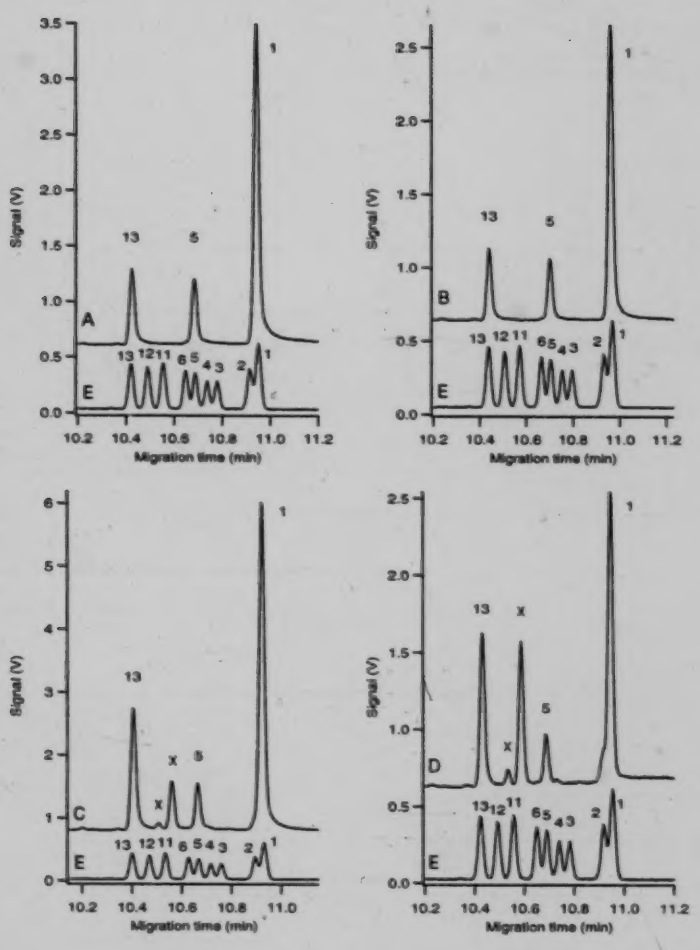

Figure 5.9 Electropherograms of the α2,3 sialylated Le^x-TMR one-pot synthesis after incubation times of 24 hours (**A**), 72 hours (**B**), 1 month (**C**), and 2 months (**D**). (**E**) Separation of 9 standard TMR oligosaccharides: linker arm- (**1**), GlcNAc- (**2**), LacNAc- (**3**), αFuc(1→2)βGal(1→4)βGlcNAc- (**4**), βGal(1→4)[αFuc(1→3)] βGlcNAc- (**5**), αFuc(1→2)βGal(1→4)[αFuc(1→3)] βGlcNAc- (**6**), αNeu5Ac(2→6) LacNAc- (**11**), αNeu5Ac(2→3)LacNAc- (**12**), αNeu5Ac(2→3)Le^x-TMR (**13**). X marks the unknown metabolic by-product peaks. These electropherograms (**A**, **B**, **C**, **D**) were y-offset for clarity.

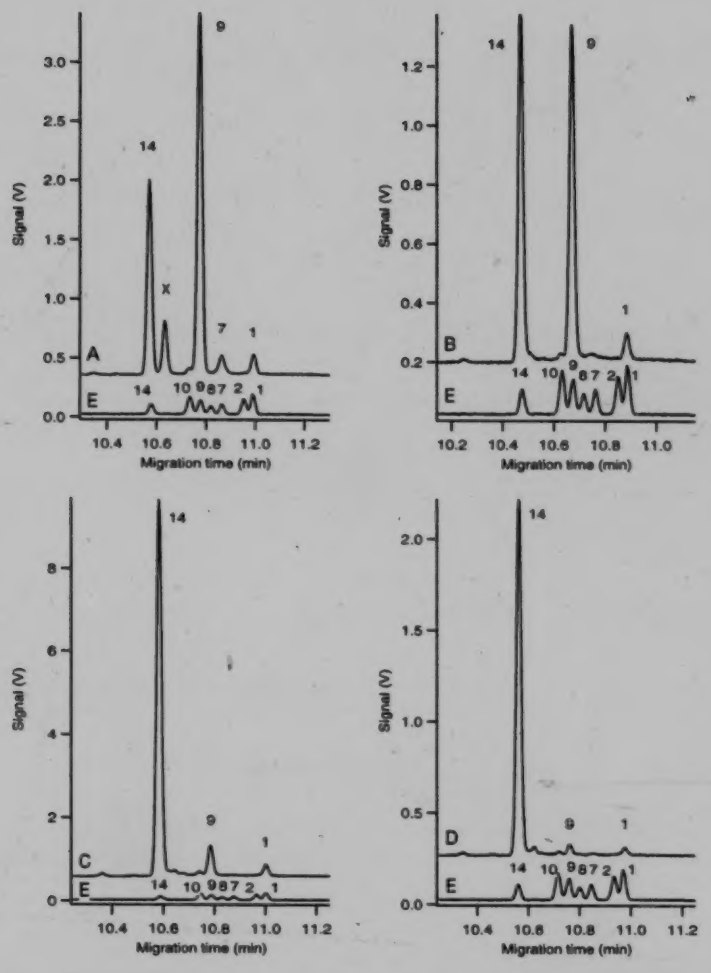

Figure 5.10 Electropherograms of the α2,3 sialylated Le^a-TMR one-pot synthesis after incubation times of 24 hours (**A**), 72 hours (**B**), 1 month (**C**), and 2 months (**D**). (**E**) Separation of 7 standard TMR oligosaccharides: linker arm- (**1**), GlcNAc- (**2**), Le^c- (**7**), αFuc(1→2)βGal(1→3)βGlcNAc- (**8**), βGal(1→3)[αFuc(1→4)]βGlcNAc- (**9**), αFuc(1→2)βGal(1→3)[αFuc(1→4)] βGlcNAc- (**10**), αNeu5Ac(2→3)Le^a-TMR (**14**). X marks the unknown metabolic by-product peak. These electropherograms (**A, B, C, D**) were y-offset for clarity.

to an oligosaccharide containing a fucosyl derivative at the 3-OH position of GlcNAc in LacNAc or the 4-OH position of GlcNAc in Lewis^c (see **Schemes 5.3 & 5.4**).

Three enzymes, isolated bovine milk β1,4 galactosyltransferase, isolated human milk α1,3/4 fucosyltransferase, and myxoma viral α2,3 sialyltransferase, were used in a one-pot synthesis of αNeu5Ac(2→3)Le^x-TMR from the monosaccharide, GlcNAc-TMR. **Fig. 5.9** shows electropherograms of the reaction mixtures after incubation times of 24 hours, 72 hours, 1 month, and 2 months. The area under each peak was determined using the data analysis program, Igor Pro ver. 2.04. The area under each peak was divided by the total area to calculate the % conversion. These data are summarized in **Table 5.3** to illustrate the increase in production of αNeu5Ac(2→3)Le^x-TMR over the course of two months incubation.

The one-pot synthesis of αNeu5Ac(2→3)Le^a-TMR from Le^a-TMR was done in a similar manner, with isolated human milk α1,3/4 fucosyltransferase and myxoma viral α2,3 sialyltransferase. **Fig. 5.10** shows the separation electropherograms of the reaction mixtures after incubation times of 24 hours, 72 hours, 1 month, and 2 months. The % area of each peak during these incubation times are summarized in **Table 5.4**.

In the one-pot synthesis of αNeu5Ac(2→3)Le^x-TMR, the presence of hexosaminidase in the myxoma viral enzyme extract reduced the amount of GlcNAc-TMR to zero after less than 24 hours incubation. After 1 day, more than 70% of total TMR was the linker arm-TMR, and this value stayed unchanged until after 1 month. After 1 month incubation, only 14% Le^x-TMR remained and 16% had been converted to αNeu5Ac(2→3)Le^x-TMR. Over the course of 2 months, the amount of

Table 5.3 Percent area of each peak in the electropherograms of the αNeu5Ac(2→3)Le^x-TMR one-pot synthesis.

TMR-oligosaccharide (peak #)	% area of each peak[a]			
	Incubation time			
	24 hours	72 hours	1 month	2 months
2,3 sLe^x (peak 13)	15.5%	16.3%	21.8%	23.8%
Le^x (peak 5)	13.9%	14.3%	7.79%	7.06%
Linker-arm (peak 1)	70.6%	69.4%	60.7%	48.4%
Unknowns[b] (peaks X)	0.00%	0.00%	9.66%	20.8%

[a] The area under each peak was calculated using integration in the data analysis program, Igor Pro ver. 2.04. The area of each peak was divided by the total area to calculate the percentage.

[b] These peaks were identified as unknowns because they did not co-migrate with any of the existing TMR-labeled oligosaccharide standards.

Table 5.4 Percent area of each peak in the electropherograms of the αNeu5Ac(2→3)Le^a-TMR one-pot synthesis.

TMR-oligosaccharide (peak #)	% area of each peak[a]			
	Incubation time			
	24 hours	72 hours	1 month	2 months
2,3 sLe^a (peak 14)	29.2%	49.1%	89.2%	94.6%
Le^a (peak 9)	55.6%	47.2%	7.76%	3.04%
Le^c (peak 7)	3.58%	0.00%	0.00%	0.00%
Linker-arm (peak 1)	3.12%	3.65%	3.08%	2.37%
Unknowns[b] (peak X)	8.50%	0.00%	0.00%	0.00%

[a] The area under each peak was calculated using integration in the data analysis program, Igor Pro ver. 2.04. The area of each peak was divided by the total area to calculate the percentage.

[b] These peaks were identified as unknowns because they did not co-migrate with any of the existing TMR-labeled oligosaccharide standards.

αNeu5Ac(2→3)Le^x-TMR formed slowly increased to 24%, while only 7% Le^x-TMR remained. The total TMR between αNeu5Ac(2→3)Le^x-TMR and Le^x-TMR remained a constant 30%.

There were two unknown peaks detected in the electropherograms of the mixtures after 1 and 2 months incubation. These unknown peaks seemed to have resulted from conversion of the linker arm-TMR, because the total TMR distributed between these peaks remained at about 70% throughout. The identities of these peaks were not confirmed, but they may have been formed from the action of a nonspecific protease that cleaved one of the amide bonds in linker arm-TMR. The resulting compounds would carry a net positive charge. This could be confirmed by synthesizing the compounds chemically, and testing co-migration with the sample. Another explanation for the presence of these peaks might be addition of a charged species (phosphate, sulphate groups) to the linker arm.

In the one-pot synthesis of αNeu5Ac(2→3)Le^a-TMR, the starting material was Le^c-TMR and therefore, the presence of hexosaminidase did not affect the concentration of the starting material. Very little degradation was found in this reaction even after 2 months. After 24 hours, Le^a-TMR accounted for more than 55% of the TMR compounds, while αNeu5Ac(2→3)Le^a-TMR accounted for almost 30%. Over a 2 month incubation, the amount of αNeu5Ac(2→3)Le^a-TMR slowly increased to about 95% of total TMR. The unknown peak in panel **A** of **Fig. 5.10** had the same migration time as the unknown with a migration time close to 10.6 minutes in panel **D** of **Fig. 5.9**. Disappearance of this unknown peak in the synthesis of αNeu5Ac(2→3)Le^a-TMR over time could not be explained. If this was a product of

linker arm-TMR conversion, as seen in the synthesis of αNeu5Ac(2→3)Le^x-TMR, it would have remained at 8.5% area throughout the 2 months incubation period.

5.4 Conclusions

Capillary electrophoresis with laser-induced fluorescence was used to detect two different and unusual glycosyltransferases with extremely low activities. One was a *Helicobacter pylori* α1,2 fucosyltransferase cloned and expressed in a strain of *E. coli*, and the other was a Brazilian myxoma virus α2,3 sialyltransferase gene expressed in the European rabbit kidney RK_{13} cell line. They both showed novel activities compared with the corresponding natural mammalian enzymes. These unusual activities, and their products, were detected and identified using CE-LIF, a task which had previously been impossible by the use of standard Sep-Pak radiochemical assays. The usefulness of CE-LIF, compared with radiochemistry, was most evident in the case where the extract contained glycosidases that depleted the substrate thereby preventing glycosyltransferase activity in the reactions. Conventional radiochemical assays were unable to separate product(s) from substrate and could not identify the product in cases where more than one linkage was possible. Furthermore, radiochemistry was unable to detect any degradation product which was not labeled with radioisotope. CE-LIF allows a fast, efficient alternative to the radiochemical assay for low level enzyme expression and substrate degradation detection.

CE-LIF has been used in our laboratory in a variety of studies not reported in this thesis. The technique has been used in the detection of oligosaccharide processing in 10^5 bone marrow cells, in comparisons of levels of glycosyltransferases in different types of cells (such as HL60, platelets, endothelial cells, and neutrophils) during differentiation, and in determinations of the relative rates of transfer of

unusual substrates by the enzyme to the natural substrate. The incorporation of an inverted microscope will allow us to perform single cell analysis for the understanding of heterogeneity in cells.

5.5 References

1. Palcic, M. M., Heerze, L. D., Pierce, M., and Hindsgaul, O. (1988) *Glycoconjugate J.* **5**, 49-63.

2. Schachter, H., Brockhausen, I., and Hull, E. (1989) *Methods Enzymol.* **179**, 351-397.

3. Brockhausen, I., Carver, J. P., and Schachter, H. (1988) *Biochem. Cell Biol.* **66**, 1134-1151.

4. Stults, C. L., Sullivan, M. T., Macher, B. A., Johnston, R. F., and Stack, R. J. (1994) *Anal. Biochem.* **219**, 61-70.

5. Nakamura, M., and Sweeley, C. C. (1987) *Anal. Biochem.* **166**, 230-234.

6. Sears, P., and Wong, C.-H. (1998) *Cell. Mol. Life Sci.* **54**, 223-252.

7. Toone, E. J., Simon, E. S., Bednarski, M. D., and Whitesides, G. M. (1989) *Tetrahedron* **45**, 5365-5422.

8. David, S., Auge, C., and Gautheron, C. (1991) *Adv. Carbohydr. Chem. Biochem.* **49**, 175-237.

9. Drueckhammer, D. G., Hennen, W. J., Pederson, R. L., Barbas, C. F., Gautheron, C. M., Krach, T., and Wong, C.-H. (1991) *Synthesis* , 499-525.

10. Ichikawa, Y., Look, G. C., and Wong, C.-H. (1992) *Anal. Biochem.* **202**, 215-238.

11. Wong, C.-H., Halcomb, R. L., Ichikawa, Y., and Kajimoto, T. (1995) *Angew. Chem. Int. Ed. Engl.* **34**, 521-546.

12. Crawley, S. C., and Palcic, M. M. (1995) in *Modern Methods in Carbohydrate Synthesis* (Kahn, S. H., and O'Neil, R. A. eds.) pp. 492-517, Harwood Academic Publishers.

13. Varki, A. (1993) *Glycobiology* **3**, 97-130.

14. Hendrix, M., and Wong, C.-H. (1996) *Enantiomer* **1**, 305-310.

15. Paulson, J. C., and Colley, K. J. (1989) *J. Biol. Chem.* **264**, 17615-17618.

16. Lowe, J. B. (1991) *Seminars Cell Biol.* **2**, 289-307.

17. Kleene, R., and Berger, E. G. (1993) *Biochim. Biophys. Acta* **1154**, 283-325.

18. Schachter, H. (1994) in *Molecular Glycobiology* (Fukuda, M., and Hindsgaul, O. eds.) pp.88-162, Oxford University Press, UK.

19. Wang, G., Boulton, P. G., Chan, N. W. C., Palcic, M. M., and Taylor, D. E. (1998) submitted.

20. McCarthy, K., Taylor-Robinson, C. H., and Pillinger, S. E. (1963) *Lancet* 2, 593-598.

21. Jackson, R. J. (1997) International Patent Application Publication No. WO97/18302.

22. Zhang, Y., Le, X., Dovichi, N. J., Compston, C. A., Palcic, M. M., Diedrich, P., and Hindsgaul, O. (1995) *Anal. Biochem.* **227**, 368-376.

23. Gokhale, U. B., Hindsgaul, O., and Palcic, M. M. (1990) *Can. J. Chem.* **68**, 1063-1071.

24. Le, X., Scaman, C. H., Zhang, Y., Zhang, J., Dovichi, N. J., Hindsgaul, O., and Palcic, M. M. (1995) *J. Chromatogr. A* **716**, 215-220.

25. Bradford, M. (1976) *Anal. Biochem.* **72**, 248-254.

26. Priells, J. P., Monnom, D., Dolmans, M., Beyer, T. A., and Hill, R. L. (1981) *J. Biol. Chem.* **256**, 10456-10463.

27. Palcic, M. M., Venot, A. P., Ratcliffe, R. M., and Hindsgaul, O. (1989) *Carbohydr. Res.* **190**, 1-11.

Chapter Six

Conclusions

6.1 General Discussion and Conclusions

Cell surface oligosaccharides have been implicated in many physiological and pathological phenomena (1). Their functions in cell-cell recognition and signaling are well studied (2), and they are also involved in receptor binding for lectins (3-5), viri such as HIV (6), bacteria (7), and antibodies (8). Some oligosaccharides are associated with malignant transformation and tumour progression (9). Glycosyltranferases that catalyze the biosynthesis of glycoconjugates have been associated with oncogenesis since it has been found that an increase in, or lack of, certain glycosyltransferase activities in malignant cells govern such changes in glycosylation (9, 10). Understanding glycosyltransferases can provide essential information on diseases diagnosis (11, 12) and play a key role in the drug discovery process (13, 14).

Difficulties in studying glycosyltransferases include limited availability of substrates, a paucity of enzyme protein from mammalian sources and structural information thereupon, and detection of oligosaccharides that do not absorb in the UV-VIS range. Capillary electrophoresis with laser-induced fluorescence detection (CE-LIF) not only provides a method with high sensitivity and separation efficiency compare to conventional chromatographic separations such as HPLC (15, 16) and size exclusion chromatography (17), it also circumvents the use of radiochemicals in these assays. A two-step labeling process introduces a fluorescent tag, tetramethylrhodamine (TMR), to oligosaccharide acceptors for CE-LIF (18). Micellar electrokinetic capillary electrophoresis (MEKC) is then used to separate oligosaccharides that are electronically neutral, and separation is based on their

partition between the micelle and the buffer in the capillary (19). The post-column detection was based on a sheath flow quartz cuvette with low scattering characteristics. The sheath flow buffer focuses analytes coming out of the capillary, thereby, providing a very low detection limit of one hundred fluorescent molecules (20).

This thesis focuses on the application of CE-LIF in the detection of minute glycosyltransferase enzyme activity (chapter 2), on development of an intracellular enzyme inhibition method for two different enzymes (chapters 3 and 4), and on detection and characterization of novel, genetically-engineered glycosyltransferases for use in oligosaccharide synthesis (chapter 5).

In chapter 2, the biosynthesis of Lewis^x determinants in two strains of *Helicobacter pylori* was investigated. Lewis^x is expressed on the *H. pylori* cells and flagella sheaths, and this masks them from the mammalian host immune system. α1,3 fucosyltransferase and β1,4 galactosyltransferase activities were detected in *H. pylori*, and the Lewis^x biosynthetic pathway was found to be similar to that in human cells. A new glycosidic linkage was detected in a galactosyltransferase assay in the UA 861 strain, which was confirmed by methylation analysis to be an α1→6 linkage. A recent report showed UA 861 expressed lipopolysaccharides that terminate with glucosylated *N*-acetyllactosamine (21). Monteiro *et al.* suggested it is likely an α1,6 glucosyltransferase, rather than an α1,6 galactosyltransferase reported in Chan *et al.* (22).

In chapter 3, the development of an intracellular enzyme inhibition assay was described. The enzyme used for developing this method was an α-glucosidase I in

the HT29 human colon adenocarcinoma cell line. A synthetic substrate, αGlc(1→2)αGlc(1→3)αGlc, that was covalently linked to TMR was used in the assay. The potencies of two α-glucosidase I inhibitors, 1-deoxynojirimycin and castanospermine, were assessed as inhibitors of substrate degradation in this intracellular assay. IC_{50} values obtained for 1-deoxynojirimycin and castanospermine were 320 μM and 165 μM, respectively. Their IC_{50} values obtained in this manner should reflect the bioavailability of the inhibitors in the intracellular compartment where the enzyme is localized because the inhibitors have to cross cell membranes to effectively inhibit α-glucosidase I, which is localized in the luminal space of the endoplasmic reticulum. These IC_{50} values for inhibition of intracellular metabolism were significantly higher than those obtained versus purified glucosidase I enzymes, an observation similar to that of Kang and coworkers (23), which might be attributed to poor accessibility of the inhibitors to the enzyme. The efficacy of a novel carbohydrate-based compound, 1,5-trans-*C*-glucose, as an inhibitor of α-glucosidase I was determined in this assay and was found to be ineffective at concentrations up to 5 mM.

In chapter 4, the newly developed intracellular enzyme inhibition assay was applied to determine an IC_{50} value for a compound which had been reported previously by Lowary and Hindsgaul to be a blood group A-transferase inhibitor (24). The compound, 3-amino-3-deoxy-[αFuc(1→2)]βGal-*O*-octyl, was reported to have a K_i of 200 nM against the blood group A-transferase isolated from human serum (24). The IC_{50} was determined here to be 282 μM because endogenous donor, UDP-GalNAc, biosynthesized in the cells was used instead of being added to the culture

medium. The IC_{50} value obtained here was substantially higher than the K_i of 200 nM reported by Lowary and Hindsgaul (24), might attributed to the poor bioavailability of the inhibitor to the enzyme in the luminal space of the Golgi compartments where the enzyme resides. Experiments in which HT29 cells were radiolabeled with [^{35}S]-methionine indicated that inhibition by 3-amino-3-deoxy-[αFuc(1→2)]βGal-*O*-octyl was specific for A-transferase. Results showed glycoprotein formation to be similar in control and inhibitor-treated samples, although fewer blood group A structures were expressed on cells treated with inhibitor.

In chapter 5, CE-LIF was used to detect and characterize minute activities associated with two novel enzymes, an *H. pylori* α1,2 fucosyltranferase cloned in *E. coli* cells and a Brazilian myxoma viral α2,3 sialyltransferase infected into a European rabbit kidney RK_{13} cell line. Conventional radiochemical assays are able to determine the amount of enzyme activities and not able to separate products from each other or determine the exact position and type of linkage of the newly added monosaccharide. In both cases we confirmed the specificity of the novel enzyme, while providing fast separation of product(s) from substrate and allowed identification of each individual product formed. The *H. pylori* α1,2 fucosyltranferase was confirmed to transfer fucose via an α1→2 linkage to Lewis^c, Lewis^a, and Lewis^x; the addition of fucose to the two latter acceptors is not permitted in the mammalian equivalents. The Brazilian myxoma viral α2,3 sialyltransferase was confirmed to transfer sialic acid to LacNAc, Lewis^c, Lewis^x, and Lewis^a via an α2→3 linkage. Addition of sialic acid to Lewis^a and Lewis^x is not permitted in the mammalian biosynthetic pathway. Thus, CE-LIF allowed the determination of the

novelties of both α1,2 fucosyltranferase and α2,3 sialyltransferase as their abilities to transfer monosaccharide to acceptors that are normally not permitted in their mammalian counterparts.

In conclusion, CE-LIF was proven to be a fast and effective method to separate and determine enzymatic products in a single analysis involving several enzymes that work in a concerted fashion. CE-LIF has been adapted to glycosyltransferase studies, other than those described above, such as to compare rates of transfer of substrate analogues to their usual substrate (25), in metabolic fingerprinting assays, in the monitoring of several glycosyltransferases and glycosidases simultaneously, in single cell analyses (26), and in detection of enzymatic products in stem cells (Chan, N. W. C., unpublished data).

One of the difficulties in the study of this newly developed *in vivo* inhibition assay with CE-LIF detection is the choice of cells. There are different responses to each substrate in different cell lines including uptake and localization. Also some cell lines have high activities of certain glycosyltransferases while others contain no activity. Moreover, the same cell line, such as the HT29 cell line used throughout this thesis, can show metabolic variations during passages which is a characteristics of cultured cells. However, the choice of cell line can resemble the type of tissue that will be used for screening the drug of interest. CE is not as reproducible as HPLC due to changes in the migration times (factors involved include temperature changes, fluctuations in the buffer content and capillary wall compositions), peaks are identified by co-migration with authentic standards in each runs instead of by their elution times as in HPLC.

The choice of fluorescent tag, tetramethylrhodamine (TMR), provided a relatively stable fluorescent response regardless of any changes to the oligosaccharide. As shown in the electropherograms of separations of standards in Chapter 5, the signal from each standard had roughly the same fluorescent intensity (within weighing errors).

The usefulness of CE-LIF can be enhanced by coupling to mass spectrometry. The combination of MEKC with mass spectrometry was reviewed by Yang and Lee (27) for direct identification of analytes, and for structural confirmation and analysis in MS-MS mode. For identification of unknown metabolites from the *in cella* enzyme assays described in this thesis, direct coupling to a mass spectrometer would certainly be an advantage.

The intracellular enzyme inhibition assay can also be used in different glycosyltransferase systems. Another important enzyme controlling the branching of asparagine-linked oligosaccharides is UDP-GlcNAc: α-D-mannoside β1,6 *N*-acetyl glucosaminyltransferase (GnT-V, EC 2.4.1.155) and it is directly associated with metastasis (28, 29). Recently, two competitive inhibitors were reported by Lu *et al.* (30) that showed promise for use as metastatic cancer treatment drugs (K_is less than 10 μM in both cases). Some of the highly metastatic cell lines, such as murine tumour cells MDAY-D2 (28) and transformed BHK cells (29), have high levels of GnT-Vs. With the availability of the GnT-V substrate, βGlcNAc(1→2)αMan(1→6) βMan-*O*gr, coupled to fluorescent marker (TMR), the efficacy of these inhibitors can be determined inside cells.

In both chapters 3 and 4, the inhibitor concentrations within the cells were not determined due to the difficulties in tracing the location and amount of the compounds that do not absorb in the UV-VIS range. Inhibitor can be modified to have a different fluorescent label, such as fluorescein, from that of the substrate. Installation of a second laser, such as a 488 nm Argon ion laser, and monitoring the intensities of the inhibitor simultaneously with substrate transformations on electropherograms can provide information for inhibitor intracellular concentrations which can not be determined with current method. This setup allows monitoring the concentration and metabolism of inhibitors inside cells with a separate electropoherogram corresponding to a different emission wavelength. If inhibitors were metabolized, it would be possible to observe any degradations from the electropherograms.

6.2 References

1. Varki, A. (1993) *Glycobiology* **3**, 97-130.
2. Hakomori, S.-I., and Igarashi, Y. (1995) *J. Biochem.* **118**, 1091-1103.
3. Feizi, T. (1993) *Curr. Opin. Struct. Biol.* **3**, 701-710.
4. Crocker, P. R., and Feizi, T. (1996) *Curr. Opin. Struct. Biol.* **6**, 679-691.
5. Liener, I. E., Sharon, N., and Goldstein, I. J. eds. (1986) *The Lectins: Properties, Functions and Applications in Biology and Medicine*, Academic Press, New York.
6. Feizi, T., and Larkin, M. (1990) *Glycobiology* **1**, 17-23.
7. Karlsson, K.-A. (1995) *Curr. Opin. Struct. Biol.* **5**, 622-635.
8. Hakomori, S.-I., and Kannagi, R. (1983) *J. Natl. Cancer Inst.* **71**, 231-251.
9. Dennis, J. W. (1992) in *Cell Surface Carbohydrates and Cell Development* (Fukuda, M. ed.) pp. 161-194, CRC Press, Boca Raton.
10. Yamashita, K., Tachibana, Y., Okhura, T., and Kobata, A. (1985) *J. Biol. Chem.* **260**, 3963-3939.
11. Orntoft, T. F. (1992) *Apmis. Supplementum* **27**, 181-187.
12. Stanley, P., and Ioffe, E. (1995) *FASEB J.* **9**, 1436-1444.
13. Jacob G. S. (1995) *Curr. Opin. Struct. Biol.* **5**, 605-611.
14. McAuliffe, J. C., and Hindsgaul, O. (1997) *Chem. Ind.* **5**, 170-174.
15. Schachter, H., Brockhausen, I., and Hull, E. (1989) *Methods Enzymol.* **179**, 351-397.
16. Brockhausen, I., Carver, J. P., and Schachter, H. (1988) *Biochem. Cell Biol.* **66**, 1134-1151.

17. Nakamura, M., and Sweeley, C. C. (1987) *Anal. Biochem.* **166**, 230-234.

18. Zhang, Y., Le, X., Dovichi, N. J., Compston, C. A., Palcic, M. M., Diedrich, P., and Hindsgaul, O. (1995) *Anal. Biochem.* **227**, 368-376.

19. Terabe, S. T. (1991) in *Micellar Electrokinetic Chromatography*, pp.1-7, Beckman Instruments, Inc., CA.

20. Zhao, J. Y., Dovichi, N. D., Hindsgaul, O., Gosselin, S., and Palcic, M. M. (1994) *Glycobiology* **4**, 239-242.

21. Monteiro, M. A., Rasko, D., Taylor, D. E., and Perry, M. B. (1998) *Glycobiology* **8**, 107-112.

22. Chan, N. W. C., Stangier, K., Sherburne, R., Taylor, D. E., Zhang, Y., Dovichi, N. J., and Palcic, M. M. (1995) *Glycobiology* **5**, 683-688.

23. Kang, M. S., Liu, P. S., Bernotas, R. C., Harry, B. S., and Sunkara, P. S. (1995) *Glycobiology* **5**, 147-152.

24. Lowry, T. L., and Hindsgaul, O. (1994) *Carbohydr. Res.* **251**, 33-67.

25. Sujino, K., Uchiyama, T., Seto, N. O. L., Wakarchuk, W. W., Hindsgaul, O., and Palcic, M. M. (1998) *in preparation*.

26. Krylov, S. N., Arriaga, E., Zhang, Z., Chan, N. W. C., Palcic, M. M, and Dovichi, N. J. (1998) *in preparation*..

27. Yang, L., and Lee, C. S. (1997) *J. Chromatogr. A* **780**, 207-218.

28. Dennis, J. W., Laferté, S., Waghorns, C., Breitman, M. L., and Kerbel, R. S. (1987) *Science* **236**, 582-585.

29. Dennis, J. W. (1988) *Cancer Surveys* **7**, 573-595.

30. Lu, P.-P., Hindsgaul, O., Li, H., and Palcic, M. M. (1997) *Carbohydr. Res.* **303**, 283-291.